

Dry beneficiation of fine coal using a fluidized dense medium bed

AN Terblanche
21292922

Dissertation submitted in fulfilment of the requirements for the degree *Magister in Chemical Engineering* at the Potchefstroom Campus of the North-West University

Supervisor: Dr M le Roux
Co-supervisor Prof QP Campbell

September 2013

Declaration

I, ANDRE NARDUS TERBLANCHE (8902205083081), hereby declare that this dissertation entitled: DRY BENEFICIATION OF FINE COAL USING A FLUIDIZED DENSE MEDIUM BED, which was done for the completion of a Magister degree in Chemical Engineering, has never been submitted to any other academic institution and is my own work. Some of the information contained in this dissertation has been gained from various journal articles; text books etc., and has been referenced accordingly.

A.N. Terblanche

Witness

ABSTRACT

Beneficiation of fine coal (**+500 μm –2000 μm**) is a worldwide problem in the mining industry, especially dry beneficiation of fine coal. Coal beneficiation can be divided primarily into two methods, namely wet- and dry beneficiation. Wet beneficiation methods are utilized more in today's industry because of the sharp separation efficiency that can be achieved. These processes include wet jigging, dense medium cyclones, spiral beneficiation etc. Due to the lack of a sufficient water supply in some regions around the world including South Africa, dry beneficiation methods are becoming more popular.

Recent mechanized mining methods caused the fraction of fines from coal mines to increase over the years. However, due to old inefficient technologies, coal fines contained in slurry ponds could not be beneficiated and had to be discarded. One new dry beneficiation technology that has been used and researched extensively is the fluidized dense medium bed (FDMB) technology.

The purpose of this study is to determine whether fine coal can be successfully beneficiated with a FDMB. It also has to be determined whether adding magnetite and introducing a jigging (pulse) motion to the air feed will increase the separation efficiency of the fluidization process.

Witbank seam 4 and a Waterberg coal was used in experiments during this study. A coarse (+1180 μm –2000 μm), fine (+500 μm –1180 μm) and a mix of the two samples were prepared and tested.

It was found that adding magnetite to the feed of the fluidized bed did not increase the separation efficiency. However, previous studies indicated the opposite results with regards to magnetite addition. The difference in results obtained could be prescribed to the ultrafine nature of the magnetite and the small coal particles size range used. If the presence of fine particles in the bed increases, the stability of fluidization decreases. In turn, the separation efficiency of the process decreases.

School of Chemical and Minerals Engineering

Subjecting the feed air flow to a pulsating motion did not have a significant effect on separation. Good results were still obtained with jigging experiments, although not better than with normal fluidization.

Stratification of coal particles according to quality was evident by the results obtained during experiments. The quality of coal increases from the bottom to the top of the bed. Overall the fluidized bed, in the absence of magnetite, was found to be a sufficient de-ashing process and further research on this technology could be very beneficial to the coal industry.

Keywords: fluidized bed separation, coal preparation, dry beneficiation, fine coal beneficiation, density separation.

ACKNOWLEDGEMENTS

I would like to thank the following individuals and organizations for their contributions to the execution of this study. It would not have been possible to accomplish this if not for them:-

- First of all and most importantly, I would like to thank my Creator, Saviour and heavenly Father. Without **God** giving me my talents, I would not have accomplished what I have.
- I would like to thank my supervisor and mentor **Dr. Marco le Roux** for his guidance, motivation and helpful contribution to this project which made it all possible.
- I would also like to thank my co-supervisor **Prof. Quentin Campbell** for all his positive insights throughout this project.
- Thank you to **Mr. Johan de Korte** of **Coaltech** for his valuable insights and financing given to this study which made it possible.
- A much appreciated thanks to **SAMMRI** for partly funding this project.
- Special word of thanks to the following people for their moral support during this project. To **Jana van Rensburg** and **Theron Smith** with whom I shared an office with for the last two years. Their help and positivity always encouraged me. I would also like to thank my **family** for their love and support throughout my whole study. I love you all.
- Finally, I would like to give a much appreciated thanks to **Janine van der Bank**. Her loving smiles and hugs came just at the right times. Thank you for believing in me and supporting me unconditionally.

Publications and presentations

The work done during this dissertation has been presented at the following conferences around South Africa:

- Annual student coal symposium: North-West University, Potchefstroom, 26 June 2012.
- South African minerals to metals research institute workshop: Vineyard hotel and conference centre, Cape Town, 5 August 2013.
- MINPROC annual student presentation: Vineyard hotel and conference centre, Cape Town, 7 August 2013.
- 18th Southern African coal science and technology indaba (Fossil fuel foundation): Stonehenge conference centre, Parys, 14 November 2013.

An article has been published and will be presented at the XXVII International Mineral Processing Congress (IMPC) on 20-24th October 2014 at Hotel Sheraton, Santiago, Chile.

Website link – <http://www.impc2014.org/english/>

LE ROUX, M., CAMPBELL, Q.P., TERBLANCHE, A.N. 2014. Dry beneficiation of fine coal using a dense medium fluidized bed. XXVII International Mineral Processing Congress (IMPC). October.

CONTENTS

Title Page	1-1
Declaration	1-2
Abstract	1-3
Acknowledgements	1-5
Publications and presentations	1-6
Contents	1-7
DVD – Contents	1-11
List of symbols	1-12
List of tables	1-14
List of figures	1-16
Chapter 1: Introduction	1-19
1.1 Background and motivation.....	1-19
1.2 Objectives	1-21
1.3 Scope of investigation	1-22
Chapter 2: Literature survey	2-24
2.1 Background.....	2-24
2.2 Coal	2-24
2.2.1 Origin of coal.....	2-24

School of Chemical and Minerals Engineering

2.2.2	Properties of coal.....	2-25
2.3	South African coal and market relations.....	2-25
2.4	Sizing of coal particles	2-27
2.5	Coal washing	2-27
2.5.1	Wet beneficiation	2-27
2.5.2	Wet jigging.....	2-28
2.6	Dry beneficiation	2-30
2.6.1	Dry jigging.....	2-31
2.6.2	Fluidization.....	2-32
2.6.3	The principle of fluidization	2-32
2.6.4	Minimum fluidization velocity	2-35
2.6.5	Pressure and velocity relations in a fluidized bed	2-38
2.6.6	Classification of particles in a fluidized bed.....	2-40
2.7	Dry beneficiation of coal using a fluidized bed.....	2-41
2.7.1	Magnetically stabilized fluidized beds	2-43
2.7.2	Vibrated gas-fluidized bed.....	2-43
Chapter 3: Experimental		3-45
3.1	Safety in the lab	3-45
3.2	Equipment.....	3-45
3.2.1	Fluidized bed	3-45
3.3	Feed material.....	3-51

School of Chemical and Minerals Engineering

3.4	Coal sample preparation	3-51
3.5	Analyses of the coal	3-53
3.6	Experimental planning.....	3-54
3.7	Experimental procedure	3-55
Chapter 4: Results and discussion		4-58
4.1	Introduction	4-58
4.1.1	Pre-experiment results	4-59
4.2	Interpretation procedure of the data	4-62
4.3	Repeatability of experiments	4-63
4.4	Statistical analysis.....	4-65
4.4.1	Introduction	4-65
4.4.2	Statistical analysis: Case 1	4-67
4.4.3	Statistical analysis: Case 2.....	4-73
4.5	Discussion of selected runs.....	4-79
4.5.1	Run 2	4-79
4.5.2	Run 6	4-87
4.5.3	Run 11	4-93
Chapter 5: Conclusions and recommendations		5-101
5.1	Conclusions	5-101
5.2	Recommendations for the future	5-102
Bibliography.....		6-103

School of Chemical and Minerals Engineering

Appendix A – Experimental results 7-108

A.1. Feed coal washability data tables 7-108

A.2 Repeatability graphs 7-109

Appendix B..... 8-116

DVD – Contents

A large amount of information including experiment videos are contained in a DVD attached as a part of this dissertation. The DVD also contains the following relevant information:

- Information and contact details on the author
- The complete dissertation
- Picture gallery of the experimental setup
- Experimental run videos
- Articles used during this dissertation including additional relevant reading material
- Statistical data tables and graphs (Appendix B)
- Experimental results data tables and graphs (Appendix B)

List of Symbols

Description	Units
A_t - Cross-sectional area of the bed cylinder	(m^2)
Ar - Archimedes' number/constant	-
E_p - Ecart probable moyen value	(g/cm^3)
f - Critical vibration frequency	(Hertz)
F_b - Effective buoyancy force of air on particle	(N)
F_{gd} - Frictional drag force of air on particle	(N)
F_{sd} - Drag force of air dense medium on particle	(N)
g - Gravity acceleration constant	(m/s^2)
G - Gravitational force on particle	(N)
h - Height of particle bed	(m)
L_{mf} - Length of fluid bed	(m)
Δp_b - Pressure drop within particle bed	(Pa)
Q - Air flow rate to fluidized bed	(m^3/s)
$Re_{p,mf}$ - Reynolds number	-
u_{mf} - Minimum fluidization velocity	(m/s)
W - Weight of particle bed	(N)

Greek symbols

Description	Units
δ_{75} - 75% partition coefficient	(g/cm ³)
δ_{25} - 25% partition coefficient	(g/cm ³)
ε - Voidage between particles in bed	-
μ - Viscosity of the feed gas	(Pa.s)
μ_{mf} - Viscosity of the feed gas at minimum fluidization	(Pa.s)
ρ - Relative density	(g/cm ³)
ρ_g - Density of the gas	(g/cm ³)
ρ_s - Density of the solid	(g/cm ³)
φ - Sphericity of the particles	-

List of Tables

Table 2-1: Cost of dry coal beneficiation processes.....	2-30
Table 2-2: Ep value comparison of the various coal washing processes.....	2-31
Table 3-1: Analyses standards	3-53
Table 3-2: South Africa's domestic and export coal specifications.....	3-54
Table 3-3: Thermal coal grade specifications in South Africa.....	3-54
Table 3-4: Experimental plan.....	3-55
Table 4-1: Bed height and bed layer comparison.....	4-58
Table 4-2: Witbank FF pre-test results.....	4-61
Table 4-3: Witbank SF pre-test results	4-62
Table 4-4: Waterberg pre-test results	4-62
Table 4-5: Standard deviation (Run 2).....	4-64
Table 4-6: Standard deviation (Run 3).....	4-64
Table 4-7: Standard deviation (Run 8).....	4-65
Table 4-8: Standard deviation (Run 9).....	4-65
Table 4-9: Independent variable (x_1) options	4-66
Table 4-10: Altered experimental plan	4-66
Table 4-11: Case 1 data values.....	4-67
Table 4-12: Case 2 data values	4-74
Table 4-13: Run 2 data results	4-81

School of Chemical and Minerals Engineering

Table 4-14: Run 6 data results 4-89

Table 4-15: Run 11 data results 4-95

Table 7-1: Washability data table: Witbank filter feed 7-108

Table 7-2: Washability data table: Witbank spiral feed..... 7-108

Table 7-3: Washability data table: Waterberg 7-109

List of Figures

Figure 1-1: Scope of investigation	1-23
Figure 2-1: Coalfields in South Africa	2-26
Figure 2-2: The working principle of a jigging process	2-29
Figure 2-3: Forces acting on a particle during fluidization	2-34
Figure 2-4: Fluid-like properties of particles in a fluidized bed.....	2-35
Figure 2-5: Pressure vs. velocity diagram of uniformly sized sand particles.....	2-39
Figure 3-1: Schematic presentation of the fluidized bed flow diagram	3-47
Figure 3-2: Pressure probe marked for each bed height.....	3-47
Figure 3-3: Variable area flow meters (air) with regulator valves	3-48
Figure 3-4: Air distributor system.....	3-49
Figure 3-5: Fluidized bed equipment (150mm)	3-49
Figure 3-6: Sample cutting tool.....	3-50
Figure 3-7: Magnetite – coal separation equipment	3-50
Figure 3-8: Spiral feed coal sample	3-52
Figure 4-1: Washability curve – Witbank FF	4-59
Figure 4-2: Washability curve – Witbank SF	4-60
Figure 4-3: Washability curve – Waterberg.....	4-60
Figure 4-4: Case 1 interaction graph of y_1 (Δ density g/cm^3).....	4-68
Figure 4-5: Case 1 interaction graph of y_2 (Δ ash %).....	4-70

School of Chemical and Minerals Engineering

Figure 4-6: Case 1 interaction graph of y_3 (Δ CV MJ/kg).....	4-71
Figure 4-7: Case 1 interaction graph of y_4 (Δ d50 particle size μm)	4-72
Figure 4-8: Case 2 interaction graph of y_1 (Δ density g/cm^3).....	4-75
Figure 4-9: Case 2 interaction graph of y_2 (Δ ash %).....	4-76
Figure 4-10: Case 2 interaction graph of y_3 (Δ CV MJ/kg).....	4-77
Figure 4-11: Case 2 interaction graph of y_4 (Δ d50 particle size μm)	4-78
Figure 4-12: Run 2 minimum fluidization graph.....	4-80
Figure 4-13: Run 2 pressure vs. bed height graph.....	4-81
Figure 4-14: Run 2 density curve.....	4-82
Figure 4-15: Run 2 ash curve	4-83
Figure 4-16: Run 2 calorific value curve.....	4-84
Figure 4-17: Run 2 moisture content curve.....	4-85
Figure 4-18: Run 2 ash vs. bed height graph.....	4-86
Figure 4-19: Run 2 performance curve	4-87
Figure 4-20: Run 6 minimum fluidization graph.....	4-88
Figure 4-21: Run 6 pressure vs. bed height graph.....	4-88
Figure 4-22: Run 6 density curve.....	4-89
Figure 4-23: Run 6 ash curve	4-90
Figure 4-24: Run 6 calorific value curve.....	4-91
Figure 4-25: Run 6 moisture content curve.....	4-91
Figure 4-26: Run 6 ash vs. bed height graph.....	4-92

School of Chemical and Minerals Engineering

Figure 4-27: Run 6 performance curve 4-93

Figure 4-28: Run 11 minimum fluidization graph..... 4-94

Figure 4-29: Run 11 pressure vs. bed height graph..... 4-95

Figure 4-30: Run 11 density curve..... 4-96

Figure 4-31: Run 11 ash curve 4-97

Figure 4-32: Run 11 calorific value curve..... 4-98

Figure 4-33: Run 11 moisture content curve..... 4-98

Figure 4-34: Run 11 ash vs. bed height graph..... 4-99

Figure 4-35: Run 11 performance curve 4-100

Figure 7-1: Run 2 density repeatability graph 7-109

Figure 7-2: Run 2 ash repeatability graph..... 7-110

Figure 7-3: Run 2 CV repeatability graph..... 7-110

Figure 7-4: Run 3 density repeatability graph 7-111

Figure 7-5: Run 3 ash repeatability graph..... 7-111

Figure 7-6: Run 3 CV repeatability graph..... 7-112

Figure 7-7: Run 8 density repeatability graph 7-112

Figure 7-8: Run 8 ash repeatability graph..... 7-113

Figure 7-9: Run 8 CV repeatability graph..... 7-113

Figure 7-10: Run 9 density repeatability graph 7-114

Figure 7-11: Run 9 ash repeatability graph..... 7-114

Figure 7-12: Run 9 CV repeatability graph..... 7-115

Chapter 1: Introduction

In this chapter a brief introduction and motivation behind this project will be discussed. The objectives and scope of the investigation will also be given.

1.1 Background and motivation

Water is the most abundant natural resource on earth. However, water is scarce in some arid regions around the world. This is particularly true for some countries with vast coal reserves such as India, China, Russia, America and South Africa, some of which have a shortage of clean process water near coal reserves. Transporting water to these areas where there is a shortage would be very expensive and unpractical to maintain (Houwelingen & de Jong, 2004).

Throughout most of South Africa water is a scarce commodity especially during winter (Philander, 2010). A deeper study into South Africa's water resources revealed that only 1200m³ of fresh water is available per capita per year. Moreover, South Africa has an average rainfall of 464mm per year (Zhao *et al.*, 2010a). To place this into perspective, a study indicated that for one ton of coal, 3 – 5 tons of process water is needed in a wet jigging process (Chen & Wei, 2003). In the Waterberg area, which has one of the largest coal deposits in South Africa, large scale plant development could be limited in future due to insufficient water supplies (Eberhard, 2011).

Vast coal reserves were recently discovered in Mongolia. More than 200 coal deposits were found which consists of 152 billion tons of coal (Erdenetsogt *et al.*, 2009). China, which is geographically located next to Mongolia, is the largest steel producer in the world. According to Levin (2012) there is enough coal in Mongolia to fuel China's substantial demand for the next 50 years. Aminov (2011) also stated that by 2015, Mongolia will be responsible for 52% of China's coking coal supply. However, Mongolia is a perfect example of a country with enormous coal reserves but insufficient process water in some regions to run an economically viable wet beneficiation process. The only viable alternative is to implement dry coal beneficiation processes.

School of Chemical and Minerals Engineering

Coal can be washed by using several methods in the industry today. The purpose of washing is to remove impurities contained in the coal. These cleaning processes can be divided into two primary groups namely: wet and dry beneficiation methods. Wet beneficiation methods require vast amounts of process water as emphasized by Chen and Wei (2003). Of these two processes wet beneficiation is currently the most implemented method due to the sharper separation efficiencies achieved compared to that of dry washing processes. Considering the major problem of a clean water shortage worldwide, the focus of research should be on effective dry beneficiation methods of coal (Yang *et al.*, 2012a).

A dry beneficiation method which could be a possible solution to the problem of low levels of water availability is the fluidized dense medium bed (FDMB) technology. This technology is classified as a dense medium beneficiation which uses gas and solid particle interactions as well as the law of gravity to stratify coal according to density (Luo *et al.*, 2007).

Over the years several research articles have been written on every aspect of fluidization, and it was found that this technology holds many advantages especially in the coal washing industry (Mohanta *et al.*, 2013). Chen and Yang (2003) describes these advantages as:

- **High precision:** Coal with a size range of 50 – 6 mm can effectively be separated with Ep values of 0.05-0.07. These values compare favourably with the existing heavy medium wet beneficiation.
- **Low investment:** The same capacity dry beneficiation plant can be constructed at half the costs compared to a wet beneficiation plant. This is due to the fact that no complicated and costly slurry treatment is needed when handling dry coal.
- **No environmental pollution:** This technology only requires low pressure compressed air. It also operates smoothly with very little noise pollution. The dust emitted by the equipment is within the provisions of environmental laws.
- **Wide ranges of beneficiating densities:** Beneficiating densities range from 1.3 to 2.2 g/cm³ and can be created by adding magnetite powder to the bed. This technology can either remove heavy gangues and/or lower density clean coal depending on the required product.
- **No moisture penalties:** Due to the fact that only air is used in this process, means that no cleaning water is needed and the product coal is not penalized due to excessive moisture levels (Luo *et al.*, 2008).

School of Chemical and Minerals Engineering

- **Product thermal quality:** A dryer product with a higher calorific value per ton of coal is produced (Sahu *et al.*, 2009).
- **Transportation costs:** Due to a low moisture content, transportation of the coal does not include the additional cost of transporting the weight of water (England *et al.*, 2002).

However, research on dry coal beneficiation methods is mostly conducted on coarse coal (+6 mm) which yielded promising results but these are not applicable to fine coal fractions (-2000 + 500 μ m). In recent years coal fines produced by the modern mechanized mining procedures have increased dramatically. Due to these modern methods, up to 15% of run-of-mine coal is in the minus 500 μ m size fraction (England *et al.*, 2002). Slurry ponds were constructed to dispose of this fine fraction because older technologies could not beneficiate this finer fraction. However, recent environmental law policies prohibit the construction of slurry ponds and alternative waste systems need to be implemented (filter presses, centrifuges etc.) to store coal without contaminating fresh water sources due to acid mine drainage.

Methods of dry fine coal beneficiation are therefore important to consider due to the vast amount of valuable fine coal that is discarded every year.

1.2 Objectives

Fluidization is a fairly new technology when it comes to the washing of coal. Studies have been done on the separation performance of a fluidized bed with South African coals ranging from 50 – 3 mm (He *et al.*, 2013; Zhao *et al.*, 2010a). Previous research done on (hence forth defined as “**fine**” South African **coal (-2000 + 500 μ m)**) lacks data and publications when the fluidization process is discussed.

The main focal point of this study is to prove the validity of using fluidized bed technology to upgrade dry fine coal. In order to accomplish this objective, the project will be divided into the following integrated parts:

1. Verification of previous results. Terblanche (2011) found that an air dense fluidized bed stratifies fine coal (-1000 + 212 μ m) according to density. Also, Roux (2012) found that if a jiggling motion is introduced to the air feed, improved separation of fine coal (-1180 + 212 μ m) is achieved. (Note: a smaller **80mm** fluidized bed was used in

School of Chemical and Minerals Engineering

the aforementioned experiments and for this study a bigger **150mm** will be constructed).

2. Determining the best possible separation scenario (refer to Section 1.3).
3. Determining whether the separation efficiency of the fluidized bed increases, by changing the following variables:
 - Coal feed PSD (particle size distribution),
 - Dense medium addition to the feed and,
 - Method of air flow subjection (jigging).

For these objectives to be achieved, a scope of investigation was set up.

1.3 Scope of investigation

The scope of this study has been constructed to illustrate and answer the research questions outlined in the objectives. Important factors to note regarding the scope are:

- A fluidized bed (**150mm ID and 160mm OD**) will be designed, constructed and tested.
- Keeping the results of Terblanche (2011) and Roux (2012) in mind, the above mentioned variables will be changed to observe the effect on separation efficiency of the fluidized bed.

The next step would be to try and provide explanations of previous observations by doing extended experimental work. This will be implemented by the following systematic experimental scenarios:

- Normal fluidization,
- Jigging/pulsed air flow fluidization,
- Magnetite fluidization (normal fluidization with magnetite present) and,
- Magnetite and jigging fluidization.

If reasonable results are obtained, it would make future research on fine coal fluidization at the North-West University easier. A schematic presentation of the scope is illustrated in Figure 1-1.

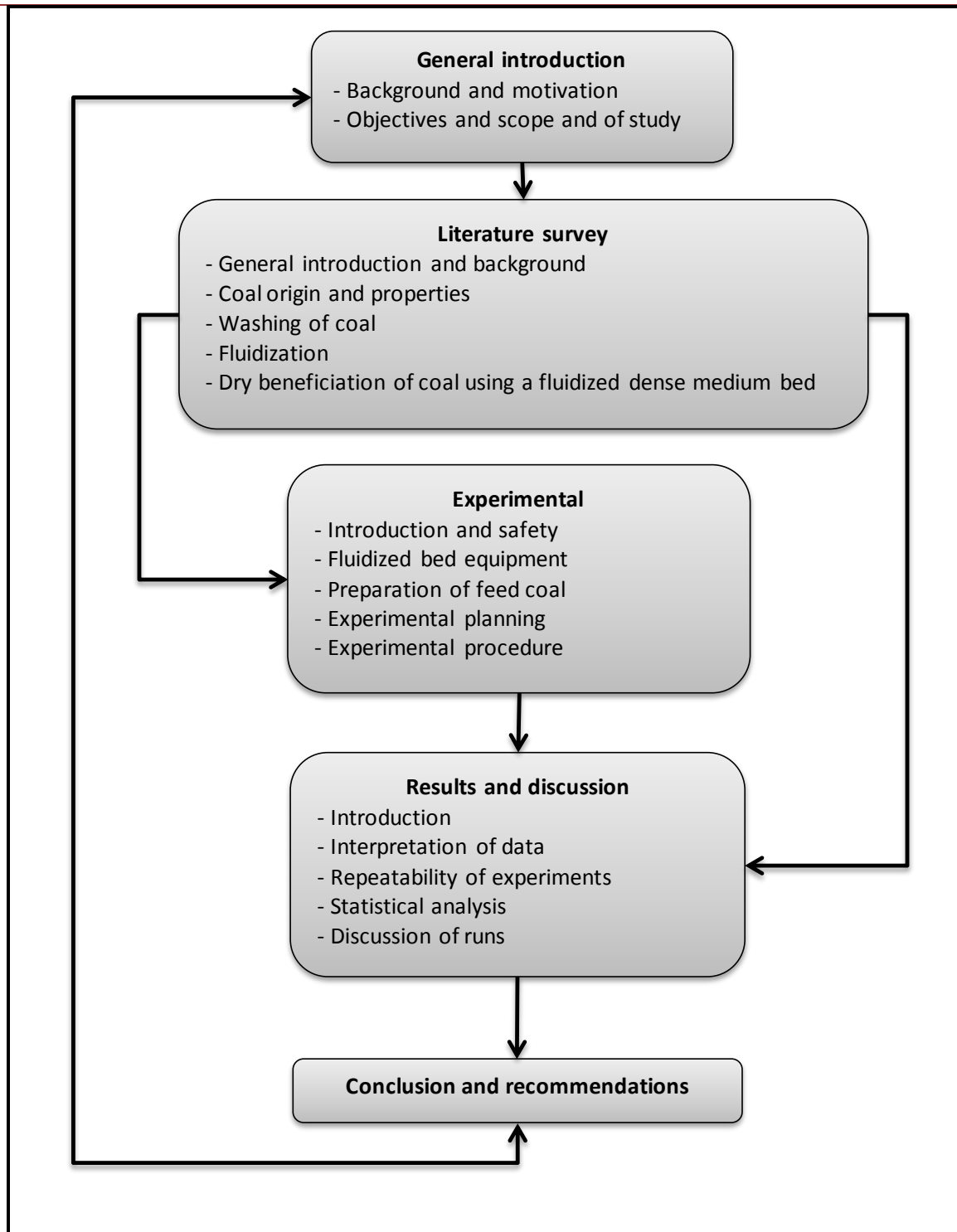


Figure 1-1: Scope of investigation

Chapter 2: Literature survey

In this chapter a literature survey is conducted on the beneficiation methods of coal. A comparison between wet and dry coal washing processes is discussed. Due to the scope of this study the dry beneficiation methods of cleaning coal is discussed and reviewed in detail. Finally the properties and classifications of a fluidized bed are presented.

2.1 Background

The coal industry currently uses primarily two beneficiation processes which can be classified as wet and dry methods. Wet beneficiation processes are utilized more frequently because of its sharp separation efficiency (Wei *et al.*, 2003). However, due to a shortage of process water in some regions around South Africa, China, Russia and Mongolia the need for an effective dry beneficiation method is becoming more appealing to coal producers. In countries such as Mongolia, temperatures could range from 35°C to -35°C in one day. The negative effect this has on coal production is sliming of the coal water mixture making handling of the slurry difficult. Therefore, conducting thorough research on methods which require no process water is imperative if coal production is to continue in these arid and/or cold areas (Chen & Yang, 2003).

2.2 Coal

2.2.1 Origin of coal

Coal originated about 200-300 million years ago and was formed by the decomposition of vegetative matter from dense forests and plants. The rotting vegetation formed thick beds of peat which over time was covered by sandstone, shale's and silts. As time progressed with increasing temperature and pressure the peat beds were altered, or *metamorphosed*, to create a sedimentary rock which is known as coal (Wills & Napier-Munn, 2006; England *et al.*, 2002). The Northern and Southern hemisphere coal seams differ in terms of initial temperature changes and basic plant composition. The Northern hemisphere coals were formed in hot humid coastal swamps whereas the Southern hemisphere coals underwent a cold increasing to warm temperature change due to the ice age (England *et al.*, 2002).

2.2.2 Properties of coal

The colour of coal varies from brown to black depending on the age and rank of the coal (Wills & Napier-Munn, 2006). Coal is capable to combust when exposed to oxygen which makes it one of the most important energy sources on earth. The chemical composition and properties of coal vary in accordance with the original plants it was derived from (Osborne, 1988). The rank of coal can be identified by the extent of alteration of the peat beds from which it was derived with less alteration indicating a lower ranking coal and vice versa (Wills & Napier-Munn, 2006, England *et al.*, 2002).

The specific gravity of coal depends on the rank, inherent moisture and percentage ash in the coal. It ranges from 1.2-1.8 g/cm³ and is a very important property on which many coal separation processes are based (Leonard & Hardinge, 1991). The density of coal is primarily the property on which coal is separated in modern coal beneficiation plants.

2.3 South African coal and market relations

In South Africa the principle coalfields are the Witbank-Middelburg, Northern KwaZulu-Natal, Ermelo, Free State and Waterberg coalfields (England *et al.*, 2002, Jeffrey, 2005). It was estimated that in the year 2000 there were about 51-55 billion tons of recoverable coal reserves left in South Africa of which at least 70% comes from the Witbank, Highveld and Waterberg coalfields (Jeffrey, 2005, Eberhard, 2012). Figure 2-1 presents a map of South Africa's coalfields. The areas on the map marked numbers 2 and 7 will be the main focus during experiments in this study as the coal used in the experiments come from these areas.

The coal reserves in South Africa consist of 96% bituminous coal mainly produced as steam coals. The seams containing these minerals are thick and close to the surface making extraction of the coal inexpensive. Half of the bituminous coal reserves are 4-6m thick and the ash percentage of the coal varies. The ash percentage can be as high as 65% in some seams in the Waterberg fields making the cleaning process crucial if the coal is to be exported (Eberhard, 2011).

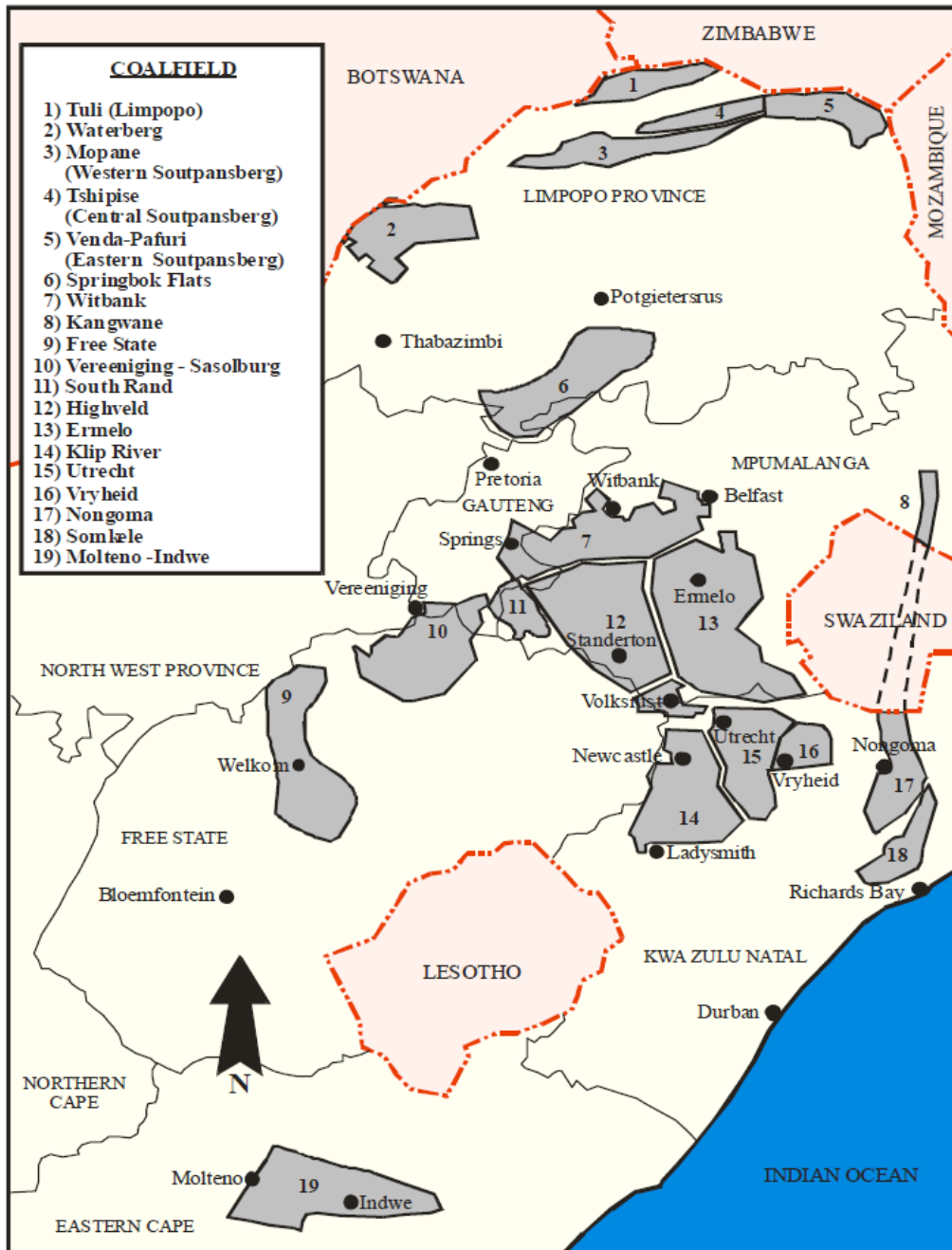


Figure 2-1: Coalfields in South Africa (taken from Eberhard, 2011:44)

South Africa is ranked 6th in the world as a coal producer with 247 million tons produced per annum. As a coal exporter, South Africa is ranked 5th and it exports 67 million tons per annum. The South African coal economy is noteworthy compared to the rest of the world due to the low production cost of coal. This together with the fact that South Africa is accessible for both Europe and the East for trading makes it evident that the coal market in South Africa is an important contributor to local GDP (Eberhard, 2011).

2.4 Sizing of coal particles

The particle size distribution of coal is an important factor to consider when selling on the market. Export coal normally has a nominal size of 50-0 mm (refer to Table 3-2). In recent years, as stated in the introduction, coal fines produced by modern mechanized mining methods increased substantially. Up to 15% of run-of-mine coal is in the -500 μm size fraction (England *et al.*, 2002).

Fine dry coal becomes an environmental problem due to dust pollution and wet coal/slurry on the other hand could cause transportation/handling problems (England *et al.*, 2002). Eberhard (2012) stated that about 60 million tons of coal is discarded every year putting the environmental impact mentioned above in perspective. These facts indicate that South Africa's current discard coal amounts to roughly 1 billion tons (Eberhard, 2012).

It is therefore evident that research on fine coal beneficiation is of utmost importance to reduce environmental problems concerning mainly water pollution.

2.5 Coal washing

Coal washing can also be referred to as ore dressing and/or mineral dressing (terms also used include: upgrading of coal, beneficiation of coal, cleaning of coal and separation of coal). Coal washing includes processes in which the valuable material (coal) is separated from the waste material (gangue, rocks, ash etc.) (Wills & Napier-Munn, 2006). Coal can be washed on both a dry and wet basis as mentioned above. The focus of this literature study will be primarily on the dry beneficiation of coal.

2.5.1 Wet beneficiation

In the current coal industry the most popular method used to wash coal is wet beneficiation. Lack of process water reserves is and will in future become an inevitable problem with wet cleaning methods (Zhao *et al.*, 2011). These methods use a considerable amount of water and in some regions of South Africa water is very scarce. Chen and Wei (2003) emphasized the severity of this problem by stating that to jig (wet jigging) one ton of coal, 3-5 tons of process water is required and fresh water needs to be added continuously during the jigging process. An advantage that is keeping wet beneficiation processes implemented to this day,

is the sharp separation efficiency achieved (Wei *et al.*, 2003). Wet beneficiation methods of treating fine coal include (England *et al.*, 2002):

- Spiral beneficiation,
- Froth flotation,
- Oil agglomeration,
- Wet jigging (Section 2.5.2),
- Wet dense medium beneficiation (DMS) ($E_p = 0.015-0.12$) (Chikerema & Moys, 2012).

Dense medium beneficiation will be discussed in detail in the following section. The latter method (DMS) can be utilized on a wet or dry basis of coal washing.

2.5.1.1 Dense medium separation (DMS)

Dense medium separation works on the principle that density different materials can be separated according to their respective densities. In principle, if the fluid medium/dense medium has a SG of 1.6 for example, materials with a higher SG will sink (called sinks) and materials with a lower SG will float (called floats) (Chen & Wei, 2005). The advantages of DMS include (Wills & Napier-Munn, 2006), (England *et al.*, 2002):

- A sharp separation at any required relative density can be achieved ($\pm 0.005\text{g/cm}^3$),
- The separating density can accurately be controlled,
- The cut density can be changed fairly quickly if required,
- The process is applicable to a wide variety of ores.

One major disadvantage of this technology, especially in wet beneficiation processes, is the expensiveness of the dense medium. All of the dense medium cannot be recovered after the process and it is therefore necessary to continuously add more medium, making this process expensive to operate (Wills & Napier-Munn, 2006).

2.5.2 Wet jigging

Jigging, as a gravity concentration process, is one of the oldest methods still used today (Wills & Napier-Munn, 2006). Jigging works on the same principle as a fluidized bed which states that particles are stratified according to their respective densities in a pulsating water

process. This is achieved by vertical water pulsations on the solid particles during the jigging process. Mukherjee *et al.*, (2009) stated that for a given frequency of pulsation, the stratification of the particles increased as the amplitude of the pulsation intensified. Although the amplitude of the pulse is very important, the frequency of the pulse cannot be ignored. In Figure 2-2 the working principle of the jigging process is illustrated.

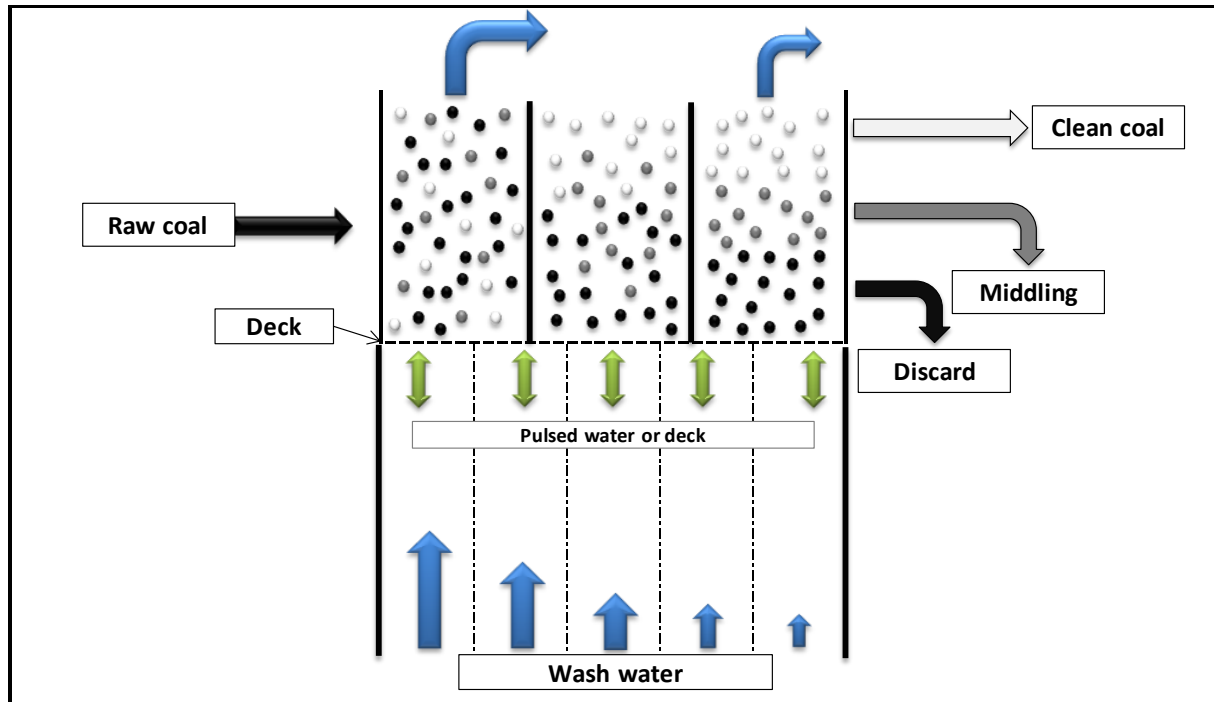


Figure 2-2: The working principle of a jigging process (adapted from England, 2002)

Figure 2-2 illustrates that raw coal enters the jigging process, thereafter wash water is pulsed through the particle bed causing the denser coal particles to drop to the bottom and the lighter coal particles to float to the top. When the material reaches the end of the process, the particle bed is cut in three different sections which constitutes the clean -, middling – and discard coals. Important to note is that good separation of coal can be achieved if the feed is fairly close sized (e.g. 3-10mm) (Wills & Napier-Munn, 2006). The aforementioned principle is also applicable to the fluidization process which works on a similar density separation as the jigging process.

The jigging process can also be utilized as a dry process implying that instead of pulsating water through the solid particles, air is used. Dry jigging of coal is discussed in Section 2.6.1.

2.6 Dry beneficiation

There are several methods of dry coal beneficiation which include hand picking, air jigging, magnetic separation, microwave separation, FDMB's and electrostatic separators. The coal particles are separated based on its physical properties such as density, magnetic conductivity, size, shape and radioactive properties (Chen & Yang, 2003, Kumar *et al.*, 2010). This project primarily focuses on beneficiation of dry fine coal using a dense medium fluidized bed (DMFB).

In Table 2-1 the cost comparison of different dry coal beneficiation processes is shown. It is evident from Table 2-1 that the DMFB separator is the most cost effective with regards to the production of thermal coal to power stations and compares well to other technologies in terms of technical specifications.

Table 2-1: Cost of dry coal beneficiation processes (taken from Sahu *et al.*, 2009)

Process	Product quality (Kcal/kg)	Yield (%)	Process operating cost (\$/t)	Cost delivered to power station (\$/Gcal)
Conventional	5947.11	84.2	1.79	1.94
Rare earth magnetic separator	6281.5	68.4	1.55	2.16
Air dense medium fluidized bed separator	6281.5	80.6	1.91	1.91
Electrostatic separator at mine	6639.75	59.9	5.01	2.65
Electrostatic separator at power station	6639.75	59.9	1.42	2.51
Air table	6281.5	71.4	1.78	2.12

The financial comparison was done on a per heat unit delivered to the power station. This factor also takes into account the reduced transportation costs due to lower moisture levels in the product coal (Sahu *et al.*, 2009). The fluidized bed therefore has an economic advantage over any other wet beneficiation process which is evident from Table 2-1. As mentioned before, although wet beneficiation processes are more costly than dry methods it is currently applied more often because of the sharpness in separation achieved with this

technology. When looking at the efficiency of a process, a widely used parameter is the Ecart Probable Moyen (Ep) value. This value is calculated using Equation 1.

$$E_p = \frac{\delta_{75} - \delta_{25}}{2}$$

Equation 1: Ecart probable Moyen equation

Where,

δ = relating partition coefficient density (g/cm³), (Yang *et al.*, 2012a).

Table 2-2 illustrates the comparison of Ep values produced by four different wet and dry coal cleaning technologies.

Table 2-2: Ep value comparison of the various coal washing processes (taken from Chikerema & Moys, 2012)

Various coal washing methods				
Method	Dry air fluidized bed	Air jig	FGX coal separator	Wet dense medium separation
Ecart Probable Moyen (Ep)	0.04–0.15	0.20–0.30	0.15–0.30	0.015–0.12

From Table 2-2 it is evident that the dry air fluidized bed has an Ep value that compares well to that of the other coal washing processes mentioned. By identifying that the separation efficiency of this dry coal beneficiation process is favourable, the need for research on this technology is emphasized.

2.6.1 Dry jigging

Dry jigging, also referred to as pneumatic jigging, is a coal particle separation process achieved by pulsating air through the particle bed as seen in Figure 2-2. This dry jigging method replaces the wash water in the Figure 2-2 with air.

According to Sampaio *et al.*, (2007) a bed of sunken product (denser particles) in the jig is formed, which acts as a barrier for the middling and lighter particles which reduces the chances of heavy particles reporting to the product stream (misplacement of particles). This phenomenon is significant due to the fact that it diminishes the displaced distribution effect

which is discussed in the following section. Moreover and with respect to the outcome of this study the problem is also common to the fluidization process.

Studies done by Sampaio *et al.*, (2007) indicate that coal with a high ash percentage can be upgraded by using a pneumatic jig. The results obtained concluded that the ash percentage of the coal was reduced by 4% and the sulphur content by 1.15%. It should be noted that the coal had an initial ash of 52%, indicating a low quality coal.

In another coal jigging study, done by Feil *et al.*, (2012), coal from the Barro Branco seam in Brazil was cleaned using a dry batch jig. Results indicated that when the coal was jigged at a specific frequency (88 min^{-1}) and pulsation, efficient separation was achieved. The coal was split into 5 layers during the jigging process, with the top layer having an ash percentage of 39.1% and the bottom layer 74.93% compared to a feed ash of 54.89% which in turn indicates good fairly separation.

Therefore subjecting the feed air of a fluidized bed to a jigging motion could possibly add to the separation efficiency of the process.

2.6.2 Fluidization

Fluidization can best be described as a process in which solid particles are transformed into a fluid-like state by suspending it in an upward flowing liquid/gas (Kunii & Levenspiel, 1991). Fluidization in the form of a FDMB is one of the DMS processes mentioned in Section 2.5.1.1.

In an industrial sense the fluidization process started with a bang in 1942 which was in the form of catalytic cracking. Since then fluidization has been widely researched by many scientists trying to understand this interesting phenomena. But due to unreliable extrapolating data, fluidized bed research was done only on a small scale (Kunii & Levenspiel, 1991).

2.6.3 The principle of fluidization

The fluidization process is based on the principle of Archimedes namely: any object either partially or fully immersed in a liquid is buoyed up by a force equal to the weight of the fluid

School of Chemical and Minerals Engineering

displaced by the object. That is, the particles more dense than the fluid/dense medium will sink to the bottom of the bed, and the lighter particles will float to the top (Luo & Chen, 2001).

Experimental results show that some misplaced light and heavy particles cannot be explained by the principle which Chen and Wei (2005) called the displaced distribution effect (Chen & Wei, 2005, Sahu *et al.*, 2009). There are variations to this effect which are known as the displaced movement effect and the displaced viscosity effect. The former increases with decreasing air flow while the latter is influenced when the feed air velocity either increases or decreases (Chen & Wei, 2005).

When studying fluidization, the falling sphere model is used to describe the rheological characteristics of the particles in the bed. Experimental results indicated that the particles in a fluidized bed behave similarly to a Bingham fluid. To obtain the plastic viscosity and yield stress, a linear regression of the measured terminal settling velocity can be used which was obtained experimentally. Both of the previously mentioned properties increase with increasing particle feed size (Chen & Wei, 2005). The forces that influence particles in a fluidized bed are (Sahu *et al.*, 2009):

- Gravity,
- Pressure,
- Frictional drag forces between the air and coal particles, the air and medium, and the medium and coal particles.

Figure 2-3 illustrates the forces acting on a solid particle in a fluidized bed.

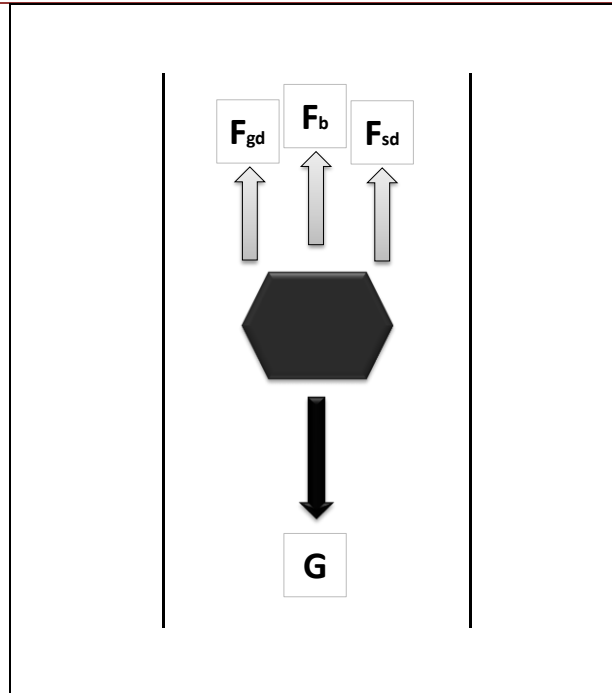


Figure 2-3: Forces acting on a particle during fluidization (adapted from Sahu *et al.*, 2009)

As seen in Figure 2-3, there are four primary forces acting on a coal particle in a fluidized bed. These forces include but are not limited to (Sahu *et al.*, 2009):

- Gravitational force of the particle (G),
- Friction drag force of the air acting on the particle (F_{gd}),
- Drag force of the air dense medium exerted on the particle (F_{sd}),
- Effective buoyancy force acting on the particle (F_b).

Since the diameter of the coal particle is much larger than that of the dense medium particles, the frictional drag force of the air on the coal particles (F_{gd}) can be neglected, therefore reducing the system to three primary forces acting on a particle during fluidization.

Particles in a fluidized bed act like a fluid when air flows upward between the particles, hence the name 'Fluidized Bed'. In Figure 2-4, the pseudo-fluid like properties of a fluidized bed is illustrated and explained in the subsequent paragraph.

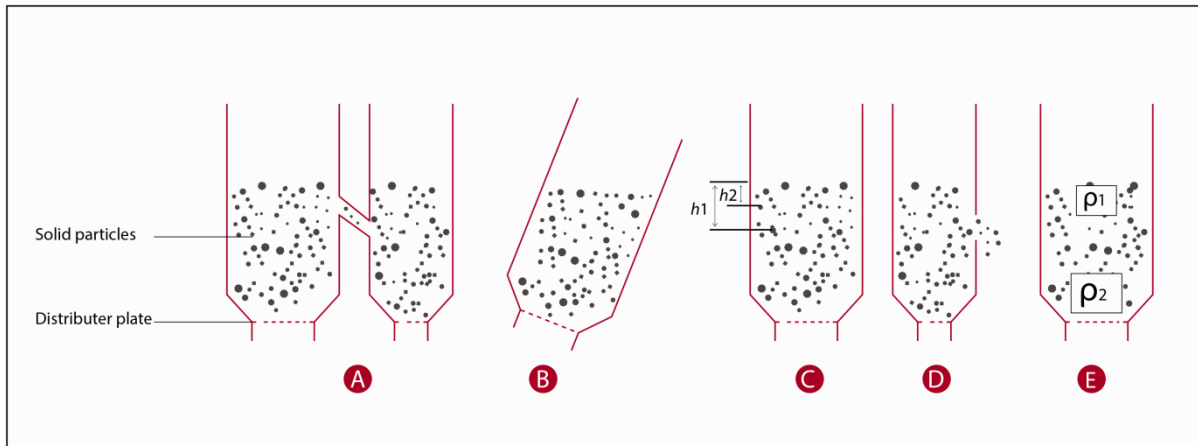


Figure 2-4: Fluid-like properties of particles in a fluidized bed (adapted from ZHAO *et al.*, 2011)

Figure 2-4 (a) shows that the upward flowing gas will fluidize particles in two connected chambers to the same height. If the vessel is inclined, the particle bed surface will still remain horizontal (b). In Figure 2-4 (c) the illustrated characteristic is that the pressure difference between two points in the bed is equal to the hydrostatic head of the bed. In (d) it is evident that should there be a hole in the wall of the bed the particles will spray out similar to a liquid. Lastly but most importantly, especially with regard to this project, less dense particles will float to the top of the bed and heavier/more dense particles will drop to the bottom of a fluid bed as shown in Figure 2-4 development (Luo & Chen, 2001).

Another important parameter to consider when separating fine coal in a fluidized bed is the gas velocity. The gas velocity must fall exactly in between the minimum fluidization and bubbling velocity to ensure effective separation. Therefore precision control needs to be implemented when conducting experiments (Luo *et al.*, 2002). In Section 2.6.4 the gas velocity (also known as the fluidization/minimum fluidization velocity) is discussed and the equation derived.

2.6.4 Minimum fluidization velocity

The hydrodynamics of a fluidized bed are very complex and need to be understood to improve the performance of this technology. It depends on the properties of the solids, distributor properties, factors that depend on the forces between particles and gas properties (Escudero & Heindel, 2011). It is also not uncommon for independent operating parameters of the fluidized beds to interact with each other. It is therefore important to understand the

School of Chemical and Minerals Engineering

interactions of the parameters with one another in order to better comprehend such a complex system (Mohanta *et al.*, 2013).

The fluidization velocity is proportional to the drag force needed to deliver a suspension of the solid particles (Escudero & Heindel, 2011). Studies done by Gupta *et al.*, (2009) indicate that there are seventy nine correlations that could possibly predict the minimum fluidization velocity needed for a particle bed to fluidize. The equation derived by Kunii and Levenspiel (1991) is widely used in research and industry.

Parameters affecting the minimum fluidization velocity of the gas are (Escudero & Heindel, 2011):

- Particle properties,
- Fluid properties,
- Bed geometry.

These parameters are important to consider when designing a fluidized bed. The extent of the effect on the minimum fluidization velocity can be directly correlated as seen in the derived equation.

The derivation of the minimum fluidization velocity equation requires that a uniform up flow of gas/liquid is assumed. This can be achieved by the installation of a well-designed distributor plate at the bottom of the fluidized bed. According to Kunni and Levenspiel (1991) minimum fluidization occurs when:

(drag force created by upward moving gas) = (weight of particles)

From which the equation can be written, with Δp always positive,

$$\Delta p_b A_t = W = A_t L_{mf} (1 - \varepsilon_{mf}) [(\rho_s - \rho_g) \frac{g}{g_c}]$$

Equation 2

By rearranging Equation 2 the minimum fluidization is achieved when,

School of Chemical and Minerals Engineering

$$\frac{\Delta p_b}{L_{mf}} = (1 - \varepsilon_{mf})(\rho_s - \rho_g) \frac{g}{g_c}$$

Equation 3

According to Kunii and Levenspiel (1991) the superficial velocity at this minimum fluidizing condition is given by,

$$\frac{1.75}{\varepsilon_{mf}^3 \varphi_s} \left(\frac{d_p u_{mf} \rho_g}{\mu} \right)^2 + \frac{150(1 - \varepsilon_{mf})}{\varepsilon_{mf}^3 \varphi_s^2} \left(\frac{d_p u_{mf} \rho_g}{\mu} \right) = \frac{d_p^3 \rho_g (\rho_s - \rho_g) g}{\mu^2}$$

Equation 4

Rearranging delivers,

$$\frac{1.75}{\varepsilon_{mf}^3 \varphi_s} Re_{p,mf}^2 + \frac{150(1 - \varepsilon_{mf})}{\varepsilon_{mf}^3 \varphi_s^2} Re_{p,mf} = Ar$$

Equation 5

Where the Reynolds number is given by Equation 6,

$$Re_{p,mf} = \frac{d_p u_{mf} \rho_g}{\mu}$$

Equation 6

And the Archimedes number is written as,

$$Ar = \frac{d_p^3 \rho_g (\rho_s - \rho_g) g}{\mu^2}$$

Equation 7

Therefore it can be simplified that the minimum fluidization gas velocity for small particles is as given by (Kunii & Levenspiel, 1991):

$$u_{mf} = \frac{d_p^2 ((\rho_s - \rho_g) g \varepsilon_{mf}^3 \varphi_s^2)}{150 \mu (1 - \varepsilon_{mf})} \quad Re_{p,mf} < 20$$

Equation 8: Minimum fluidization velocity equation

Where,

School of Chemical and Minerals Engineering

u_{mf} = minimum fluidization velocity (m/s),

d_p = particle diameter (m),

ρ_s = density of the particles (kg/cm³),

ρ_g = density of the gas (kg/cm³),

g = gravity acceleration constant (m/s²),

ϵ_{mf} = voidage between particles,

ϕ_s = sphericity of the particles (perfect round spheres = 1),

μ = viscosity of the gas/fluid (Pa s).

Equation 8 also known as the Ergun equation indicates that if the particle size (d_p) increases, the minimum fluidization velocity increases quadratic. Similarly, if the voidage (ϵ_{mf}) between particles is increased the minimum fluidization velocity will also increase. This is significant as the experimental plan had to be altered due to minimum fluidization restrictions encountered during experiments. When considering the density of the particles an observation was made that when the density increases, the minimum fluidization velocity also increases proportionally which is also indicated by Equation 8.

Sahu *et al.*, (2009) emphasized the importance of correctly choosing the exact fluidization velocity. Not only will inefficient separation occur, the misplacing effect of both viscosity and motion will be intensified when the bed is operated at the incorrect velocity. The precise minimum fluidization velocity of a specific coal sample is therefore of utmost importance to choose and correctly implement to ensure successful operation of the fluidized bed technology.

2.6.5 Pressure and velocity relations in a fluidized bed

It is not always possible to visibly observe the degree of fluidization in a fluidized bed however to determine an estimation of the degree of fluidization, a pressure vs. gas velocity (ΔP -vs- u_0) diagram can be constructed. Figure 2-5 depicts a graph an ideal fluidization scenario. The particles used to construct this graph are uniformly sized and the curve up to point A is a straight line relating to a Pressure vs. Velocity ratio of 1:1.

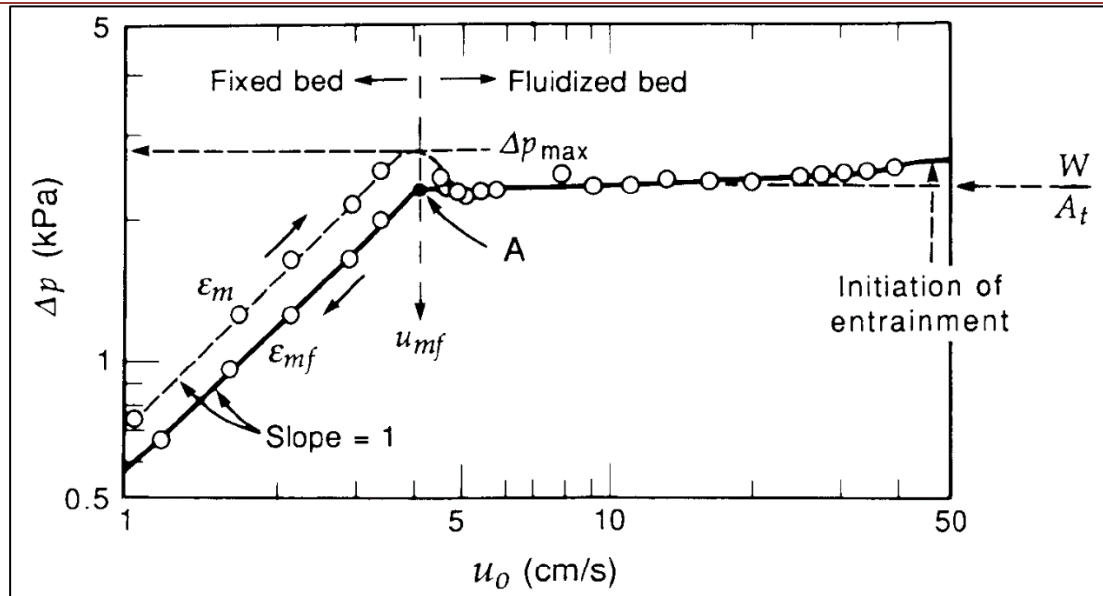


Figure 2-5: Pressure vs. velocity diagram of uniformly sized sand particles (taken from Kunii & Levenspiel, 1991)

As seen in Figure 2-5 the data line reaches a point Δp_{\max} where the bed pressure is slightly higher than the static pressure of the bed. This point is also called the minimum fluidization point. If the gas velocity is increased slightly, bubbles will start to form and the bed of particles will transform from a static bed into a fluidized bed (Kunii & Levenspiel, 1991).

Effective and complete fluidization occurs at the minimum fluidization point. It is therefore practical to choose the fluidization velocity slightly higher than the minimum fluidization value to ensure complete fluidization.

Important to the conclusion of the degree of fluidization is to evaluate the bubbles within the particle bed. The bubbles have a direct relation to the velocity at which the bed is fluidized. Moreover, the effect of the bubbles on fluidization has a dual character with advantages that include (Luo *et al.*, 2012):

- The bubbles passing through the material bed shock the bed, causing the particles to loosen allowing better separation and a higher capacity within the bed,
- Particles remix due to the bubbles formed.

The latter point could be seen as a disadvantage of the bubbling effect. But because a more uniform bed density is formed by this effect, better separation of the particles after the mixing can be expected. A uniform bed density is a requirement for complete fluidization as

mentioned in Section 2.7 (Chen & Wei, 2005). This fact makes mixing bubbles an advantage due to the creation of a uniform bed density.

Large bubbles have the following disadvantages on fluidization:

- Fine high quality coal particles are caught in bursting bubbles and are misplaced to the tailings section. The misplaced distribution effect discussed in Section 2.6.3 is the aforementioned result of the large bubbles,
- The large bubbles shock the bed to an extent that the height and heterogeneity of the bed fluctuates over time, causing insufficient separation due to inconsistency.

2.6.6 Classification of particles in a fluidized bed

The particle properties are very important parameters when implementing fluidization (Escudero & Heindel, 2011). Geldart carefully observed the behaviour of different particles in a fluidized bed (Kunii & Levenspiel, 1991). Four different types of particles were clearly identified and sorted into groups: Group A, B, C and D particles. The four groups are briefly explained (Kunii & Levenspiel, 1991):

Group A: This group consists of particles with a density lower than 1.4 g/cm^3 and has a small mean particle size. These particles will fluidize easily and form controllable bubbles at low gas velocities.

Group B: The particle size in this group ranges from $40 - 500 \mu\text{m}$. The density ranges from $1.4 - 4 \text{ g/cm}^3$ and will fluidize with vigorous bubbling present. As the bed height increases, the bubble size also increases.

Group C: This particle group includes very fine powders. It is very difficult to fluidize these particles because the gas/fluid force on the particles is weaker than the forces between each particle making fluidization almost impossible.

Group D: Group D consists of large and or very dense particles making fluidization very difficult due to large exploding bubbles. Because of the high density of the particles, severe channelling and back mixing occur.

The coal used in this project belongs primarily to Group A of the particle types mentioned. Therefore the coal should fluidize efficiently. However, adding magnetite which is a fine

powder could cause problems during experiments. The magnetite used throughout this study forms part of the group B particles mentioned. Therefore vigorous bubbling can be expected when fluidizing fine magnetite.

2.7 Dry beneficiation of coal using a fluidized bed

The first known account of coal beneficiation using a fluidized bed was in 1926. A paper was published and a patent issued by Yancey and Fraser on the process of using river sand with a bulk density of 1.45 g/cm³ to clean coal (50 – 10 mm) (Mohanta *et al.*, 2013; Houwelingen & de Jong, 2004). However the separation performance was never tested for this process on a pilot or industrial scale.

Later dry beneficiation of coal was introduced on a dry density based separation using only gas-solid fluidized beds (Zhao *et al.*, 2011). The dry beneficiation of coal using a fluidized bed was tested by numerous researchers and on coal ranging from 50 – 6 mm. The density separation was successful, achieving an E_p value of 0.05 (Luo *et al.*, 2003; Wei *et al.*, 2003; Luo & Chen, 2001). The first dry coal beneficiation plant in China was established by the China University of Mining and Technology (CUMT) with an annual output of 320 000 tons and a similar E_p value of 0.05 (Chen & Wei, 2005).

Further research by the CUMT on the entire size range of coal (300 – 0 mm) lead to the following results regarding dry coal beneficiation processes:

- **Vibrated air-dense medium fluidized bed**

An E_p value of 0.065 was achieved with a yield of 80.20%. In the process the ash percentage was reduced from 16.57% to 8.35%.

- **Dual-density fluidized bed for three-product beneficiation**

Three products are yielded by this technology: clean, middling and discard coals. The upper layer has a density of ± 1.52 g/cm³ and the lower layer ± 1.87 g/cm³.

- **Triboelectric cleaning technology of pulverized coal (< 1 mm)**

This technology yielded ultra- low ash coal (< 2%) in experiments with a coal size of 43 μm .

- **Deep air-dense medium fluidized bed (> 50 mm)**

An E_p value of 0.02 was achieved with this technology with coal in the 300 – 50 mm size range.

School of Chemical and Minerals Engineering

For coal to successfully separate according to density in a fluidized bed, micro bubbles and stable dispersion fluidization must occur. Also, the three dimensional bed densities have to be stable over time and the bed has to have a low viscosity and high fluidity (Chen & Yang, 2003; Chen & Wei, 2005).

According to Chen and Yang (2003) fluidization of dry coal has the following advantages (Chen & Yang, 2003; Luo & Chen, 2001):

- **High precision:** Coal with a size range of 50 – 6 mm can effectively be separated with E_p values of 0.05-0.07. This value compares favourably with the existing heavy medium wet beneficiation.
- **Low investment:** The same capacity dry beneficiation plant can be constructed for half the costs compared to a wet beneficiation plant mainly due to the fact that no complicated and costly slurry treatment is needed when handling dry coal.
- **No environmental pollution:** This technology only requires low pressure compressed air. It also operates smoothly with very little noise pollution and the dust emitted by the equipment is within environmental laws.
- **Wide ranges of beneficiating densities:** Beneficiating densities ranging from 1.3 to 2.2 g/cm³ can be created by adding magnetite powder to the bed. Therefore this technology can either remove heavy gangues or lower density clean coal depending on the required product.

Another advantage of this technology according to Luo *et al.*, (2008) is that no moisture penalties are given due to the dry beneficiation. Although there are many advantages to the fluidized bed technology, it has some draw backs which include (Sahu *et al.*, 2009):

- If the moisture content of the run of mine (ROM) coal is too high, inefficient separation of the coal occurs due to a reduction of fluidity within the bed (also observed in experiments done by Terblanche (2011),
- The air-feed is required to be moisture free,
- The consumption rate of the medium is high,
- During fluidization fine coal is generated which affects the overall separation density of the bed,
- As the feed coal particle size increases, the separation performance of the fluidized bed decreases (Mohanta *et al.*, 2011).

If the fluidized bed is operated at the correct parameter values these pitfalls could be overcome.

2.7.1 Magnetically stabilized fluidized beds

In this type of fluidized bed magnetic materials such as magnetite, vanadic titanomagnetite, and paigeite are added to the bed and a magnetic field is induced around the bed hence the term magnetically stabilized. Magnetically stabilized fluidized beds are especially effective when separating dry fine (6 -1 mm) coal (Maoming *et al.*, 2003). Because of the high lower size limit of the 6 mm coal, vigorous bubbling can occur and this can be suppressed by introducing a dense media such as magnetite to the bed (Fan *et al.*, 2001).

Another advantage of adding a magnetic dense media to the bed is the prevention of back mixing of the solid particles. However, the key to success with this technology is that the particles size of the dense media must be significantly smaller than the coal particles size. This is due to the fact that if the cohesive forces between the small particles are too strong, it can cause fluidization to fail (Luo *et al.*, 2002; Zhao *et al.*, 2010c).

Experiments done by Zhao *et al.*, (2010b) indicated that hard to wash coal (13 – 6 mm) can be effectively recovered by adding paigeite powder to the bed. During the experiments the ash percentage of the feed coal was reduced from 22.37% to 9.88% for the product and discard coals respectively at a separation density of 1.5 g/cm³ with a resulting E_p value of 0.075 g/cm³ (Zhao *et al.*, 2010b).

2.7.2 Vibrated gas-fluidized bed

The segregation of coal particles in this type of fluidized bed is mainly caused by the bubbles. As the bubbles rise through the bed, an area behind the bubble with a lower solid volume is created. It is in this region where the higher density particles have the possibility of 'overtaking' the lighter particles in the downward direction. This is also similar to the separation technique utilized by bubble-driven jigging (Yang *et al.*, 2012b). Another advantage of the vibrating fluidized bed is the increase in the gas-solid interaction creating a better dispersed fluidized bed.

Moreover, the problem of aperture blinding is completely eliminated by a vibrated fluidized bed. The particles at the bottom of the bed do not 'settle' into an aperture hole as a result of

School of Chemical and Minerals Engineering

the vibrating movement. This effect also reduces channelling of the air through selective pathways within the bed (Maoming *et al.*, 2003).

Equation 9 illustrates the proposed critical vibration frequency equation. If the correct frequency can be calculated and implemented, the bubbles should burst and transform into many micro bubbles which in turn creates a more stable fluidized bed. The optimal frequency is given by (Dwari & Rao, 2007)

$$f = \left(\frac{6Q}{\pi}\right)^{-1/5} g^{3/5}$$

Equation 9: Critical vibration frequency

Where,

f = critical vibration frequency (Hertz),

Q = air flow (m³/s),

g = gravity acceleration constant (m/s²).

Studies done by Yang *et al.*, (2012b) on fine coal indicate that coal (-3 +1 mm) can be successfully beneficiated with a vibrated gas-fluidized bed having an Ep value of 0.175. Coal with a size smaller than 6 mm even down to 125µm can also be successfully separated with this fluidization method. Moreover, results obtained on a laboratory apparatus showed coal (6 – 0.5 mm) with a feed ash of 16,57% was cleaned to 8.35% ash with yields of up to 80.2% (Dwari & Rao, 2007).

In conclusion this project will include experiments on a constructed FDMB (**150 mm ID**). Coal ranging from **-2000 + 500µm** will be tested. Magnetite will be added to the bed according to a ratio recommended by Mohanta *et al.*, (2013) which is a coal to magnetite ratio of 0.7. And finally a jiggling motion of the air feed will be introduced as literature indicates a possible separation efficiency increase (Feil *et al.*, 2011; Sampaio *et al.*, 2007).

Chapter 3: Experimental

During any research project the correct experimental setup is of utmost importance to ensure accurate useful results. This was achieved by carefully considering the coal used during experiments, the design and construction of equipment as well as the experimental planning and methodology. One major aspect in any project especially related to industry size projects and work is safety. This chapter is devoted to these aspects of the study.

3.1 Safety in the lab

Good and safe housekeeping in the laboratory was essential to conduct safe and successful experiments.

3.2 Equipment

3.2.1 Fluidized bed

In any project, the correct experimental setup is of utmost importance. This type of cylindrical laboratory scale fluidized bed has not yet been implemented on an industrial scale. Therefore, to simulate industry standards on a smaller scale, a 150mm fluidized bed was designed and constructed. The 150 mm fluidized bed is an upscale from the 80mm fluidized bed used in similar experiments by Terblanche (2011) and Roux (2012) at the North-West University. By increasing the diameter of the cylindrical bed, an indication of the efficiency of the fluidized bed to separate fine coal could be determined more accurately.

During the design of the fluidized bed, research on fluidized bed scale-up factors had to be considered. The bubble size and bubble rising velocity are amongst the most important factors to consider. These depend strongly on the equipment scale. Slugging of the rising bubbles could occur during fluidization which significantly affects the fluidization performance. Some of the pitfalls associated with incorrect fluidized bed design factors include (Rüdisüli *et al.*, 2011):

- Channelling of the gas due to incorrect feed PSD and an inefficient distributor plate,
- Fluidization efficiency due to gas pathways and particle agglomeration,
- Excessively large bubbles causing back mixing of particles,

School of Chemical and Minerals Engineering

- Elutriation of the particles in the bed due to high air velocities and the attrition of coarse particles causing smaller particles increase.

The main problem with the fluidized bed up-scaling was the interdependence of important operation parameters. When one parameter changes (e.g. gas velocity) another parameter (e.g. bed diameter) does not always change accordingly. Moreover, due to the fact that fluidized beds do not always operate at the same regimes (bubbling, circulating etc.) and have different feed particle types, there are no uniform scaling factors to follow (Rüdisüli *et al.*, 2011).

Therefore the existing fluidized bed (**80mm**) at the North-West University was used as a reference to build the new fluidized bed (**150mm**). In Figure 3-1 the flow diagram of the fluidized bed is illustrated.

The air supply to the fluidized bed was provided by a laboratory compressor line. A sufficient pressure drop was needed to fluidize the coal particles. The laboratory compressor produced enough pressure and air-flow to achieve that. The flow of air through the system started at the compressor line, from there the air flowed through a low and then high air-flow meter, after which the air continued through the distributor plate which evenly distributed the air through a particle bed. The air then flowed through the bed of particles as indicated, where the coal particles was separated according to density. At the top of the bed was a 212 μ m sieve to prevent the coal from becoming airborne.

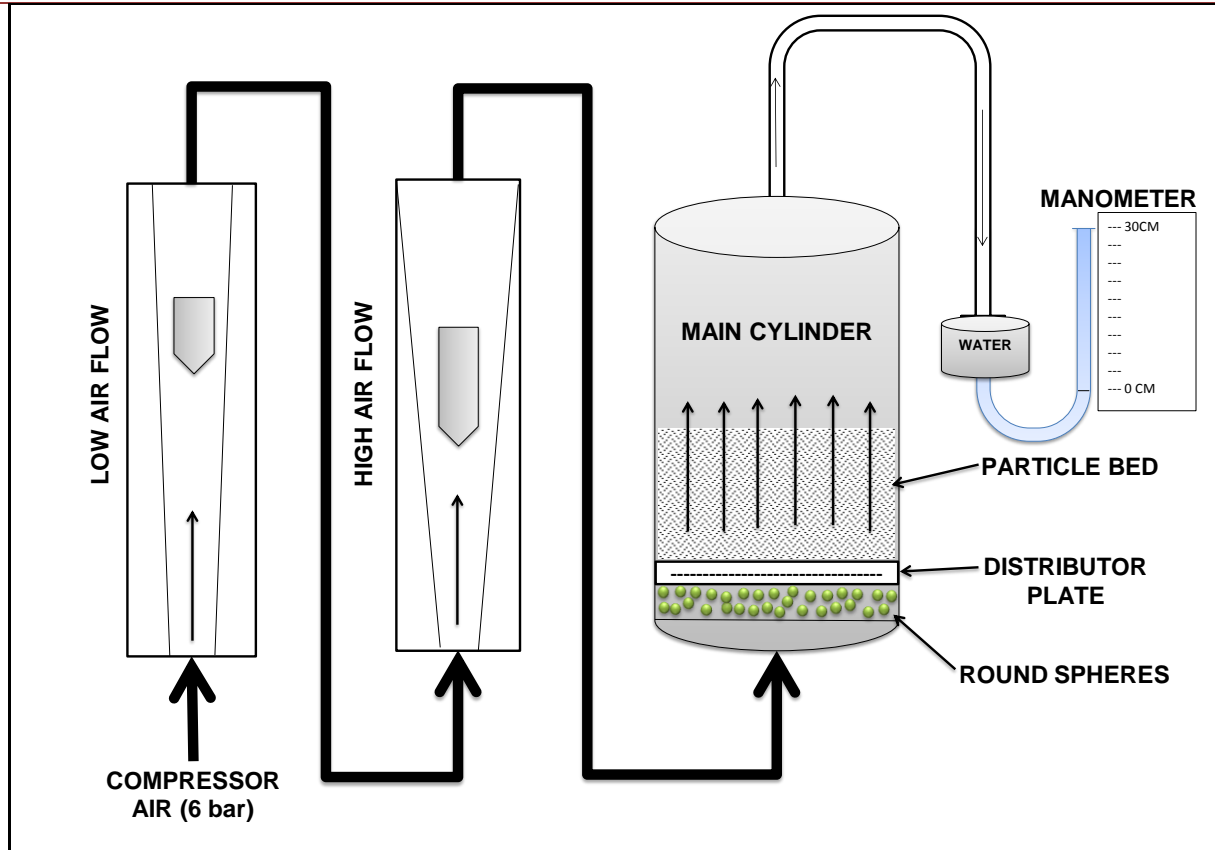


Figure 3-1: Schematic presentation of the fluidized bed flow diagram

A pressure probe was attached to the top of the bed to measure the pressure drop within the particle bed. The pressure was measured by an attached water based manometer as seen in Figure 3-1. The mentioned pressure probe is illustrated in Figure 3-2.



Figure 3-2: Pressure probe marked for each bed height

School of Chemical and Minerals Engineering

The markings on the probe indicated where pressure readings were taken as the particle bed obscures visibility of the probe when submerged.

The air control and measurement system consisted of two (high and low air flow) variable area air flow meters as seen in Figure 3-3. Also indicated by the white arrows are the regulator valves used to precisely control the air feed to the system. It is of utmost importance to control the air feed with precision if successful separation of the coal is to be achieved as mentioned in Section 2.6.5.

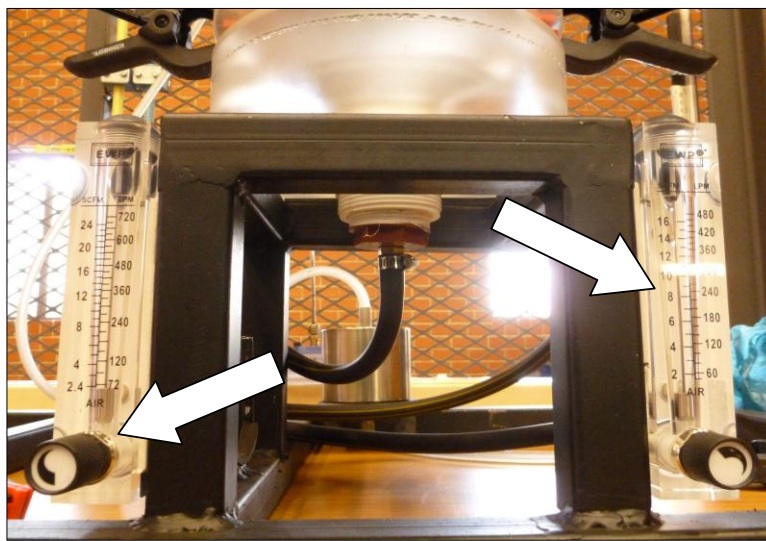


Figure 3-3: Variable area flow meters (air) with regulator valves

The main cylinder of the bed consisted of 8 removable Perspex sections. This specific configuration was designed according to recommendations made by Terblanche (2011) and Roux (2012) in order to ease sample cutting.

It was very important to evenly distribute the air through the particle bed to prevent channelling of the air through selective pathways in the bed. To accomplish this, an air distributor mechanism was constructed by placing round spheres (marbles) at the bottom of the bed. As seen in Figure 3-1, the air passed between the spheres and evenly flowed through the system without inducing a remarkable pressure drop.



Figure 3-4: Air distributor system

In this particular case marbles were used as illustrated in Figure 3-4. Also seen in Figure 3-4 is a filter cloth and perforated plate configuration constructed to prevent solid particles from falling into the air feed line. Even air distribution was achieved with this setup during experimentation.

In Figure 3-5 the constructed **150 mm** fluidized bed can be seen. Non-magnetic material was used during construction of the equipment as not to disturb the magnetic field of the fluidized bed. This could have posed a problem when using magnetite during experiments. The blue pipe on the left hand side of Figure 3-5 is the laboratory compressor supply line used to supply the bed with compressed air. As seen in Figure 3-5, the equipment was designed and constructed as simply as possible.



Figure 3-5: Fluidized bed equipment (150mm)

School of Chemical and Minerals Engineering

Figure 3-5 also illustrates that the cylinder sections were kept together with plastic clamps. This configuration was designed to ease sample cutting and increase experimental accuracy. Terblanche (2011) found that when the coal was extracted from the bed using a vacuum cleaner device, sample spillage occurred and experimental inaccuracy was the consequence. Therefore by removing the sections separately as discussed in Section 3.7, precise and accurate sample cutting was achieved with no loss of coal sample due to spillage. Figure 3-6 illustrates the sample cutting tool. A thin sheet metal plate was constructed and used to cut the coal samples in clear sections.



Figure 3-6: Sample cutting tool

An illustration of the clear and precise cut achieved can be seen in Figure 3-6 (also refer to video on attached DVD: **Sample cut demonstration**). After fluidization with the addition of magnetite to the feed, the coal and magnetite had to be separated. A 300 μ m sieve was used to firstly separate the coal and magnetite according to particle size (due to a large difference in particle size of the coal and magnetite) after which the remaining magnetite was removed using a hand magnet in a plastic bag as seen in Figure 3-7.



Figure 3-7: Magnetite – coal separation equipment (hand magnet in bag and 300 μ m sieve)

The difference in density of coal and magnetite particles was substantial. Therefore it was of utmost importance to remove all of the magnetite from the coal in order to not interfere with the density analysis.

Refer to the attached DVD for photos and videos of the experimental equipment used during this study.

3.3 Feed material

According to Eberhard (2012) South Africa has an estimated 55 billion tons of coal reserves still recoverable which are mainly found in the Witbank, Highveld and Waterberg coalfields (Jeffrey, 2005; Eberhard, 2012). Extensive research is being conducted on the Waterberg coalfields based on recent exploration efforts moreover this area is becoming the centre of coal mining in South Africa. Water constraints are currently one of the major setbacks for the washing of Waterberg coals (Eberhard, 2011).

Conducting experimental research on coal from these coalfields could benefit the entire coal community. This relates particularly to future studies and cleaning process designs. Due to the vast reserves still extractable from these coalfields important conclusions and maybe future industrial fluidized bed designs could be considered.

Coal from the Witbank and Waterberg fields were taken and tested to determine the separation efficiency of this fluidized bed. Spiral and filter feed coal from the Witbank area was used during experiments as well as a Waterberg run-of-mine coal. Export grade coal generally requires washing however achieving this with a dry process like a fluidized bed could be very beneficial to the stakeholders involved.

After the samples were received from the various sources, the coal had to be prepared for experiments, which included, drying and sizing.

3.4 Coal sample preparation

About 25kg of coal sample (per coalfield) was received with $\pm 20\%$ total moisture in the Witbank coal and $\pm 4\%$ contained in the already air dried Waterberg coal. For the samples to be successfully fluidized, the total moisture had to be $\pm 5\%$ (Terblanche, 2011). For the Witbank coal to reach this moisture level the sample was spread open and air dried for

School of Chemical and Minerals Engineering

approximately a week to drive off any excess moisture. Afterwards the coal samples were split into three and placed in buckets. The samples were then stored in a humidity controlled room to use as is during experiments.

Before commencing with experiments, three representative cuts were taken of each coalfield and analyses on the raw coal was done. These pre-tests included:

1. Proximate analysis (Ash, moisture, volatiles),
2. Calorific value (CV) test,
3. Washability test,
4. Particle size analysis.

The pre-tests were very important as a conclusion could be drawn if the coal was upgraded or not after the fluidization process. Three different coal samples were taken and used in this project as mentioned in the feed coal section. These samples are:

- 1) Witbank FF (filter feed: has been cleaned by a spiral process),
- 2) Witbank SF (spiral feed: has not been cleaned by the spiral process),
- 3) Waterberg (bright coal: run of mine coal).

The Witbank FF coal was only used to test the validity of the equipment, after which the other two samples were extensively tested in experiments. The reason behind using a spiral product was to study the de-ashing capabilities of the setup. It was envisaged that this process could lower the ash percentage of a spiral product.



Figure 3-8: Spiral feed coal sample

In Figure 3-8 the spiral feed sample during the air drying process is illustrated. When looking closely at the sample, small stones and impurities could be seen. This was an interesting observation as fluidization is also a de-stoning process which will be indicated and discussed in Section 4. The results of the pre-experimental coal tests can be seen in Section 4.

Sizing of the coal samples included, crushing the samples to – 2000 μm where after the samples were split into -1180 + 500 μm and -2000 + 1180 μm fractions.

3.5 Analyses of the coal

The coal samples were analysed by the **ALS Laboratory Group (ALS Witbank – Coal Division)** according to the ISO standards as noted in Table 3-1. ALS lab is an accredited laboratory and all of the analyses discussed in this project can be considered credible according to industry standards. Table 3-1 contains the analyses standards followed by ALS labs.

Table 3-1: Analyses standards

Test	Units	Standard
Total moisture	%	ISO 11722: 1995
Ash	%	ISO 1171:1997
Volatile matter	%	ISO 562: 2010
Fixed carbon	%	By difference
Calorific value	MJ/kg	ISO 1928: 2009
Washability analyses	-	ISO 7936:1992

If a conclusion on the degree of success of the equipment is to be given, a comparison to industry standard coal must be drawn against the fluidization coal product. In Table 3-2 and Table 3-3, the specifications on South African domestic and export coals are illustrated as well as the domestic coal grade specifications.

School of Chemical and Minerals Engineering

Table 3-2: South Africa's domestic and export coal specifications (adapted from Steyn & Minnitt, 2010)

Parameter	Units	Domestic	Export
Total moisture	% (AR)	8–12	8–12
Ash	% (AR)	15–21	15
Volatile matter	% (AR)	23–30	22-20
Calorific value	MJ/kg	24.5–27.5	27.5
Sizing	mm	0 x 6 6 x 25 25 x 40	0 x 50

Table 3-3: Thermal coal grade specifications in South Africa (adapted from Steyn & Minnitt, 2010)

Parameter	Units	A grade	B grade	C grade	D grade
Total moisture	% (AR)	12	12	8	8
Ash	% (AR)	15	16	18	21
Volatile matter	% (AR)	24	23	23	23
Calorific value	MJ/kg	> 27.5	> 26.5	> 25.5	> 24.5

The results obtained from ALS labs will be compared to the above figures throughout Section 4.

3.6 Experimental planning

During this project a pre-determined experimental plan was followed. The experimental plan can be seen in Table 3-4. The expected experiments had to be altered due to equipment restrictions which will be discussed in Section 4.

Table 3-4: Experimental plan

Waterberg & Witbank Coal				
Experimental Plan 2013				
Run	PSD range (µm)	Jigging effect	Magnetite (Vol % in feed)	Coal Sample
1	-1000 + 500	no	0	Witbank seam 4 (Filter feed)
2 (***)	-1180 + 500	no	0	Witbank seam 4 (Spiral feed)
3 (**)	-1180 + 500	yes	0	Witbank seam 4 (Spiral feed)
4	-1180 + 500	no	60	Witbank seam 4 (Spiral feed)
5	-1180 + 500	yes	60	Witbank seam 4 (Spiral feed)
6	-1180 + 500	no	0	Waterberg (Bright coal)
7	-1180 + 500	yes	0	Waterberg (Bright coal)
8 (**)	-1180 + 500	no	60	Waterberg (Bright coal)
9 (**)	-1180 + 500	yes	60	Waterberg (Bright coal)
10	-2000 + 1180(50%) + -1180 + 500(50%)	yes	0	Waterberg (Bright coal)
11	-2000 + 1180(25%) + -1180 + 500(75%)	no	0	Waterberg (Bright coal)
12	-2000 + 1180(25%) + -1180 + 500(75%)	yes	0	Waterberg (Bright coal)
13	-2000 + 1180	no	60	Waterberg (Bright coal)
14	-2000 + 1180	yes	60	Waterberg (Bright coal)
15	-2000 + 1180(25%) + -1180 + 500(75%)	no	60	Waterberg (Bright coal)
16	-2000 + 1180(25%) + -1180 + 500(75%)	yes	60	Waterberg (Bright coal)

*Repeated tests

The experimental plan included four different experimental scenarios. This was done to prove the validity of the fluidized bed equipment as well as its ability to upgrade fine coal.

The four scenarios include:

- Normal fluidization,
- Jigging/pulsed air flow fluidization,
- Magnetite fluidization,
- Magnetite and jigging fluidization.

3.7 Experimental procedure

Before any tests were done, a representative sample of each coal was extracted and pre-tests were done as discussed. The complete fluidization experiment is noted in bullet form:

- Approximately 2kg of coal sample was weighed and the sample was inserted into the open fluidized bed cylinder. If magnetite was added in the specific run, the desired feed volume ratio was first added to the bottom of the bed and then the coal was added on top of the magnetite layer.

School of Chemical and Minerals Engineering

- The regulator valve was opened until vigorous mixing of the particles occurred. This was to loosen the bed in order to create a uniform density before fluidization commenced (refer to Section 2.6.5).
- The tabular pressure probe was dropped to the bottom of the bed just above (1cm) the distributor plate.
- The air-flow was increased in increments of 20 or 30 L/min until a drop in pressure was noted (both the air-flow and pressure readings were recorded for each increment). This indicated that the minimum fluidization velocity had been reached and that the air-flow needed to be adjusted precisely to that specific velocity to ensure successful fluidization as discussed in Section 2.6.5.
- The tabular probe was pulled out in increments of 40mm as seen in Figure 3-2 whilst running at the desired air-flow. The pressure reading for each increment was recorded.
- The coal or coal-magnetite mixture was fluidized for approximately 10 minutes and closely observed (visually) to see how the bubbles were reacting, forming and bursting. When the bubbles were too big, back mixing of the particles occurred which decreased the separation efficiency of the coal. When the bubbles were too small, no separation occurred. It was therefore of utmost importance to regulate the air-flow consistently during fluidization.
- The bed was then cut into sections by removing the clamps and using the cutting tool as seen in Figure 3-6. Five (coal only) or four (coal and magnetite) cuts were made when the amount of coal/magnetite was added as indicated.
- The magnetite and coal was split using firstly a 300 μ m sieve (particle size difference between coal and magnetite) and then a hand magnet for the remaining magnetite as seen in Figure 3-7. (Note: It was important to separate almost all of the magnetite from the coal as to not interfere with the density analysis later in the experiment.)
- Each cut was split into a smaller representative sample for analysis by using a sample splitter. The average weight of the representative sample was \pm 60g of coal. (Refer to video: **Sample splitter** on the attached DVD)

On each of these layers the following coal properties were analysed:

- 1) Ash percentage (%)
- 2) Moisture content (%)

School of Chemical and Minerals Engineering

- 3) Volatile matter (%),
- 4) Fixed carbon (% by difference),
- 5) CV (MJ/kg),
- 6) True relative density (g/cm^3),
- 7) Particle size distribution (μm),

A detailed discussion of the results obtained follows in Section 4.

Chapter 4: Results and discussion

Throughout this study, a progressive planning path was followed to obtain the best possible conclusion to the objectives stated in Chapter 1. In Chapter 4 of this project the results of the experimental work will be illustrated graphically and discussed in detail after a statistical analysis is conducted to identify the most important results. Only the results identified by the statistical analysis will be discussed in detail. For the complete detailed results obtained the reader is referred to the attached DVD (Experimental results Rev 3.xls).

4.1 Introduction

As previously stated the primary objective of the project was to determine whether a FDMB is capable of upgrading fine coal. The question of the extent to which it can upgrade coal could be concluded from the results discussed in this section.

Three additional questions that should be kept in mind during this chapter are:

- 1) Can the addition of magnetite to the coal feed increase the separation efficiency of this process?
- 2) If a jiggling motion (on – off air flow) is introduced to the air feed of the process, will an increase in coal separation be observed?
- 3) What is the effect of particle size on fluidization performance?

For clarity purposes before commencing with the results discussion, Table 4-1 illustrates the bed height corresponding to a specific bed layer in the fluidized bed.

Table 4-1: Bed height and bed layer comparison

Bed height (mm)		Bed layer
40	=	Bottom layer
80	=	2
120	=	3
160	=	4
200	=	Top layer

An example as seen in Table 4-1; when referring to a 40 mm bed height the corresponding bed layer will be the bottom layer. When referring to the 80 mm bed height, the 2nd layer of the fluidized bed is referred to etc.

4.1.1 Pre-experiment results

A washability test (float – sink) was conducted on the raw coal samples. In Figure 4-1, Figure 4-2 and Figure 4-3 the washability graphs of the three samples are illustrated. With a complete ash – density distribution of the coal, an accurate estimation can be made as to the density that the coal should be separated at to achieve the highest mass yield possible.

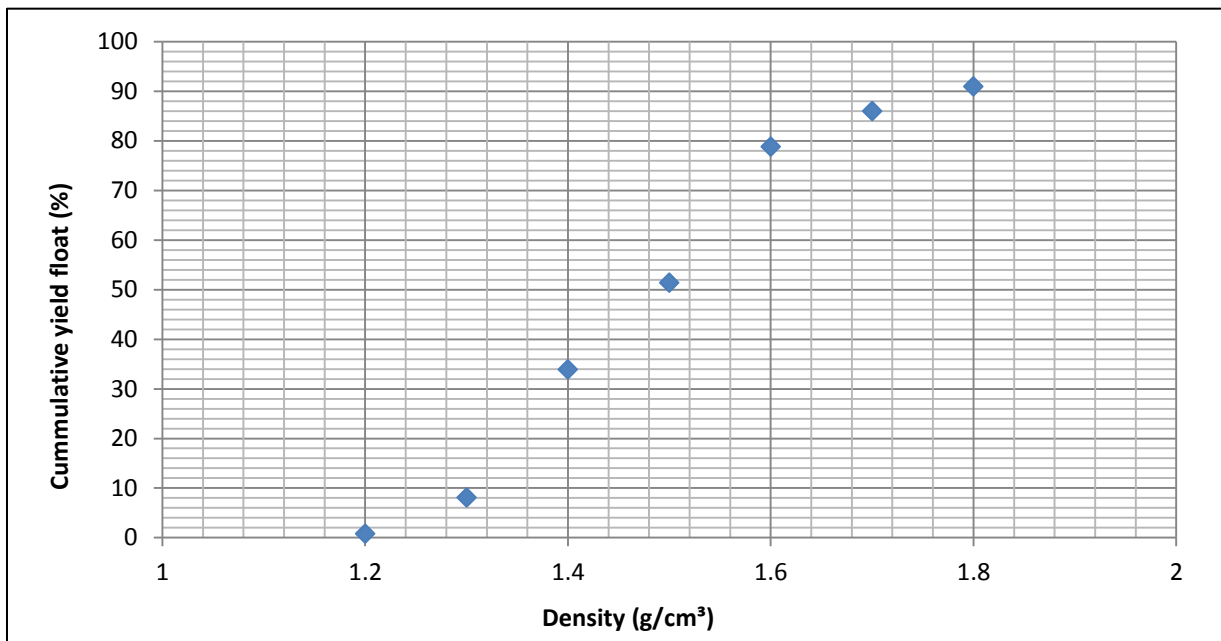


Figure 4-1: Washability curve – Witbank FF

From the washability graphs the maximum yield of the product can be calculated if the cut density is known.

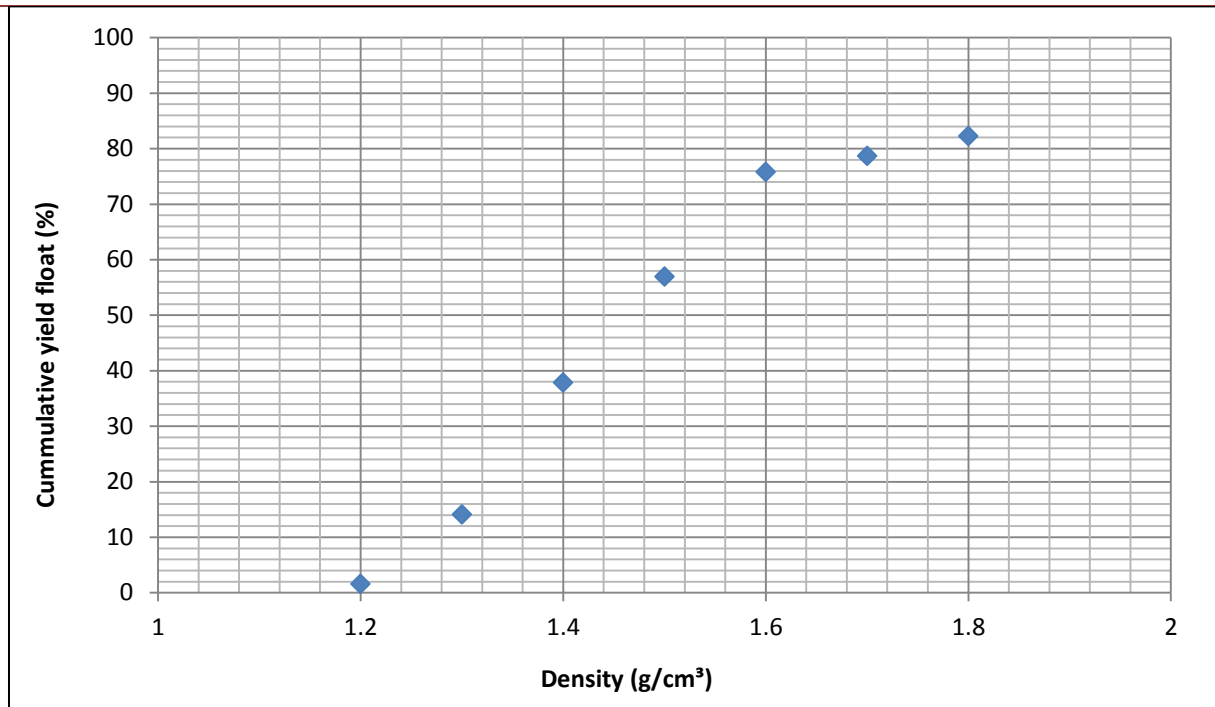


Figure 4-2: Washability curve – Witbank SF

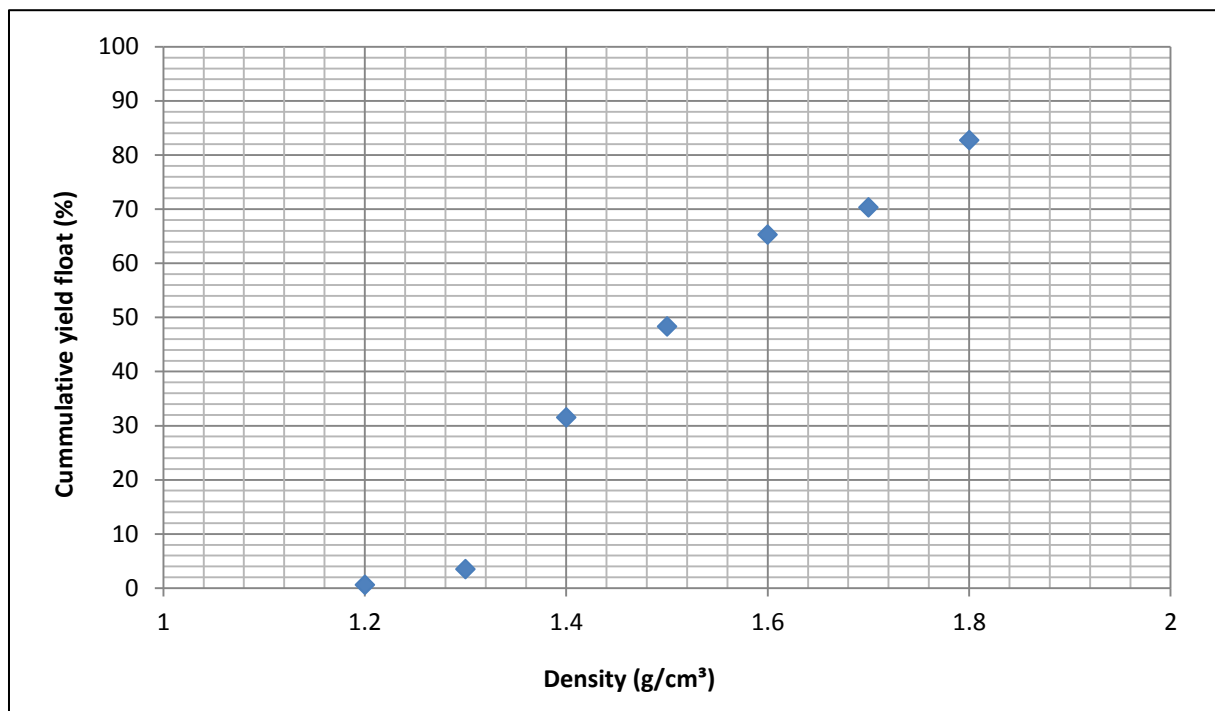


Figure 4-3: Washability curve – Waterberg

The results of the raw coal pre-tests are shown in Table 4-2 , Table 4-3 and Table 4-4.

Table 4-2: Witbank FF pre-test results

Test	Results
% Moisture (ISO 11722:1995)	4.4
% Ash (ISO 1171:1997)	19.9
% Volatile (ISO 562:2010)	23.1
% Fixed Carbon (By difference)	52.6
Calorific Value (ISO 1928:2009)	24.18 (MJ/kg)

The Witbank FF coal was only used in Run number 1, as seen in Table 3-4. All the coal samples were placed in a dry climate controlled room to be used “as is” during experiments with this sample having a moisture content of 4.4% throughout. The Witbank FF has a moderately low ash percentage (19.9%) and high CV (24.18 MJ/kg) due to the fact that it has already been cleaned by a spiral plant. Export coal is required to have a mineral content that reports as percentage ash lower than 15% and a CV higher than 27.5 MJ/kg referring to Table 3-3. However, if the fluidized bed technology is able of upgrading the coal to export quality specifications, a considerable amount of money could be saved and/or generated.

When the coal samples reached the desired moisture content, each sample was sieved and placed into respective size range buckets. The size ranges used during this study as mentioned in Section 3.4 are:

- Fine coal: -1180 + 500 μ m
- Coarse coal: -2000 + 1180 μ m

The mixtures of fine and coarse coal used can be seen in Table 3-4. The nature of the mixture is 50/50 volume base. Three different sieves were used in the PSD tests which included, a 1400 μ m, 1000 μ m and 850 μ m sieve.

The d50 and d20 of each coal sample was calculated using a graphical method. The PSD curve was constructed and the d20 and d50 lines were drawn in and manually adjusted until it intersected with the PSD curve indicating the correct values. For the Witbank filter feed coal the d20 and d50 were calculated as 763 μ m and 824 μ m respectively. The Witbank SF sample pre-test results are contained in Table 4-3.

Table 4-3: Witbank SF pre-test results

Test	Results
% Moisture (ISO 11722:1995)	5
% Ash (ISO 1171:1997)	23.8
% Volatile (ISO 562:2010)	23.7
% Fixed Carbon (By difference)	51
Calorific Value (ISO 1928:2009)	23.6 (MJ/kg)

Another Witbank coal was used in the form of a pre-spiral coal. As seen in Table 4-3 the ash percentage is higher than the post-spiral coals which can be expected. This coal sample also has a slightly higher moisture content of 5% and lower CV of 23.6 MJ/kg than the filter feed sample. The Witbank SF coal was used in Test's nr 2-5. By following the same procedure as mentioned previously, the d₂₀ and d₅₀ of the Witbank spiral feed coal was calculated as 746µm and 852µm. In Table 4-4 the final coal sample (Waterberg) pre-experiment test results are shown.

Table 4-4: Waterberg pre-test results

Test	Results
% Moisture (ISO 11722:1995)	3
% Ash (ISO 1171:1997)	18.6
% Volatile (ISO 562:2010)	21.3
% Fixed Carbon (By difference)	57.1
Calorific Value (ISO 1928:2009)	25.43 (MJ/kg)

The Waterberg coal has a lower ash percentage and higher CV than the Witbank SF coal which was the most thoroughly tested samples during this project. Tests nr 6-16 was done on the Waterberg coal sample. A mixture of the fine (75%) and coarse (25%) particles were used in the Waterberg sample. From the graphically obtained results it can be concluded that the d₅₀ of the Waterberg coal is around 1558µm with a d₂₀ of 874µm. The d₅₀ particle size of the Waterberg coal is much higher than the previous two samples due to the coarse and fine coal particle mixture created for experiments (refer to Table 3-4).

4.2 Interpretation procedure of the data

A large amount of data was acquired from each run as seen from the list of analyses at the end of Section 3. Twenty one experiments, including repeats, were done (10 coal – magnetite runs and 11 coal only runs). For each normal coal run, five layers were extracted and for each magnetite and coal mixture run, four layers were extracted. Each of these

School of Chemical and Minerals Engineering

extracted layers was analysed producing results for percentage ash, volatile matter, moisture content, fixed carbon, CV, PSD and density. The twenty one runs therefore produced 94 coal samples that had to be analysed.

Due to the share volume of data points, an ANOVA (analyses of variance) was conducted to determine the influence of the different variables on the separation capabilities of the fluidized bed. The data was split according to two main variables namely: PSD and the coal type. The variables used in the analysis are shown:

- x_1 = PSD (Case 1) and Coal type (Case 2)
- x_2 = Jigging (Yes/No)
- x_3 = Magnetite (Yes/No)

From the properties mentioned in Section 3.7, the most significant indicators of successful coal beneficiation are density, ash percentage, CV and particle size (d50). Therefore, these were chosen as the dependent variables indicated as a difference between the top and the bottom value.

- y_1 = Δ density
- y_2 = Δ ash
- y_3 = Δ CV
- y_4 = Δ size (d50)

If a statistical value signifying the extent of interaction between these variables can be obtained, an accurate conclusion can be made to which independent variable has the largest effect on coal separation. On the other hand, if a variable is found to be insignificant, the remaining variables will be used for further calculations and an optimum variable configuration will be identified from these calculations.

After the optimum operating parameters have been identified, which includes jigging magnetite, PSD and coal type, the best runs will be chosen and discussed in detail.

4.3 Repeatability of experiments

In order to validate the credibility of the fluidized bed equipment, certain experiments had to be repeated. As seen in Table 3-4 runs nr 2, 3, 8, and 9 were repeated as indicated by the

School of Chemical and Minerals Engineering

asterisk below the table. These runs were chosen as each run represented a different experimental scenario. The four experimental scenarios include: normal fluidization, jiggling fluidization, normal magnetite fluidization and jiggling plus magnetite fluidization. The normal fluidization scenario was repeated thrice as it is the most elemental and important experiment for this study. In Table 4-5 the standard deviation values of run 2 can be seen.

Table 4-5: Standard deviation (Run 2)

Bed height	Standard deviation					
	Density (g/cc)	Moisture (%)	Ash (%)	Volatiles (%)	Fixed Carbon (%)	CV (MJ/kg)
40	0.07	0.42	7.51	1.46	5.66	2.37
80	0.03	0.15	0.52	0.32	0.40	0.36
120	0.03	0.06	3.18	0.70	2.49	1.19
160	0.14	0.26	3.93	0.50	3.20	1.07
200	0.03	0.06	3.44	0.93	2.46	1.26
Average of STDEV (±)	0.06	0.19	3.72	0.78	2.84	1.25

It is clear from Table 4-5 that the results do not differ noticeably through repeats 1-3 of run 2. The average of all the layers was calculated to produce an overall standard deviation for a specific property of the coal. It is important to note that fluidized beds are very sensitive to any change in particle size, air flow, particle density, etc. (Gupta *et al.*, 2009). From Table 4-5 it can be seen that the total standard deviation of the ash for the fluidized bed is only $\pm 3.72\%$ and the standard deviation of the CV is 1.25 MJ/kg which is also very low.

In Table 4-6 the standard deviation values of run 3 is shown. The averages of the standard deviations are illustrated at the bottom of Table 4-6.

Table 4-6: Standard deviation (Run 3)

Bed height	Standard deviation					
	Density (g/cc)	Moisture (%)	Ash (%)	Volatiles (%)	Fixed Carbon (%)	CV (MJ/kg)
40	0.11	0.49	5.73	1.41	3.82	1.64
80	0.00	0.78	0.85	0.07	0.00	0.35
120	0.04	0.71	0.07	0.14	0.49	0.30
160	0.00	0.35	2.33	0.42	2.26	1.01
200	0.02	0.14	4.81	1.34	3.61	1.87
Average of STDEV (±)	0.03	0.49	2.76	0.68	2.04	1.03

It can be seen from Table 4-6 that the repeatability of the experiments is very good when keeping in mind the sensitive nature of fluidized beds. The standard deviation of the density data is only 0.03 g/cm³ with the ash and CV differences reported as 2.76% and 1.03 MJ/kg respectively.

School of Chemical and Minerals Engineering

The credibility of the experiments can therefore be approved for the normal fluidization and jiggling fluidization scenarios. Table 4-7 illustrates the standard deviation averages of run 8.

Table 4-7: Standard deviation (Run 8)

Bed height	Standard deviation					
	Density (g/cc)	Moisture (%)	Ash (%)	Volatiles (%)	Fixed Carbon (%)	CV (MJ/kg)
40	0.00	0.21	0.07	0.14	0.14	0.00
80	0.08	0.07	0.42	0.21	0.28	0.29
120	0.04	0.14	1.98	0.00	2.12	0.55
160	0.01	0.14	0.07	0.14	0.07	0.01
Average of STDEV (±)	0.03	0.14	0.64	0.12	0.65	0.21

Again it is clear that the standard deviation averages are very low. In run 8's case it is evidently lower than the previous two runs. Later in this section the separation efficiency of the various runs will be discussed. However, in the case of runs number 8 and 9 inefficient separations occurred with almost no change in the ash or CV values from the top to bottom layers. This is the suspected reason for the good repeatability of run 8 and run 9. The standard deviation of run 9 is shown in Table 4-8.

Table 4-8: Standard deviation (Run 9)

Bed height	Standard deviation					
	Density (g/cc)	Moisture (%)	Ash (%)	Volatiles (%)	Fixed Carbon (%)	CV (MJ/kg)
40	0.03	0.07	0.85	0.07	0.71	0.31
80	0.02	0.14	2.83	0.21	2.47	0.63
120	0.05	0.21	0.07	0.14	0.14	0.11
160	0.11	0.00	0.07	0.07	0.00	0.06
Average of STDEV (±)	0.05	0.11	0.95	0.12	0.83	0.28

It is evident that the standard deviation of all the properties is again very low and the repeatability of the equipment can be verified by the results obtained from these four repeated runs.

Refer to Appendix A for the rest of the repeatability graphs of the above mentioned runs.

4.4 Statistical analysis

4.4.1 Introduction

As mentioned in Section 4.2, two cases were established for the bilateral ANOVA analysis. When conducting an ANOVA analysis the interaction between the chosen variables is indicated by a p (probability) value. This interaction is based on a 90% confidence interval. The coal used in this study and overall in the world is heterogenic in nature in terms of

School of Chemical and Minerals Engineering

particle shape, size and mineral content. For this reason a 90% confidence interval was chosen and not a 95% confidence interval as normally used in research studies. A discussion of the two cases mentioned above follows.

The independent variable (x_1) options are shown in Table 4-9.

Table 4-9: Independent variable (x_1) options

PSD (Case 1)	
$x_1 = 1$ (Fine coal)	-1180 + 500
$x_1 = 2$ (Coarse coal)	-2000 + 1180(25%) + -1180 + 500(75%)
Coal sample (Case 2)	
$x_1 = A$	Witbank SF
$x_1 = B$	Waterberg

In Table 4-10 the altered experimental plan can be seen.

Table 4-10: Altered experimental plan

Altered experimental Plan 2013					
Case	Run nr	PSD	Jigging	Magnetite	Coal Sample
2	2 (a)	1	no	No	A
2	2 (b)	1	no	No	A
2	2 (c)	1	no	No	A
2	3 (a)	1	yes	No	A
2	3 (b)	1	yes	No	A
2	4	1	no	Yes	A
2	5	1	yes	Yes	A
1 & 2	6	1	no	No	B
1 & 2	7	1	yes	No	B
1 & 2	8 (a)	1	no	Yes	B
1 & 2	8 (b)	1	no	Yes	B
1 & 2	9 (a)	1	yes	Yes	B
1 & 2	9 (b)	1	yes	Yes	B
2	10	2	yes	No	B
2	11	2	no	No	B
2	12	2	yes	No	B
2	15	2	no	Yes	B
2	16	2	yes	Yes	B

This altered experimental plan was created based on data obtained from runs number 1, 13 and 14. It is irrelevant to use the data from these runs when considering the two way ANOVA analysis. Run 1, 13 and 14 contain variables e.g. a third coal sample and a third PSD, which could not be processed by the statistical analysis due to insufficient data on

specific run configurations. Refer to Table 4-9 for the variable definitions of PSD and coal sample. It is clear from Table 4-10 that in Case 1, the coal sample was kept constant (Waterberg coal) and in Case 2 the PSD was kept constant (fine fraction only).

4.4.2 Statistical analysis: Case 1

The data used in Case 1 is shown in Table 4-11.

Table 4-11: Case 1 data values

Run nr	PSD x_1	Jig x_2	Magnetite x_3	Δ density (g/cc) y_1	Δ ash (%) y_2	Δ CV (MJ/kg) y_3	Δ size (d50: μ m) y_4
6	1	no	no	0.29	16.4	6.05	388
7	1	yes	no	0.25	18.3	7.02	385
8a	1	no	yes	0.06	1.2	0.6	5
8b	1	no	yes	0.07	1.2	0.62	16
9a	1	yes	yes	0.18	1.4	0.46	7
9b	1	yes	yes	0.07	2.5	0.98	10
10	2	yes	no	0.19	10.8	4.22	687
11	2	no	no	0.23	18.4	7.9	689
12	2	yes	no	0.28	14.6	3.15	679
15	2	no	yes	0.18	4.7	1.95	109
16	2	yes	yes	0.21	8.1	3.1	147

As mentioned before, the Δ indicates the value difference between the top and bottom layers of the fluidized bed of a certain variable. The data in Table 4-11 was analysed and the following results were obtained:

The graph in Figure 4-4 was drafted to determine the effect of the three independent variables (x_n) on the dependent variable y_1 . The interpretation of an interaction graph such as the one below is explained:

The blue lines ($x_1 = 1$) in Figure 4-4 indicate fine coal and the red lines ($x_1 = 2$) indicate coarse coal. There are two evident graphs in Figure 4-4, namely the left side graph indicating $x_3 = \text{no}$, which indicates that zero magnetite was added to the feed and the right hand side indicating that magnetite (60% volume) was added during the experiment. Moreover, two points are visible in the graph with $x_2 = \text{no}$ and $x_2 = \text{yes}$. x_2 is the variable

School of Chemical and Minerals Engineering

associated with jiggling and 'yes' indicates jiggling likewise 'no' indicate no jiggling. The effect of jiggling will therefore be indicated by the slope of the lines within the error bars. A positive slope will indicate better separation with an induced jiggling motion and a negatively sloped line will indicate worse separation with jiggling. The vertical lines in the figure are indicative of the error values of the data.

Above the graph a value of $p = 0.64786$ is shown. This is the probability value mentioned in the previous section that indicates whether an interaction is noteworthy or not. The p value should be < 0.01 to be significant enough to consider (90% confidence interval). Lastly, the values on the Y axis are the Δ values of the dependent variable, in this case y_1 which is density.

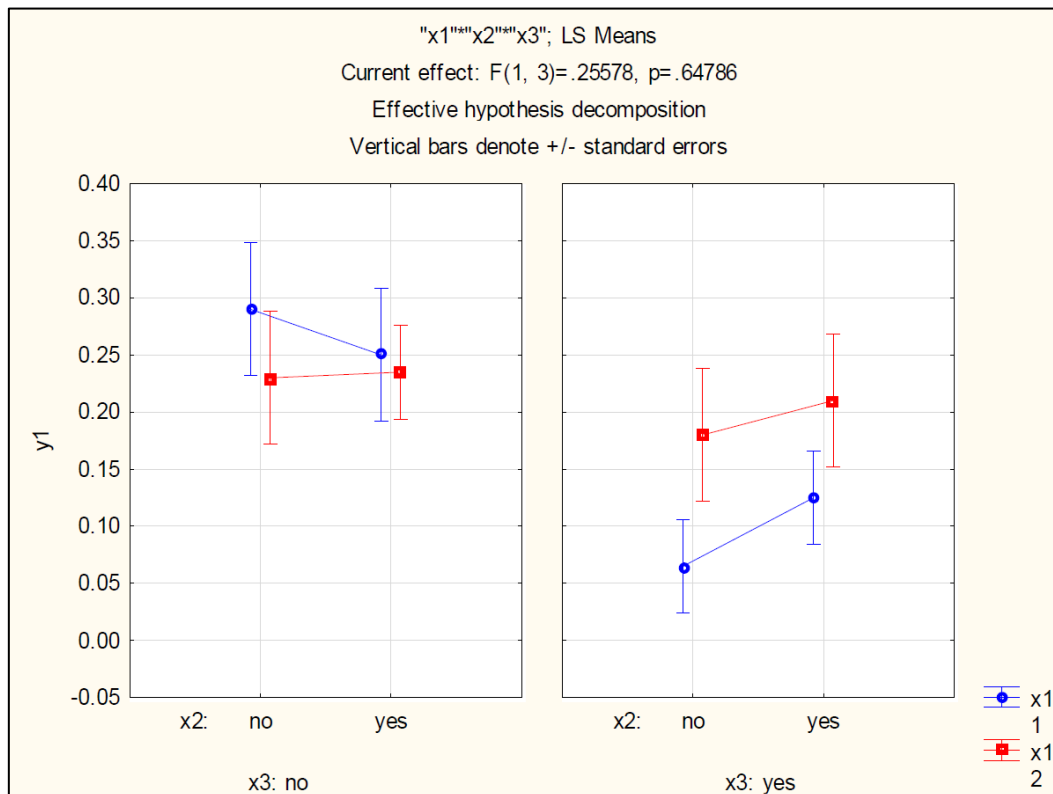


Figure 4-4: Case 1 interaction graph of y_1 (Δ density g/cm^3)

Therefore it can be stated that Figure 4-4 shows when adding magnetite to the coal feed the separation efficiency decreases as the density difference from the top to the bottom of the bed is not as high as when no magnetite is present. This is however only evident in the finer coal tests. Considering $p = 0.64786$, indicating no significant effect of particle size, magnetite addition and jiggling of the air-flow on density separation.

School of Chemical and Minerals Engineering

During experiments with magnetite present, severe channelling of the air through the particle bed occurred. When the bed of particles was initially fluidized, the increasing air velocity reached a point at which the air would suddenly and violently burst out of the bed. This is due to a high pressure drop created by the ultrafine ($d_{50} = 24\mu\text{m}$) closely packed bed of magnetite particles which causes pressure to build up and a sudden release of energy into the bed inducing big bursting bubbles. If the bubbles were well dispersed and small, it could have been an advantage in this particular case. However, due to the channelling nature of the gas through selective pathways through the bed, inefficient separation occurred during fluidization in the presence of magnetite. Although the distribution system of the equipment worked well with only coal particles, the small size of the magnetite particles caused channelling which could not be prevented.

Zhao *et al.*, (2010c) stated that when Geldart B magnetite powder is fluidized, the fluidization quality (increase of gas channelling in the bed) decreases as the static bed height increases. Although Zhao *et al.*, (2010c) mentioned that it only influences bed heights $H_s > 300$ mm; in this particular case the ultrafine magnetite particles played a more significant role on fluidization as seen in the results in Figure 4-4. It should also be noted that a rectangular fluidized bed was used during the experiments done by Zhao *et al.*, (2010c), indicating slightly different hydrodynamics within the bed compared to the cylindrical bed used in this study.

Figure 4-4 also indicates that a jiggling air feed has no significant effect on the separation efficiency of the fluidized bed however this could be due to the nature of the jiggling motion induced. The pulsing air was not calculated to be exactly 2 seconds apart with the amplitude implemented during the tests due to the manual operation of the pulsing air. Manual operated jiggling was chosen rather than automated control in order to simplify the design and construction of the equipment as this is a new technology and no publications are produced on this specific subject yet. In Figure 4-5, the interaction graph of variable y_2 (% ash) is attached.

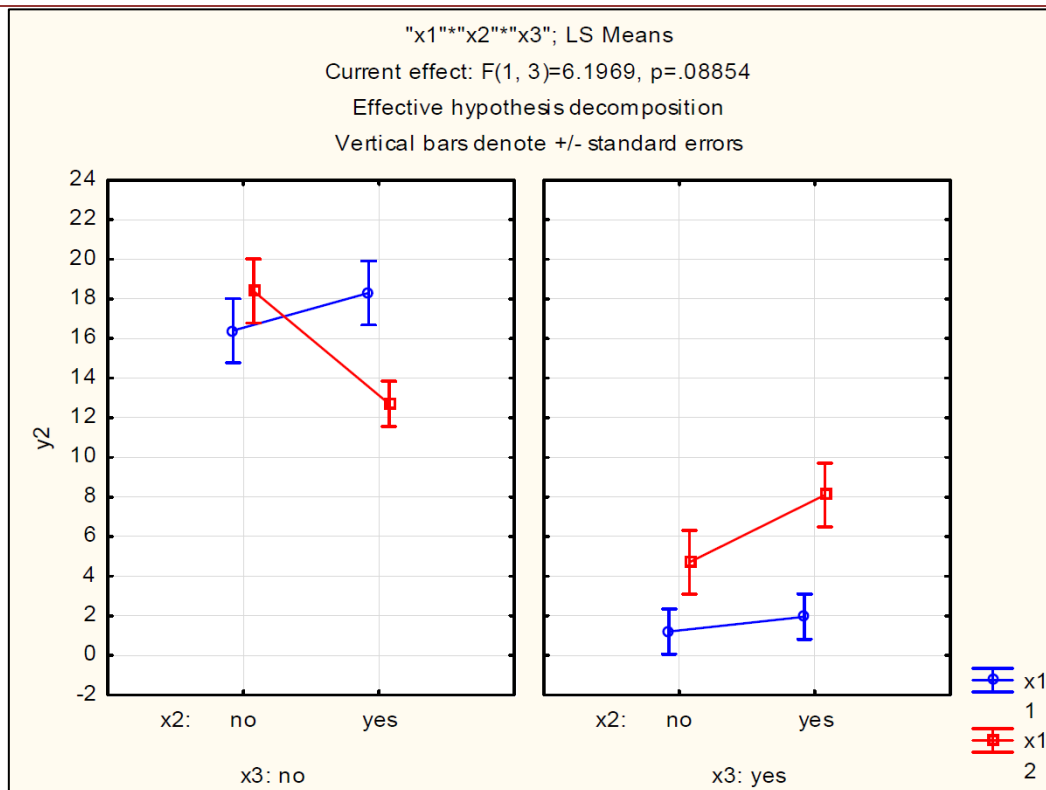


Figure 4-5: Case 1 interaction graph of y_2 (Δ ash %)

As the density of a particle is an indication of the amount of ash contained, the graph in Figure 4-5 shows similar results to that of Figure 4-4 which is that adding magnetite has a negative effect on the fluidized bed separation capabilities (Mohanta *et al.*, 2013).

Deviations in the density results can be attributed to the trace amounts of magnetite still contained in the tested coal sample which has a larger effect on density results compared to that of ash tests. In the case of magnetite tests it is therefore more accurate to interpret the effect of separation focussing on ash and CV values instead of density. However, in this particular case the results indicate similar outcomes which are that magnetite decreases separation efficiency of coarse and fine particles (the lines on the right hand side graph, lies lower than the left hand side lines). When looking at dependant variable y_3 (CV, MJ/kg) shown in Figure 4-6, similar results to Figure 4-4 and Figure 4-5 is evident.

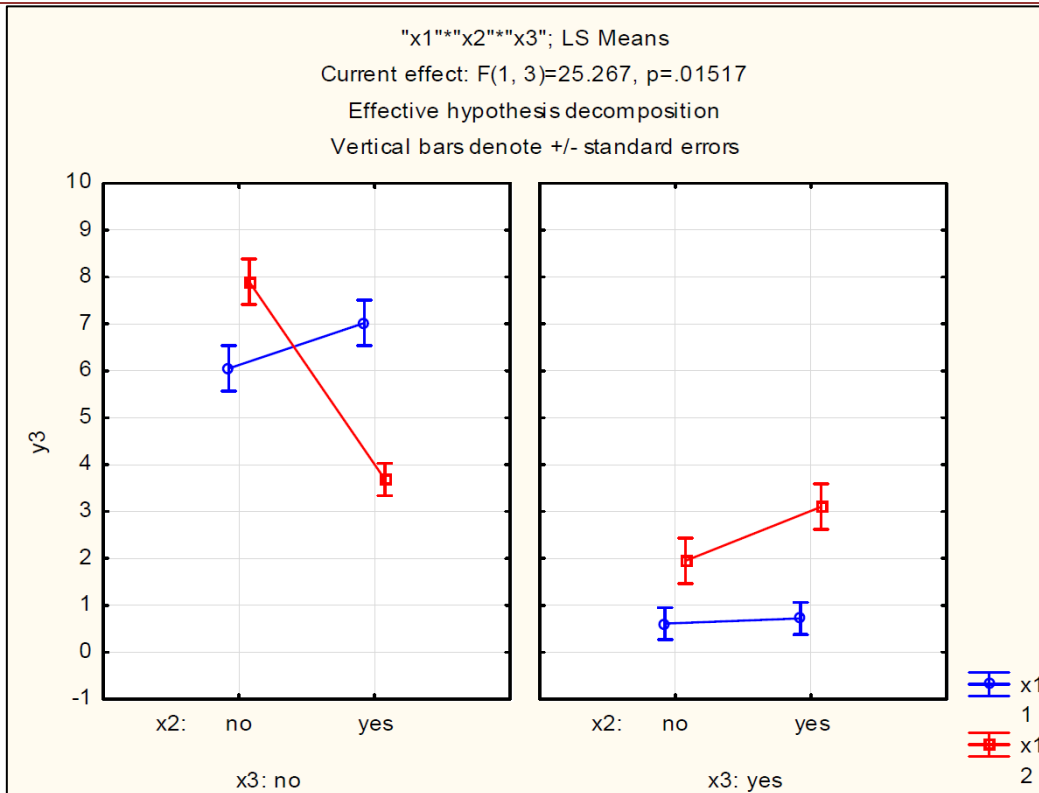


Figure 4-6: Case 1 interaction graph of y_3 (Δ CV MJ/kg)

It is clearly visible from Figure 4-6 that adding magnetite powder together with coal to the fluidized bed feed does not increase the separation efficiency of this particular fluidized bed equipment. Therefore repeatedly indicating that magnetite decreases the accuracy of test results due to contamination of the sample.

An interesting observation seen in Figure 4-5 and Figure 4-6 (excluding Figure 4-4 due to density error values) is that when zero magnetite is present, jiggling the air feed does not increase separation efficiency of coarse coal but in turn actually decreases it. The opposite is indicated when magnetite is used and surprisingly shows a slight increase in separation of coarse coal when jiggled. It is also clear that this only occurs when considering the coarser coal particles (red lines) with no significant change in separation observed by the fine coal lines (blue lines). A possible explanation to this can be that the particles separate based on size and not density when jiggled.

This observation could also be ascribed to the packing of the particles within the bed. When jiggling with magnetite present the shock produced by the pulsating air unlocks the bed causing a decrease in the observed channelling mentioned above. This was also observed

during experiments done when micro bubbles were visible and pulsed air was introduced in the presence of magnetite, which indicates that more stable fluidization and in turn better separation could be expected (Luo *et al.*, 2012; Chen & Yang, 2003; Chen & Wei, 2005). However this observation is negligible when comparing the results to that of zero magnetite fluidization which is why jigging positively influences separation with magnetite, compared to worse separation with jigging on the zero magnetite runs.

Shocking the bed with pulsating air has a negative effect on separation only when considering coarse coal particles as mentioned above. This observation could be the effect of feed particle size on fluidization. In Figure 4-7 the interaction effects of the dependent variable y_4 (Δ particle size (μm)) is illustrated.

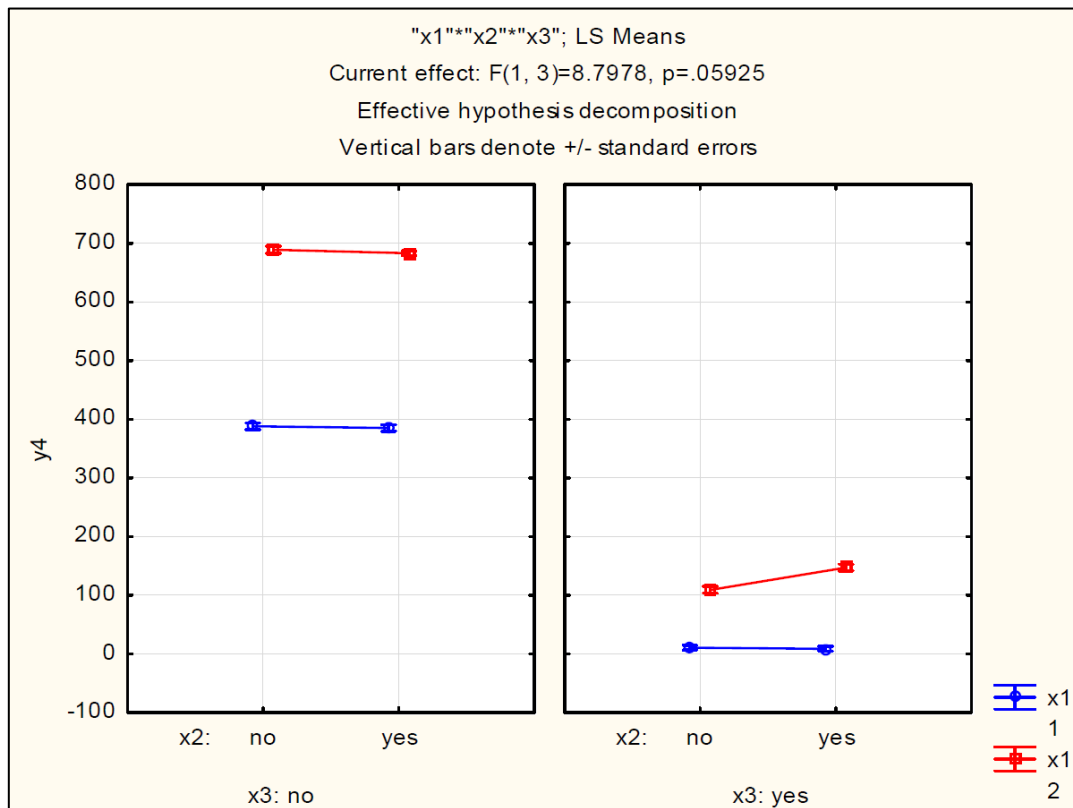


Figure 4-7: Case 1 interaction graph of y_4 (Δ d50 particle size μm)

From Figure 4-7 it is clear that when magnetite is used, a negligible effect on d50 feed particle size is observed. The effect mentioned is the separation of larger particles and smaller particles in the bed. In the presence of magnetite no separation occurred according to particles size and in fact no separation took place at all.

It is evident that in the absence of magnetite, indicated in the section on the left hand side of Figure 4-7, the coarse coal particles are separated based on size rather than the preferred density or ash separation. When studying fluidization, separation should primarily be based on density and not particle size and the feed PSD range should be chosen narrowly as this will decrease the effect of separation based on particles size (Chikerema & Moys, 2012). Refer to Section 5.2 for recommendations on how to reduce this effect.

Again no indication of better separation is observed in Figure 4-7 when a pulsating motion to the air feed is induced. There is a slight slope change evident in lines in the figures above but the error bars of most of the lines overlap. This means that the values could be anywhere in between the overlapping line areas which therefore indicates that no effect of jiggling the air feed on separation is observed.

In conclusion of Case 1 (PSD):

- Adding magnetite powder to the bed reduces separation of both coarse and fine coal,
- Jiggling the air feed slightly decreases separation of coarse coal but has no significant effect on fine coal (zero magnetite),
- Coarser coal particles fluidize better than the finer coal particles when no jiggling is present.

The best chosen runs in Case 1 is therefore, run 6/7 and 11 as indicated by the Δ values for ash and CV in Table 4-11. This is a comparison between a Waterberg coarse coal and a Waterberg fine coal normal fluidization run. The above mentioned runs will be discussed in detail in Section 4.5.

4.4.3 Statistical analysis: Case 2

The difference between case 1 and 2 is that the variable x_1 in the first case is defined as particle size distribution and in the second case it is defined as the two different coal samples used. In Table 4-12 the data values used in Case 2 is shown moreover it can also be seen that the two coal samples used are:

- A. Witbank SF
- B. Waterberg

School of Chemical and Minerals Engineering

By evaluating the results obtained in the same way as for Case 1 the effect of coal sample on separation performance can be interpreted and discussed.

Table 4-12: Case 2 data values

Run nr	Coal sample x_1	Jig x_2	Magnetite x_3	Δ density (g/cc) y_1	Δ ash (%) y_2	Δ CV (MJ/kg) y_3	Δ size (d50: μ m) y_4
2a	A	no	no	0.12	11	3.64	10
2b	A	no	no	0.14	22.1	7.05	30
2c	A	no	no	0.03	32.8	10.83	52
3a	A	yes	no	0.1	8	2.75	10
3b	A	yes	no	0.02	22.9	7.71	37
4	A	no	yes	0.02	6.1	1.76	11
5	A	yes	yes	0.19	5.1	1.94	16
6	B	no	no	0.29	16.4	6.05	388
7	B	yes	no	0.25	18.3	7.02	385
8a	B	no	yes	0.06	1.2	0.6	5
8b	B	no	yes	0.07	1.2	0.62	16
9a	B	yes	yes	0.18	1.4	0.46	7
9b	B	yes	yes	0.07	2.5	0.98	10

The interaction graph of variable y_1 is included in Figure 4-8. Throughout this section the same results are clear compared to the results found in Case 1 which indicates that magnetite addition to the coal feed decreases separation. Research has shown that adding magnetite to a fluidized bed increases separation but due to the small coal particle size it is not effective in this study. The magnetite used during this study could also be a reason for the inefficiency of separation due to its ultrafine size. All of the magnetite runs will therefore be shown but excluded from further discussions (right side of figures following).

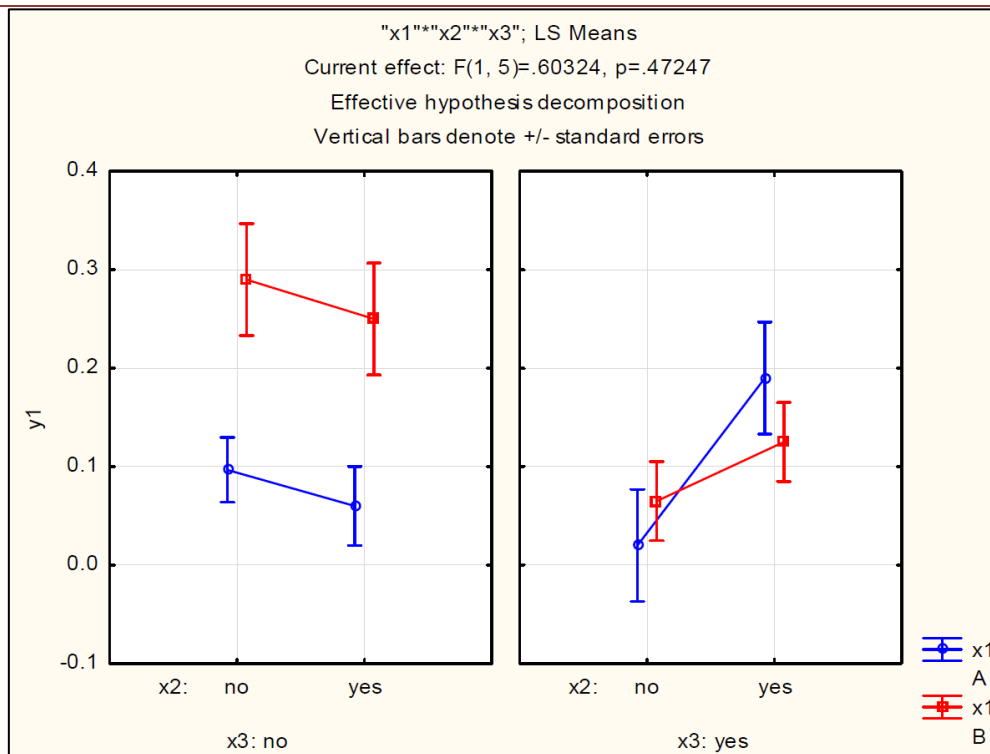


Figure 4-8: Case 2 interaction graph of y_1 (Δ density g/cm^3)

The first thing to notice is that the value of $p = 0.47247$ which indicates that no remarkable interaction is evident for each of the coal samples when considering the addition of magnetite (right side graph) in Figure 4-8. A clear difference in the density can be noticed when no magnetite is present. This is indicative of the fact that the two different coal samples separate differently according to density. This observation can also be due to the nature of the different coal samples although a better indication could be seen from the interaction graph with ash percentage as the dependent variable. The interaction curve of ash is indicated in Figure 4-9.

School of Chemical and Minerals Engineering

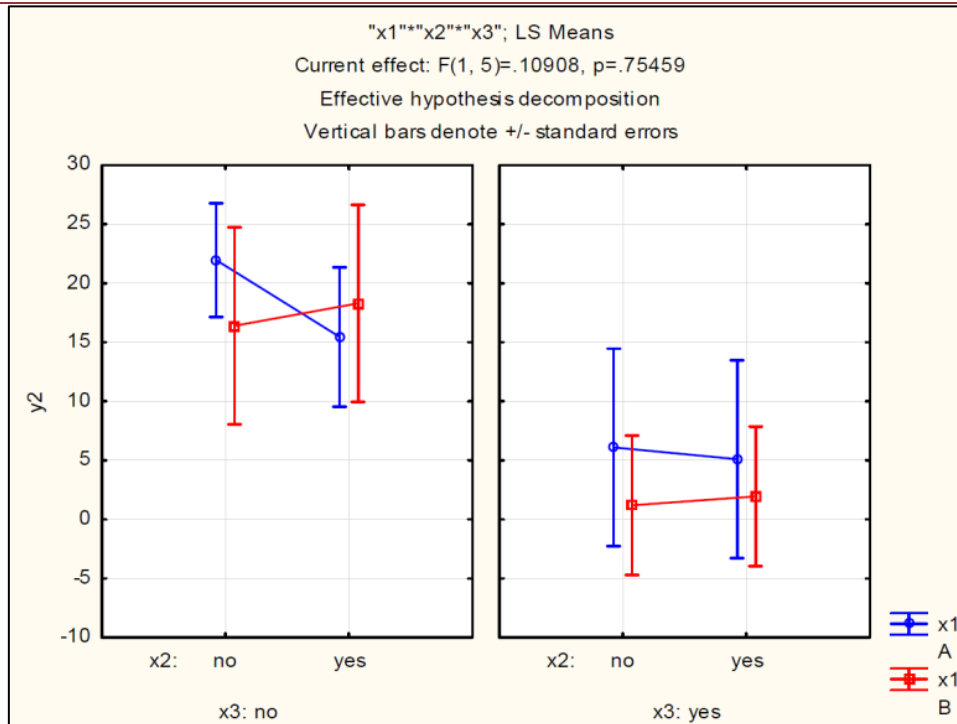


Figure 4-9: Case 2 interaction graph of y_2 (Δ ash %)

Figure 4-9 indicates that there is almost no difference in the Δ ash values of the coal samples. The ash differs from 10% to 25% for both coal samples from top to bottom. There is a slight slope evident in the lines of the graph. But due to the overlapping error bars, jiggling can also be seen as having no effect on the separation performance.

In Figure 4-10 the CV value interaction graph is illustrated. Because the ash percentage and CV value of coal can be directly correlated for the same coal sample, the same result is expected for CV values as for ash values and this seems to apply in this particular case.

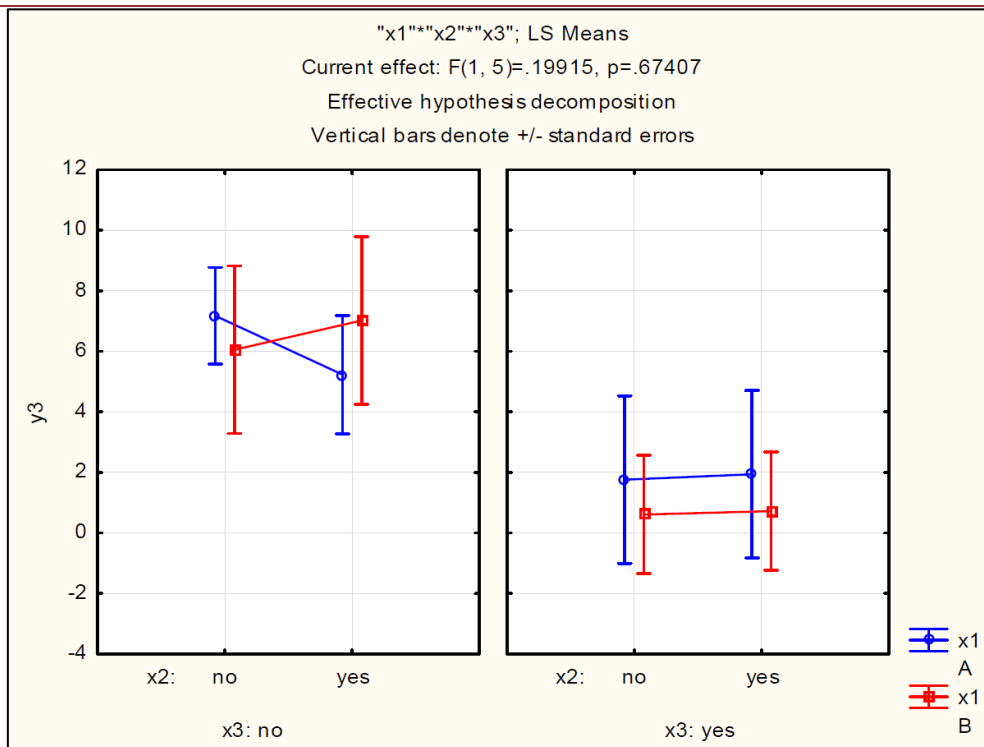


Figure 4-10: Case 2 interaction graph of y_3 (Δ CV MJ/kg)

There is a clear Δ value difference, but no difference between the coal samples in Figure 4-10. It can therefore be concluded that the coal samples fed to the fluidized bed does not affect the separation capabilities of the equipment. Although an interesting observation can be made when looking at the d_{50} particle size of the top and bottom layer of the two coal samples.

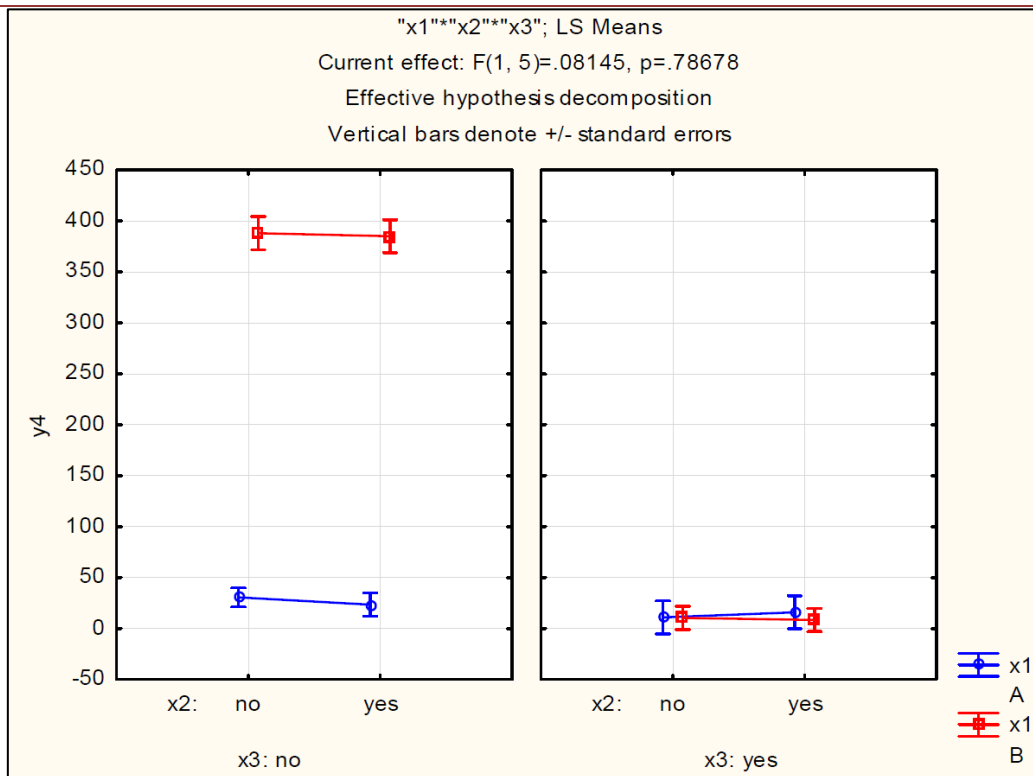


Figure 4-11: Case 2 interaction graph of y_4 (Δd_{50} particle size μm)

It is evidently clear from the interaction graph indicated in Figure 4-11 that the Witbank SF coal separates according to particle size, but the Waterberg coal does not. A possible explanation could be that because of the narrower PSD range of the Witbank coal compared to the Waterberg coal, separation is based primarily on density and not particle size and weight.

In the next section it is observed that overall, Waterberg coals show better separation results which could be expected. Waterberg coals only separate according to density and not particle size, which is the basic working principle of fluidized bed separation (density separation).

In conclusion of Case 2 (Coal sample):

- There is no significant difference in separation performance based on the statistical analysis of the two coals used,
- There is however a difference when considering particles size. The Waterberg coal does not seem to be separated according to particle size with the Witbank coal showing the opposite,

School of Chemical and Minerals Engineering

- Magnetite addition causes worse separation similar to the results of Case 1.
- Jigging the air-feed had no significant effect on coal separation.

Considering the latter point in the list above, it was decided to exclude run 3 from the discussions in Section 4.5. The best run in Case 2 is therefore, run number 2 as seen in Table 4-12. Because this is a repeated run, the average of the coal properties will be calculated and used in the following discussion.

4.5 Discussion of selected runs

As mentioned above three runs were chosen as having the best results to compare. The runs taken are:

1. Run 2,
2. Run 6,
3. Run 11.

Run 6 as seen in Table 3-4, is a normal fluidization run. Run 6 and run 7 had similar results regarding Δ ash, with run 7 having the slightly better results. However, to compare similar experimental scenarios run 6 was chosen as run 7 is a jigging run, and comparing it to run 2 and run 11 which are both normal fluidization runs will make no sense. For the same reason as discussed, run 3 was also excluded. A detail discussion of the above mentioned runs follows.

4.5.1 Run 2

The coal sample used in this run is Witbank SF. It is a lower quality coal compared to the Witbank FF used in run 1 as it has not yet been beneficiated by spirals. The ash and CV values of the feed coal are 23.8% and 23.6MJ/kg respectively. Run 2 was also a repeat run to prove the validity of the fluidized bed equipment and the details can be referred to in Section 4.3. The data displayed in the graphs that follow is the average of the three repeated runs.

As mentioned before in the literature survey it is very difficult to visually analyse if complete and efficient fluidization is occurring during an experiment. The minimum fluidization graph

gives an indication of the rate of air-flow needed to completely fluidize a bed of particles. In Figure 4-12 the fluidization graph of Run 2 is illustrated.

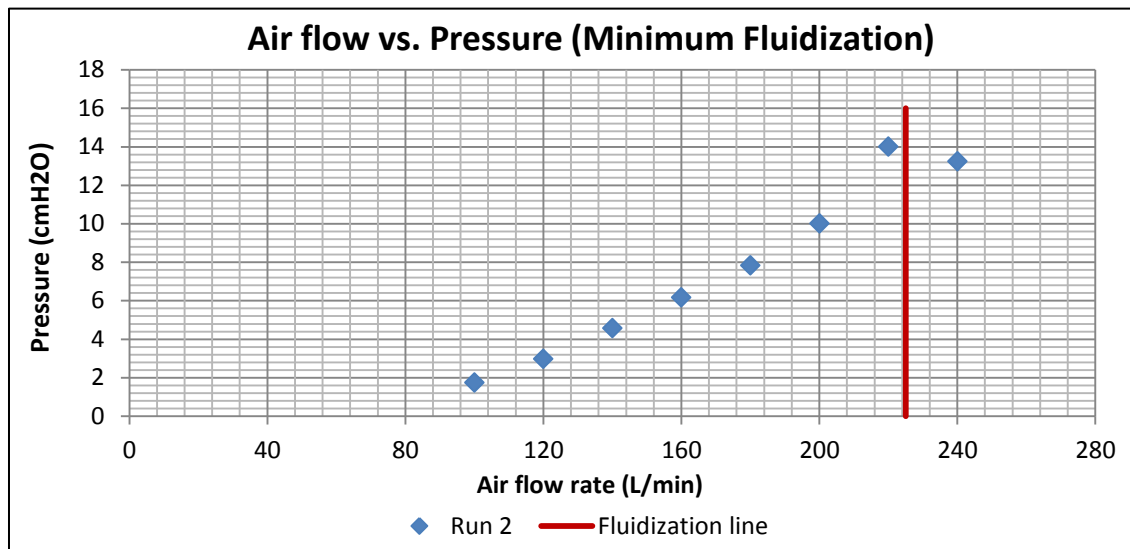


Figure 4-12: Run 2 minimum fluidization graph

It is clear from Figure 4-12 that the data reaches a maximum point ($U_{mf} = 215$ L/min) as discussed in Section 2.6.4, Figure 2-5. The procedure to construct this graph can be seen in Section 3.7. The fluidization air-flow was accordingly chosen as 220 L/min to ensure complete fluidization. This is indicated by the red line in Figure 4-12. It should be kept in mind that Run 2 is a normal fluidization run, with no jigging or magnetite added.

Another indication of the stability of fluidization can be seen in the pressure vs. bed height graph shown in Figure 4-13. The pressure was measured at the respective bed heights with the manometer displayed in Figure 3-2. An interesting observation also noted during experiments is that when magnetite was added to the bed the Pressure vs. Bed height graph did not follow a straight line trend. This observation could also be an indication of when adding magnetite to the bed unstable fluidization occurs because of the high pressure drop and vigorous bubbling. The experimental results for all of the runs are included on the DVD (**Experimental results Rev 3.xls**) attached to the back of this dissertation which can be referred to.

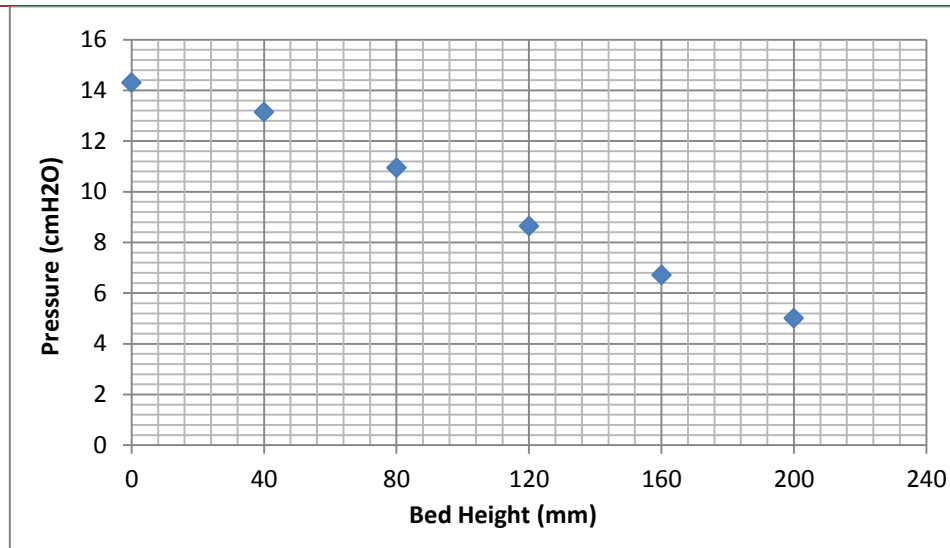


Figure 4-13: Run 2 pressure vs. bed height graph

Since a straight line trend is evident in Figure 4-13, a stable fluidized bed can be assumed. If vigorously bursting bubbles were present, the data would be scattered as the pressure would fluctuate because of vacuums produced by the bursting bubbles. However this is not the case for Run 2. After stable fluidization was reached, the rest of the procedure listed in Section 3.7 was followed and the results shown in Table 4-13 were obtained.

Table 4-13: Run 2 data results

	Density (g/cm ³)	Ash (%)	Moisture (%)	Volatile (%)	Fixed Carbon (%)	CV (MJ/kg)
Bottom layer	1.550	37.6	3.1	20.4	38.9	18.58
Layer 2	1.460	19.5	4.3	24.3	52.0	24.58
Layer 3	1.450	17.6	4.3	24.6	53.5	24.98
Layer 4	1.447	18.3	4.5	24.6	52.6	25.03
Top layer	1.473	15.6	4.4	25.0	55.0	25.75
Difference (1-5) =	0.077	22.0	1.2	4.7	16.1	7.17

It is clear from Table 4-13 that de-ashing occurs at the bottom layer of the bed. As mentioned before, the fluidized bed technology can be seen as a de-ashing process. There is also an evident decrease in CV from the top to the bottom which is to be expected when observing the ash results. In Figure 4-14 the density curve of Run 2 is illustrated. This graph of the density results is indicative of how all the property data will be presented in this section. The primary properties which will be discussed throughout Section 4.5 for each run are:

- Density (g/cm³),
- Ash (%),

School of Chemical and Minerals Engineering

- CV (MJ/kg),
- Moisture (% air-dry basis).

To conclude each run, performance curves (ash vs. yield, ash vs. bed height) will be constructed and the findings discussed.

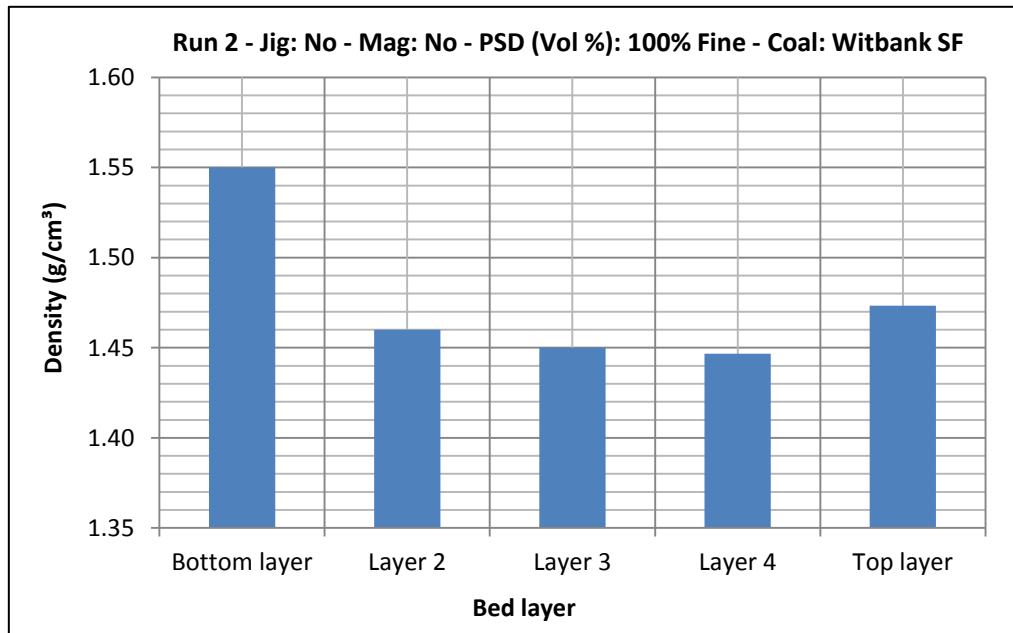


Figure 4-14: Run 2 density curve

The curve in Figure 4-14 indicates a decrease in the density of the particles in the respective layers, which in turn shows the successfulness of the hypothesis that was to be proven. The top layer (1.473g/cm^3) value which is slightly higher than the value of layer 4 (1.447g/cm^3) is within the experimental error calculated in Table 4-5. It is remarkable to note that the coal is primarily upgraded between the bottom and second layer of the bed. This is a trend that will be seen throughout the discussion of the runs. The extent to which the coal is upgraded can be seen from the ash curve in Figure 4-15 and Table 4-13.

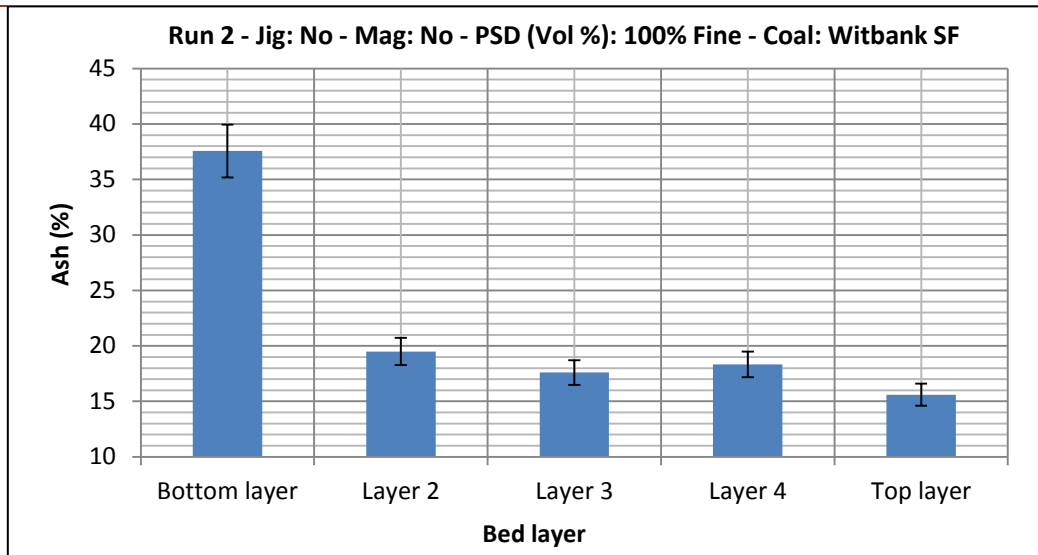


Figure 4-15: Run 2 ash curve

The results indicate that the coal was stratified in the bed from a high 37.6% ash bottom layer, to a low 15.6% ash at the top layer. This is a remarkable 22% difference as seen in Figure 4-15. Industry standards require thermal coal to have an ash percentage of 15-21% for domestic use, and < 15% for export (Steyn & Minnitt, 2010) (also refer to Table 3-2). Therefore if the product stream is taken from layer 2 upwards to the top layer, very good yields should be achieved with an ash percentage below 20. This is very promising results when considering future industry scale operations for a fluidized bed. In Figure 4-16 the CV curve is shown and as ash and CV can directly be correlated for the same coal sample, a similar trend is expected for the CV curve.

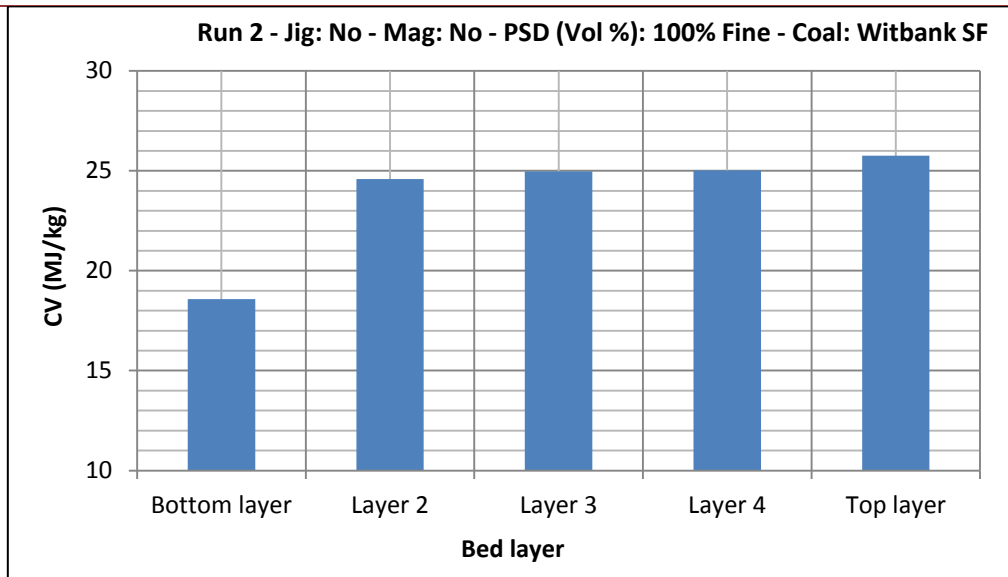


Figure 4-16: Run 2 calorific value curve

Run 2 yielded very good results with respect to CV upgrading of the coal. The CV content of the coal was increased from 18.6 MJ/kg to 25.8 MJ/kg where the feed coal had a CV of 23.6 MJ/kg. Industry standards require the CV of a domestic coal to be > 24.5 MJ/kg and > 27.5 MJ/kg for export (Steyn & Minnitt, 2010). It is clear that, similar to the ash curve, only the bottom layer CV differs substantially from the rest of the layers indicating the best separation between the bottom and second layers of the bed.

A possible explanation for the separation in this specific region could be ascribed to bubble behaviour. It was mentioned in Section 2.7 that the phenomenon of micro bubbles is an indication of stable fluidization which results in better separation. When observing a bubble as it rises through the bed of particles, the observation is that the bubble expands as it moves upward. This is due to the drop in pressure in an upward direction (Escudero & Heindel, 2011). Therefore when the air bubbles enter the bed at the bottom, they are small and described as 'micro bubbles'. Exploding bubbles at the top and middle regions of the bed could be the reason for the negligible separation in the top layers of the bed and the micro bubbles formed when entering the particle bed could be a possible explanation for the good separation occurring in the lower regions of the bed.

The last property of Run 2 that will be discussed is the moisture content. The graph of moisture content vs. bed layer is illustrated in Figure 4-17.

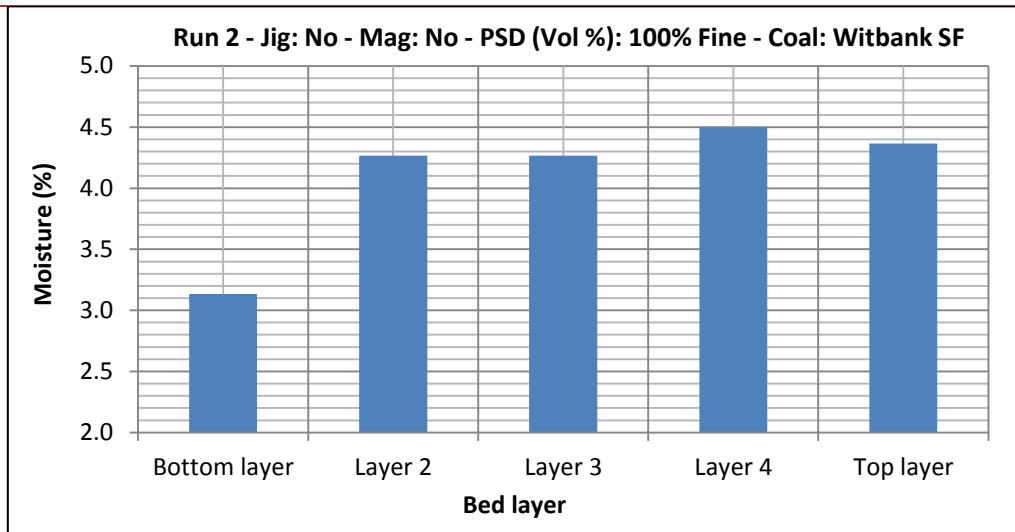


Figure 4-17: Run 2 moisture content curve

An interesting observation seen in Figure 4-17 is that the moisture content of the coal particles is greater at the top of the bed than at the bottom. One would think that the particles with a higher moisture content would be heavier and would in turn sink to the bottom of the bed however, surprisingly the opposite occurs.

A possible explanation for this is that vitrinite rich high quality coals are more porous. More water molecules can enter the particle because of the extra space (England *et al.*, 2002). During this experiment, coal with a higher moisture content, lower ash percentage and higher overall CV floats to the top of the fluidized bed which indicates the effectiveness of fluidization to separate coal according to quality. The separation can also be attributed to effective water-air equilibrium displacement.

Therefore, the fluidized bed separates the coal according to density and ash percentage and not on particle weight (moisture loaded particles) alone, indicating that the primary objective of this study was achieved. The fluidized bed is capable of upgrading fine coal (density and respectively ash/CV separation based).

From the ash data in Table 4-13 performance curves of the fluidized bed could be constructed. These graphs indicate at which bed height the sample should be cut to achieve a specific ash percentage in the product and/or discard coal and what the achievable yields could possibly be. In Figure 4-18 the ash vs. bed height graph for the discard and product streams is shown. To clarify between the difference and similarity of bed height and bed layer in this study please refer to Table 4-1.

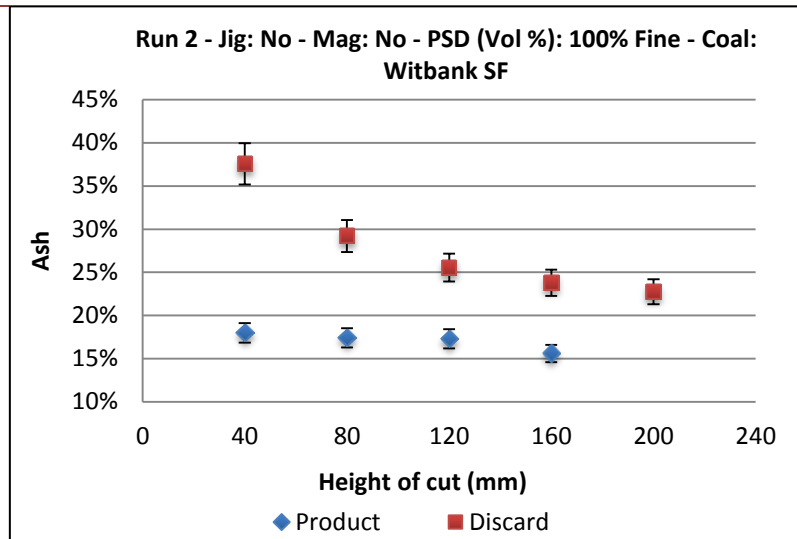


Figure 4-18: Run 2 ash vs. bed height graph

If the performance curve (Figure 4-19) together with the ash vs. bed height graph (Figure 4-18) are considered, the exact bed height can be calculated to achieve the maximum possible yield of the required product ash percentage. Another graph of significance to the performance of the fluidized bed is the yield vs. bed height graph for the discard and product coal. These graphs can be referred to in Appendix B.

Another important graph regarding fluidization is the product ash vs. yield curve. This will indicate the possible yields if a specific ash percentage in the product is required especially when the export and domestic coal specifications shown in Table 3-2 and Table 3-3 are considered. The performance curve (ash-yield curve) as it will be referred to, is illustrated in Figure 4-19.

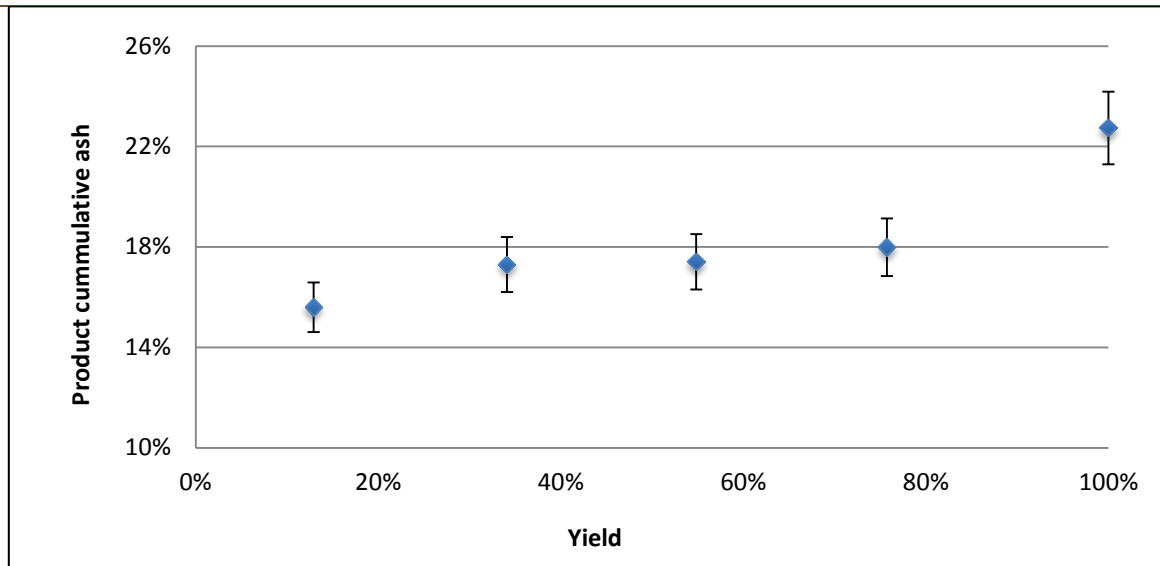


Figure 4-19: Run 2 performance curve

Figure 4-19 shows that the highest possible yield is 75.7% with a corresponding ash percentage of 18%. This is achieved by cutting the sample at a bed height of 40 mm, taking every layer upward (layer 2 to top layer) as product and discarding only 527g of the 2170g total feed.

An interesting observation from Figure 4-19 is that the ash percentage on the Y-axis has a maximum of 18% and a minimum of 15.6%. This results in a difference of only 2.4% ash in the product stream. The fluidized bed can therefore possibly be seen as 'insensitive' to product yields on condition that the same observation is seen in the following run discussions whereby it could be identified as an advantage of the fluidization process and added to the list mentioned in Section 2.7 (advantages of the fluidization process, dry fine coal washing).

4.5.2 Run 6

Run 6 as seen in Table 3-4 is a normal fluidization run. The coal used in run 6 is the Waterberg coal sample and compared to Run 2, Run 6 had almost exactly the same operating conditions. The only difference is the slightly higher air-flow which Run 6 was subjected to. The fluidization air-flow of Run 6 is 225 L/min as seen in Figure 4-20 compared to the 215 L/min in Run 2. The explanation for this could however not be ascribed to the particle size, as it was the same for both runs. The d_{20} and d_{50} of the sample is however different and could explain the higher air-flow needed to fluidize. The amount of higher density material contained in the coal has to be considered.

Figure 4-3 illustrates the washability curve of the Waterberg coal. It is evident that this coal has a higher density than the Witbank SF coal as seen in Figure 4-2. “Higher” refers to the dense fractions’ (1.6-1.8 g/cm³) mass that is larger than the Witbank SF coals’ dense fraction (Refer to Appendix A.1). This therefore explains the slightly higher air-flow needed to fluidize the Waterberg coal. The heavier particles in the Waterberg sample needs to be subjected to a higher air-flow to overcome gravity and to ensure complete fluidization.

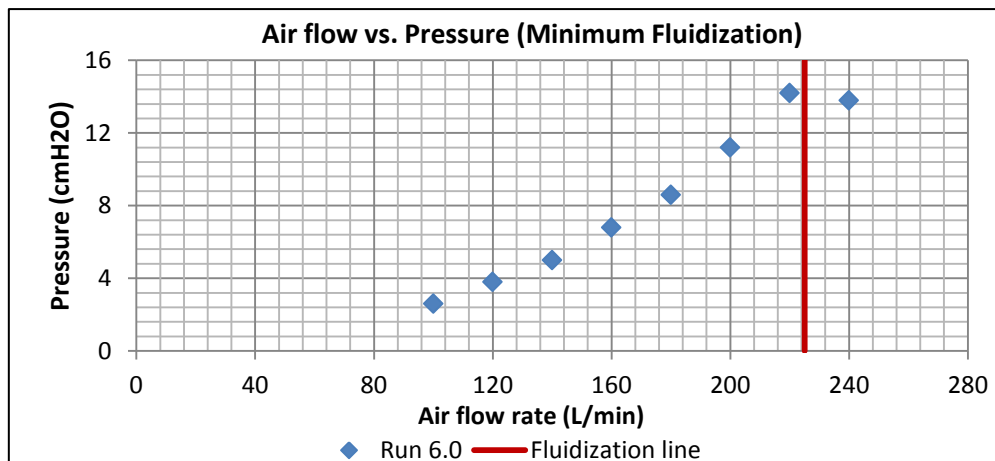


Figure 4-20: Run 6 minimum fluidization graph

From Figure 4-20 it is clear that the fluidization air-flow of Run 6 was chosen as 225 L/min. Regarding the stability of fluidization in Run 6, the graph of pressure vs. bed height is given in Figure 4-21.

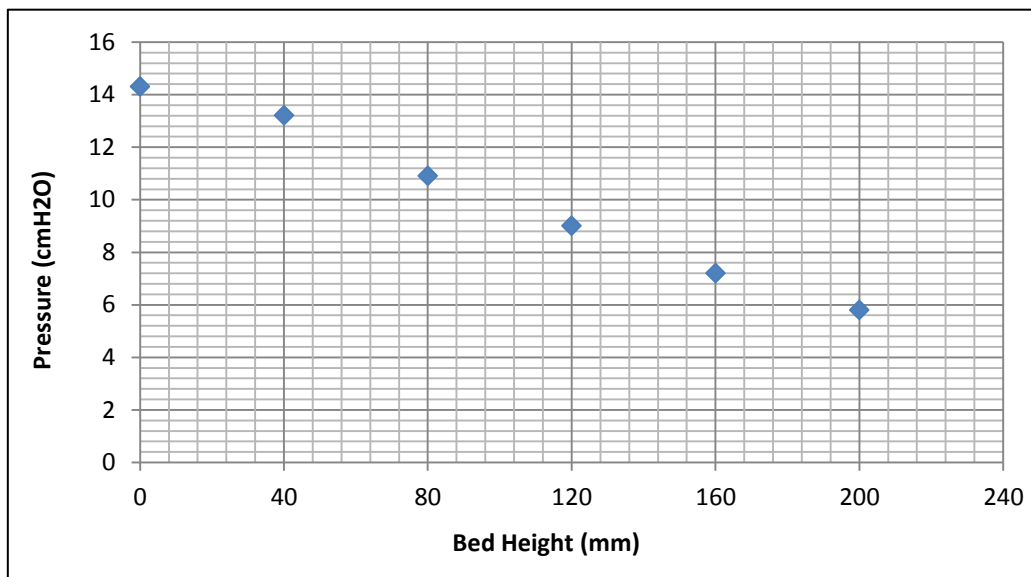


Figure 4-21: Run 6 pressure vs. bed height graph

School of Chemical and Minerals Engineering

It is evident from Figure 4-21 that Run 6 also had a stable fluidized bed similar to Run 2 indicating that good separation should also be expected. The straight line trend evident in Figure 4-21 is an indication of this as mentioned in Run 2. Indicated in Table 4-14 is the property data results of Run 6.

Table 4-14: Run 6 data results

	Density (g/cm ³)	Ash (%)	Moisture (%)	Volatile (%)	Fixed Carbon (%)	CV (MJ/kg)
Bottom layer	1.690	28.2	2.7	20.5	48.6	21.48
Layer 2	1.570	19.6	2.8	20.9	56.7	24.90
Layer 3	1.510	15.2	2.9	21.3	60.6	26.86
Layer 4	1.490	14.1	3.1	21.5	61.3	27.01
Top layer	1.400	11.8	3.2	22.3	62.7	27.53
Difference (1-5) =	0.290	16.4	0.5	1.8	14.1	6.05

Table 4-14 showed good results regarding fine coal washing. De-ashing of the coal is clear in Table 4-14 where the bulk of the separation occurred at the bottom layer.

In Figure 4-22 the density curve of Run 6 is displayed. A clear trend is visible. The separation between the bottom and 2nd layer is significant compared to the rest of the bed as seen in Table 4-14.

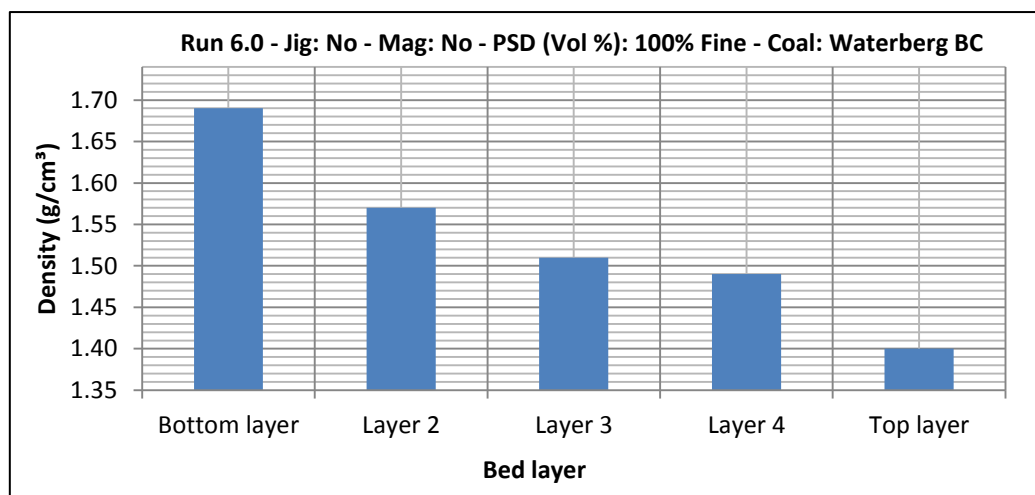


Figure 4-22: Run 6 density curve

Compared to run 2, the density curve of Run 6 has a smoother trend with the density of the bottom layer 1.69 g/cm³ gradually declining to 1.4 g/cm³ at the top.

It should be noted that the difference between Run 2 and Run 6 is the coal sample used. And from the washability tables seen in Appendix A.1, it is clear that the Witbank spiral feed has more near density material than the Waterberg coal. This is in the 1.3-1.5 g/cm³ density

School of Chemical and Minerals Engineering

region where separation primarily occurs. The Waterberg coal only has a 47.7% mass fraction in that density region compared to the 55.3% of the Witbank coal, possibly explaining the slightly different density curve trends between Run 2 and Run 6. To compare the coal washing results between Run 6 and Run 2, the ash curve of Run 6 is included in Figure 4-23.

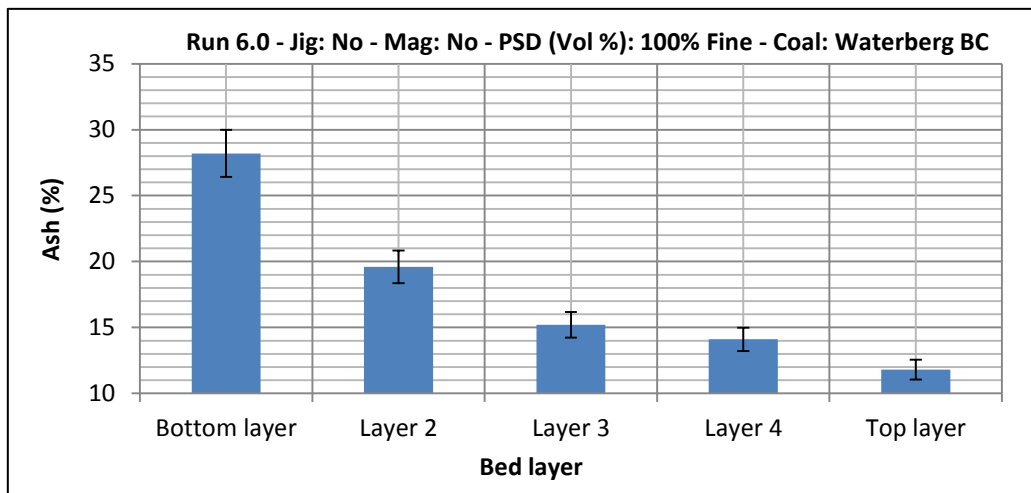


Figure 4-23: Run 6 ash curve

As the density curve of Run 6 had a smoother trend than that of Run 2, the same could be expected for the ash trend, which is evident from Figure 4-23. The ash contained in the coal in Run 6 was stratified from the bottom layer with 28.2% to the top layer with 11.8% ash. A difference of 16.4% which is around 5% less compared to that of Run 2 but considering that the Waterberg coal had a feed ash percentage of 18.6%, it can be stated that the fluidized bed can upgrade better quality coals to the same extent as worse quality coals percentage wise. This explains why a top layer of 11.8% ash was produced compared to the higher ash of Run 2 at 15.6%. Further discussions on the ash of Run 6 can be seen in the performance curve section.

In Figure 4-24 the calorific value curve of Run 6 is illustrated. As expected and to the direct correlation of ash and CV of a coal sample, the CV trend is similar to the trend seen in Figure 4-23. Thermal coal used in South Africa requires a CV value of 24.5-27.5MJ/kg as mentioned before (Steyn & Minnitt, 2010). From the CV results seen in Table 4-14, taking the top four layers and only discarding the bottom layer would produce a CV of over 25.5 MJ/kg, keeping in mind that the feed CV is 25.43 MJ/kg.

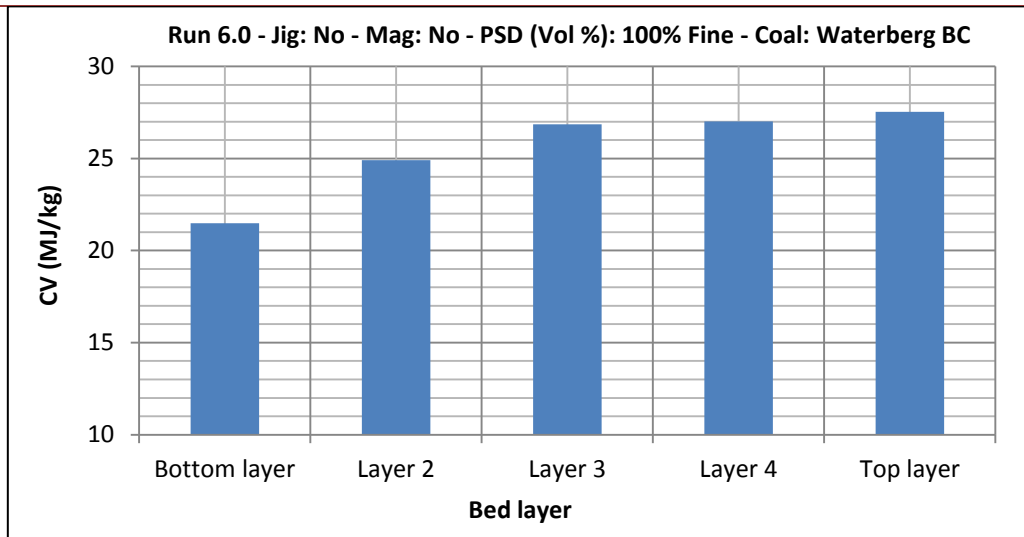


Figure 4-24: Run 6 calorific value curve

The Waterberg coal is more vitrinite rich than the Witbank SF coal used in Run 2. This explains why a higher top layer (27.5 MJ/kg) CV value was obtained compared to Run 2 with a CV of 25.8 MJ/kg. It can be stated that when fluidizing coal particles, the extent to which the coal is upgraded is directly proportional to the quality of the feed coal, making the fluidized bed relatively insensitive to the feed coal quality. This can also be seen in the statistical analysis results in Section 4.4.3, Case 2. The moisture curve of Run 6 is shown in Figure 4-25.

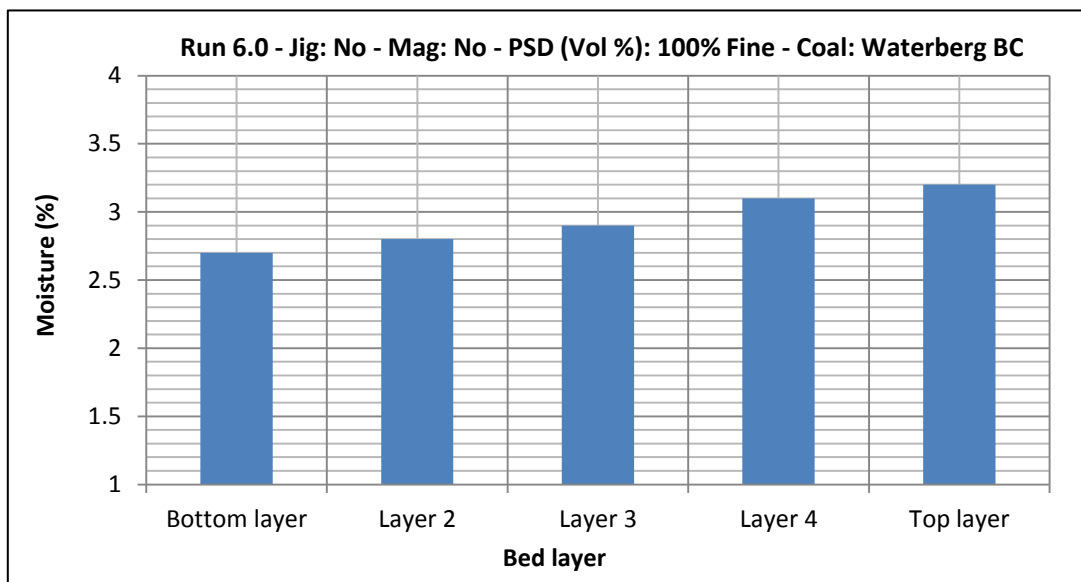


Figure 4-25: Run 6 moisture content curve

School of Chemical and Minerals Engineering

A similar trend is seen in the moisture content curve of Run 6 compared to the curve seen in Run 2. Particles with a higher moisture content are found at the top of the bed and this is a common trend throughout this study indicating the effect of fluidization on coal. The same explanation for Run 2 can be used for Run 6. The vitrinite richer porous particles float to the top of the bed (England *et al.*, 2002).

To assess the performance achieved regarding separation based on ash percentage in Run 6, the ash vs. bed height graph is depicted in Figure 4-26.

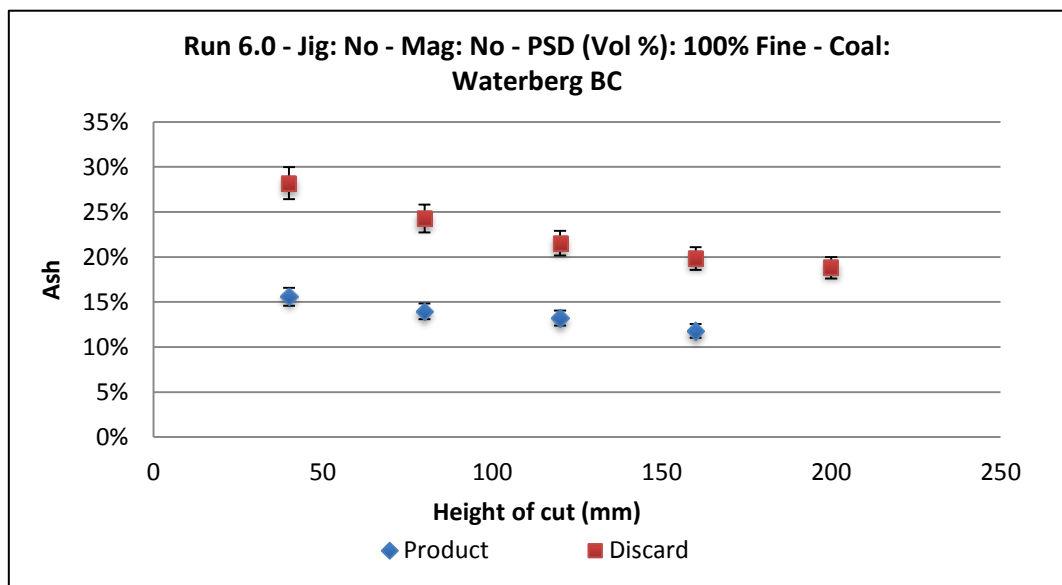


Figure 4-26: Run 6 ash vs. bed height graph

Figure 4-26 indicates that a maximum product yield of 74.6% is possible if only the bottom layer is discarded. In the coal industry it is very important for metallurgical engineers to achieve the highest possible yield with the lowest ash percentage. For a yield as high as 74.6% it is expected that the coal quality would be compromised. This is however not the case as seen in Figure 4-27. The coal ash percentage related to a yield of 74.6% is a low 15.6%.

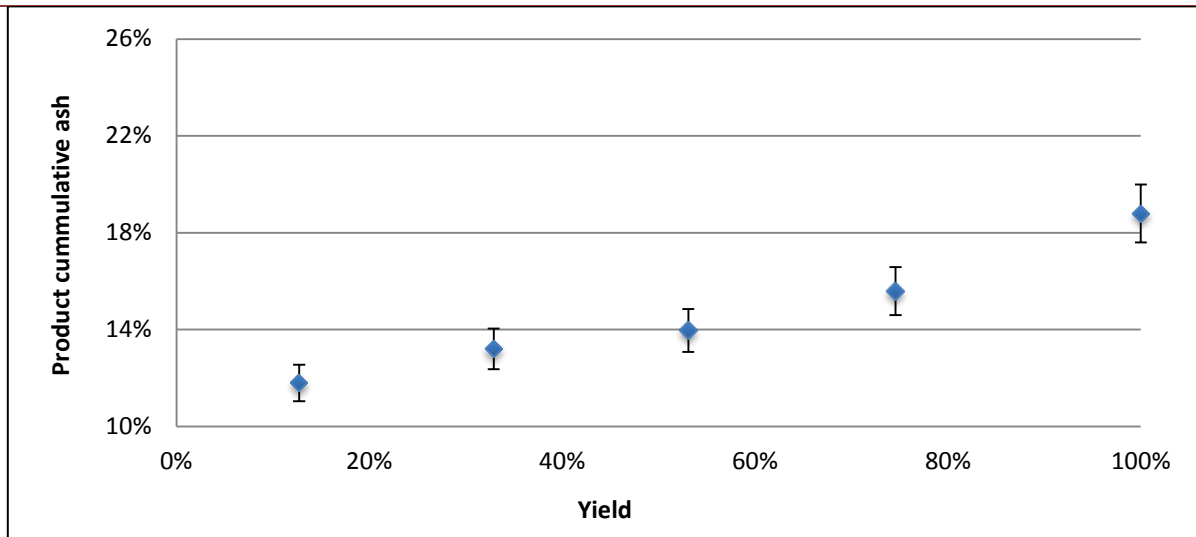


Figure 4-27: Run 6 performance curve

This makes the fluidization process an adequate process to upgrade dry fine coal. Again the insensitive nature of the process regarding yield and ash percentage is displayed in Figure 4-27. From a yield of 74.6% to a yield of 12.7%, the difference in ash percentage is only 3.8%, with an ash percentage of 11.8% related to the latter mentioned yield.

Therefore for normal fluidization without any magnetite added and no jiggling subjected to the air feed, very good results were obtained.

4.5.3 Run 11

Run 11 was the first experiment done with a mixture of a PSD as seen in Table 3-4. This is an unusual mixture of 25% coarse coal and 75% fine coal.

Particle size has a big influence on the fluidization velocity and bed characteristics as mentioned in Section 2.6.4 (Escudero & Heindel, 2011). A discussion on how run 11 came to be follows

Although Run 10 was initially scheduled to be a 100% -2000 + 1180 μ m PSD run, equipment limitations were encountered. During experimentation in Run 10 the air-flow was opened completely but no fluidization elements (bubbles or moving particles) were visible. The air supply which is the lab's compressor line did not have a sufficient air-flow rate to fluidize the particles. A mixture of 50/50 coarse and fine particles was then added to the bed but the air-flow was still insufficient. However, subjecting the bed to a jiggling motion of air resulted in

complete fluidization. Run 10 was therefore a 50/50 mixture of coarse and fine coal with a jiggling motion as seen in Table 3-4. Run number 11 was then set to be a 75% fine and 25% coarse coal run as normal fluidization could only be achieved with this PSD.

The high air-flow requirement is the result of the larger particle feed to the bed. When the particle size increases, the voids between the particles also increase and in turn this requires a higher air-flow to create a sufficient pressure drop to completely fluidize the material bed. This air-flow was too high for the lab compressor to supply resulting in the unusual PSD mixture.

Only when the 25% coarse and 75% fine material was used as the feed to the bed, was the air-flow adequate for normal fluidization which is the configuration used in Run 11. In Figure 4-28 the fluidization graph of Run 11 is illustrated.

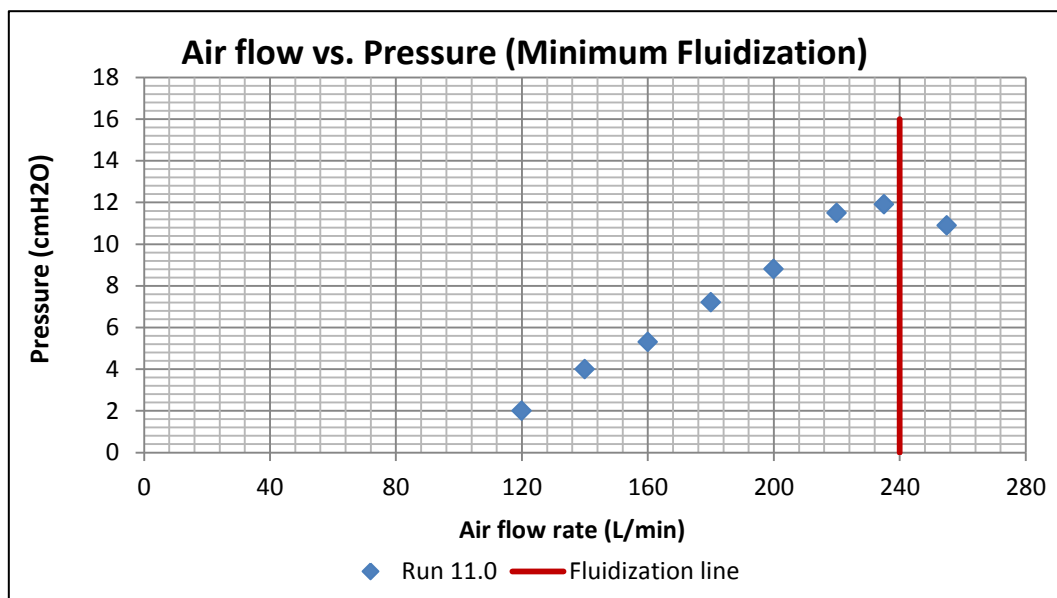


Figure 4-28: Run 11 minimum fluidization graph

As expected, the minimum fluidization air-flow (235 L/min) is higher because of the larger particles present. As a result of the larger particles, the pressure drop at a specific air-flow is also lower compared to finer particles at the same air-flow. This is evident in Figure 4-29.

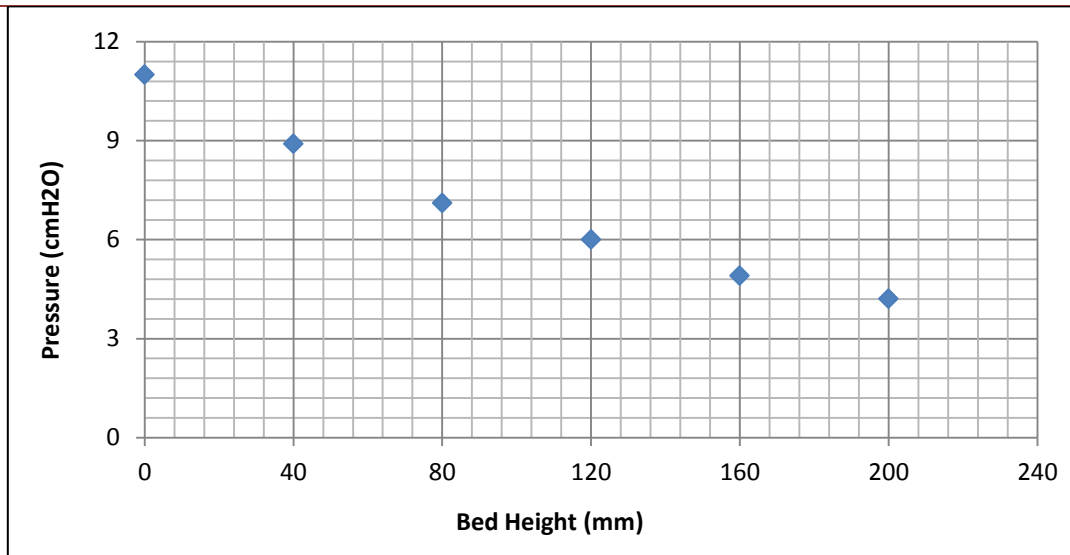


Figure 4-29: Run 11 pressure vs. bed height graph

At the bottom of the bed where the pressure was the highest, the pressure is 11 cmH₂O. However in the case of Run 6 it was 14.3 cmH₂O. The explanation of this event could be the coarser particles present in Run 11. Due to the fact that there is a bigger voidage between coarser particles, the pressure requirement is less than for smaller particles explaining the lower bottom pressure in Run 11. In Figure 4-29 the trend visible is a straight line, indicating stable fluidization as mentioned in the previous run discussions. The data obtained in Run 11 is shown in Table 4-15.

Table 4-15: Run 11 data results

	Density (g/cm ³)	Ash (%)	Moisture (%)	Volatile (%)	Fixed Carbon (%)	CV (MJ/kg)
Bottom layer	1.540	31.2	2.2	20.0	46.6	19.74
Layer 2	1.540	19.5	2.7	21.1	56.7	25.07
Layer 3	1.470	15.9	2.7	21.6	59.8	26.21
Layer 4	1.380	13.5	2.7	22.2	61.6	27.21
Top layer	1.310	12.8	2.6	22.7	61.9	27.64
Difference (1-5) =	0.230	18.4	0.4	2.7	15.3	7.90

Very good results are evident for Run 11. The de-ashing capabilities of the fluidized bed can again be seen in the test results of Run 11. A reduction of ash from bottom to top of the bed is 18% which indicated good separation within the bed. Included in Figure 4-30 is the density curve of Run 11.

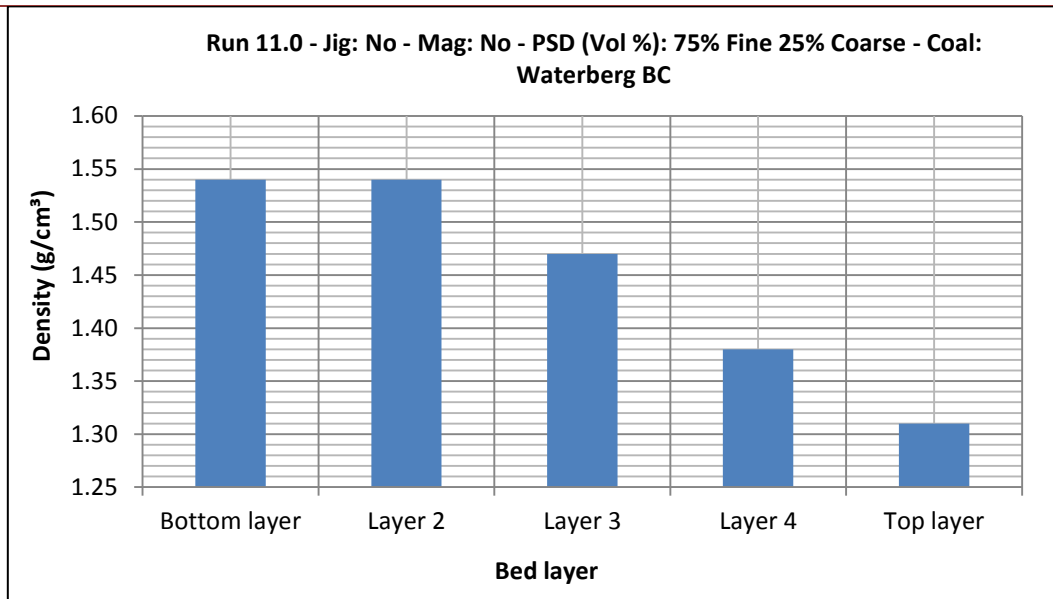


Figure 4-30: Run 11 density curve

The density at both the bottom and second layer is 1.54 g/cm³. In gravity separation, the probability of a particle to appear in the discard or product stream is a strong function of its size (Mohanta *et al.*, 2011). This could have resulted in a larger particle with a lower density appearing in the bottom layer and in turn in the tested sample due to its size. This possibly explains the uniform density of the bottom two layers achieved.

It is evident from Figure 4-30 that the density trend declines slightly more gradually than that of Run 6 when looking at the bottom and second layer density. This is a common trend in runs with coarser particles added and can be referred to in the included figures and tables on the attached DVD. A possible explanation could be the stability of the bed. As mentioned above if coarser particles are added to the bed a lower pressure drop is induced. This in turn causes the bubbles to increase in size more gradually than the bubbles in the finer material bed. This in turn induces more stable fluidization but not necessarily better separation.

The density curve is not the only indication of the separation efficiency of a fluidized bed. An ash curve of Run 11 is indicated in Figure 4-31.

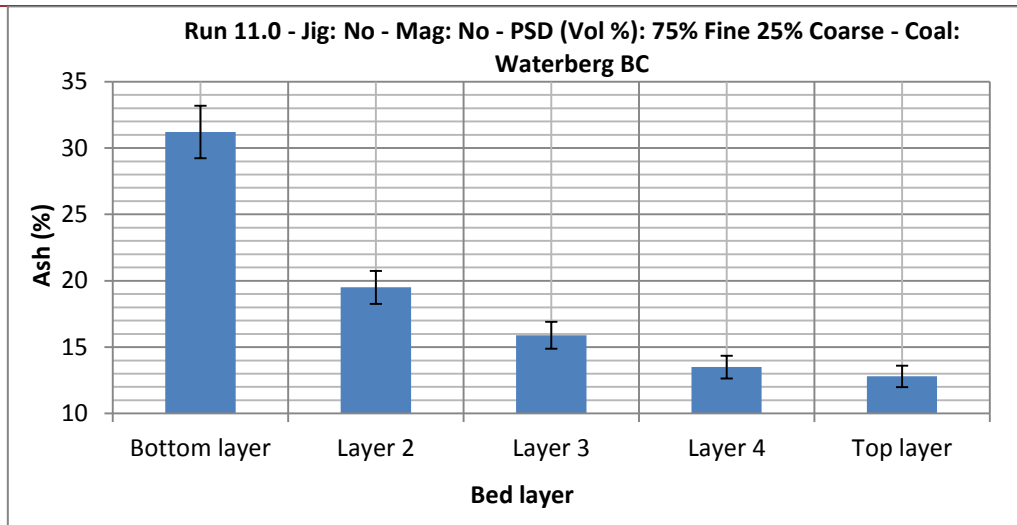


Figure 4-31: Run 11 ash curve

The above mentioned gradual trend is also visible in the ash curve. The ash in the top layer is 12.8% and 31.2% at the bottom layer. The coal sample used in Run 6 is the same for Run 11 and as mentioned although Run 11 shows a higher ash percentage at the top compared to Run 6. Keeping in mind that coarser particles were used during Run 11, the explanation of the slightly higher top layer ash value is possibly due to better liberation. When liberating coal particles, the finer particles have been liberated to a higher extent giving more exposure to the valuable minerals (Wills & Napier-Munn, 2006). This causes the lower ash percentage produced in the top layer of Run 6 (finer coal) compared to Run 11's (coarser coal) top layer ash percentage. The CV curve of Run 11 is illustrated in Figure 4-32.

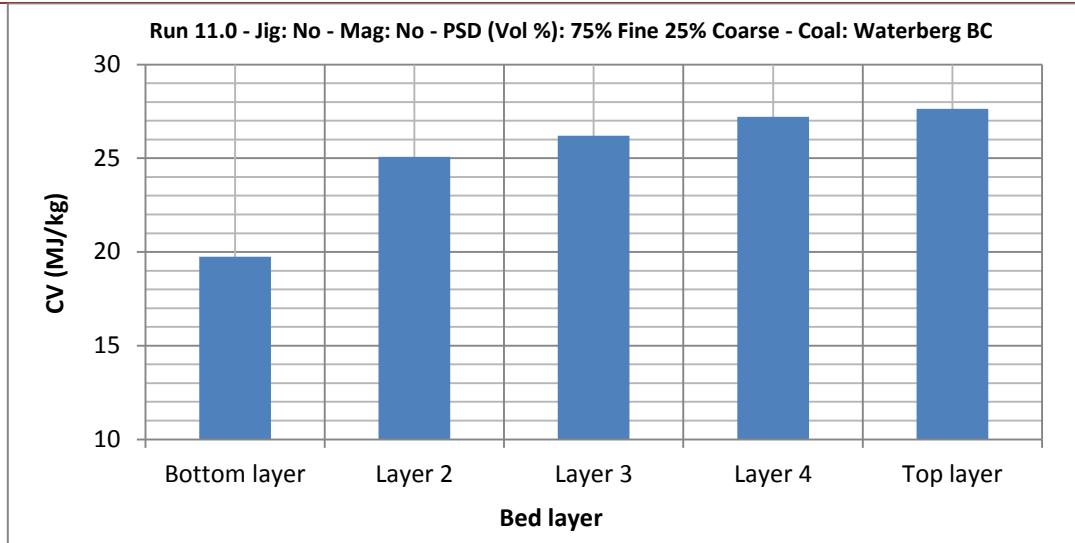


Figure 4-32: Run 11 calorific value curve

Figure 4-32 shows a similar trend to the ash curve above. A gradual increase in CV from bottom to top is evident. If only the top layer is taken as product, the yield would be 14.5% with a CV content of 27.64 MJ/kg. When considering the values in Table 3-2, this layer could be sold as export quality coal.

A balance has to be found between yield and ash/CV to produce the most efficient possible product stream. The fluidized bed technology can therefore be used to clean fine run-of-mine coal. It can also be used as an intermediate process to upgrade already washed fine coal to export quality standards. The moisture curve of Run 11 is shown in Figure 4-33.

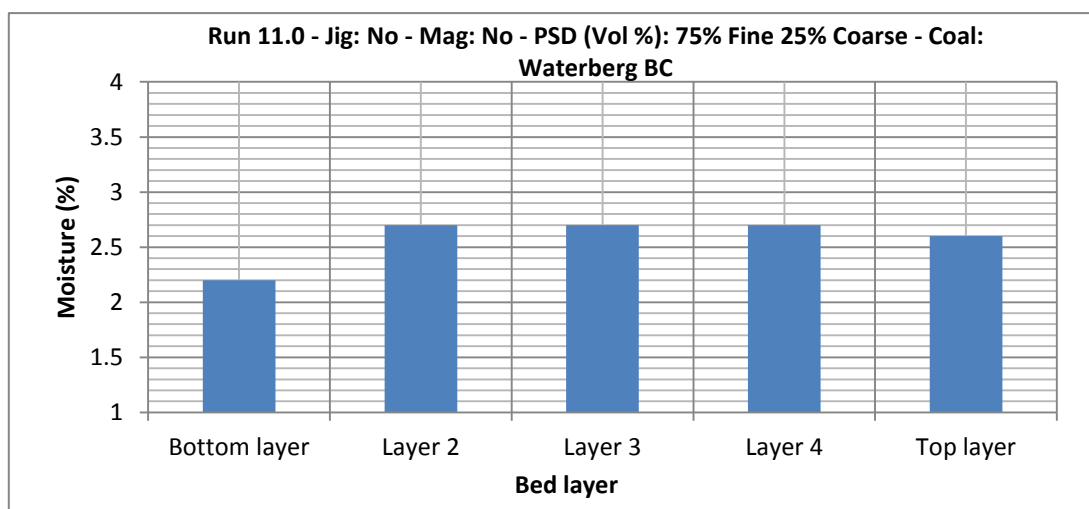


Figure 4-33: Run 11 moisture content curve

School of Chemical and Minerals Engineering

The vitrinite richer coal is found at the top of the bed again. Another explanation, added to the already mentioned explanations illustrated in Run 2 and Run 6, could be that the coal is dried to a higher extent at the bottom compared to the top possibly due to smaller bubbles present at the bottom of the bed. This increases the contact area of the gas and coal particles at the bottom layer. However, the dry compressor air used in the experiment has a low enough moisture content to prevent significant drying of the coal which is why the moisture content does not differ substantially.

In Figure 4-34 the ash vs. bed height graph of Run 11 is illustrated. It is very clear that low ash percentage product yields are possible.

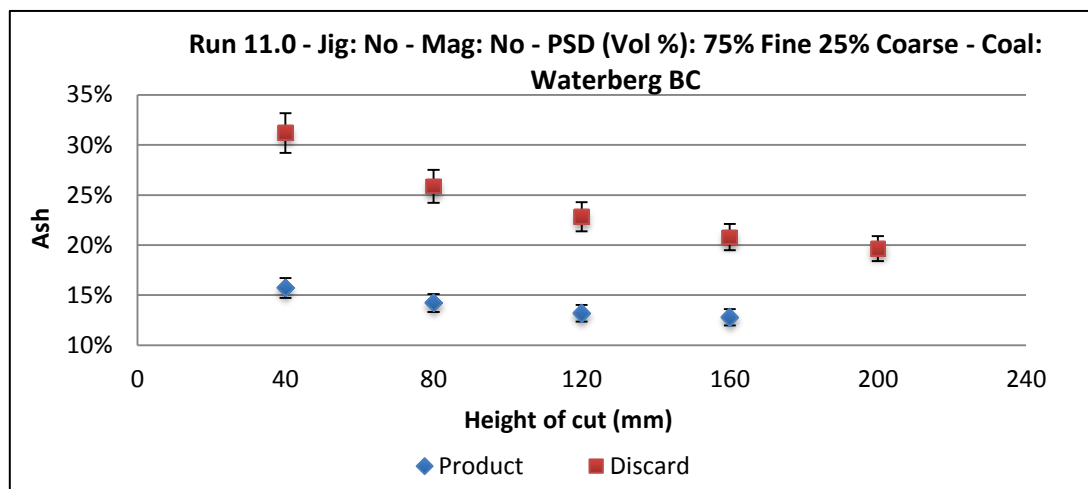


Figure 4-34: Run 11 ash vs. bed height graph

The performance curve indicated in Figure 4-35 again shows the insensitivity of the fluidized bed to ash yields.

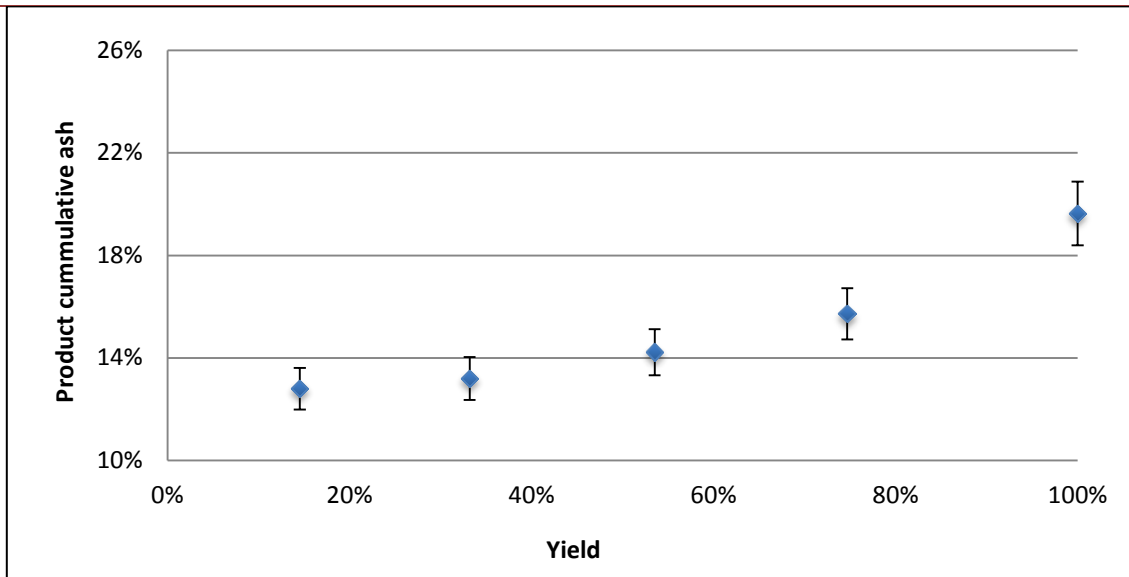


Figure 4-35: Run 11 performance curve

The highest possible yield achievable is 74.7% with a corresponding ash percentage of 15.7% which is very good in comparison with the values with the values found in Table 3-2. Due to the fact that three different runs (Run 2, 6, and 11) produced very similar performance results, it can be stated that the fluidized bed used during this study is insensitive to ash yields.

It should also be noted that the coal samples used had a fairly low ash percentage and including high ash coals in future experiments would be an interesting study to consider. Overall the designed and constructed **150mm** fluidized bed produced promising results with regards to the washing of fine South African coals from the Waterberg and Witbank areas.

For the complete experimental results obtained during this study, the reader is referred to the attached DVD (Appendix B: **Experimental results Rev 3.xls**)

Chapter 5: Conclusions and recommendations

In this chapter, the final conclusions from this study will be presented. Recommendations to further develop this project will also be made in this Chapter.

5.1 Conclusions

The primary objective of this study as stated in Section 1.2 was to prove the validity of a fluidized bed to stratify fine coal according to density which in turn reflects the quality of the coal.

- This objective was successfully accomplished during the study. A fluidized bed (**150 mm ID**) was constructed which was capable of stratifying coal according to density. The best results showed a difference in ash percentage ranging from 15.6% at the top layer to 37.6% at the bottom. The corresponding CV's were 25.75 MJ/kg and 18.58 MJ/kg respectively. The feed properties of the coal were recorded as having an ash percentage of 23.8% and a CV of 23.6 MJ/kg. Therefore a clear stratification of the coal according to quality became evident.
- Mentioned in the objectives was to verify previous results found by Terblanche (2011). The results indicated that coal could be separated according to density by only using air as a dense medium. This was verified as mentioned in the point above during Run 2 where only air was used to fluidize the fine coal.
- Upgrading of the coal occurred almost exclusively in the bottom layer of the bed. This application would be ideally suited as a de-ashing operation where a coal just below specification could be upgraded to a yield above 75%.
- ANOVA analysis indicated that the addition of magnetite to form a dense medium bed, or the application of pulsed air flow to create a jiggling effect, did not have a significant effect on the separation capabilities of the fluidized bed. Best results were obtained when the fluidized bed was operated without applying these two variables.
- Adding magnetite to the feed caused severe channelling during fluidization which in turn led to ineffective separation of the coal. The fineness of the magnetite particles caused an extreme pressure drop across the bed. This limited the force in the upward airflow, resulting in channelling instead of lifting the entire bed.

- The ash vs. yield graphs of the respective runs showed that the fluidized bed technology is relatively insensitive to ash yields.

5.2 Recommendations for the future

- The main bed cylinder could be attached to a vibrating screen and Equation 9 could be used to calculate and adjust the frequency to an intensity which would “break” the rising bubbles. This should produce micro-bubbles which according to Yang *et al.*, (2012b) are required for efficient beneficiation of the coal using a vibrated fluidized bed.
- Experiments on the jiggging frequency and amplitude could be conducted to find the optimum configuration for a specific PSD feed range. This is recommended because indications of better distribution of the gas were observed in some of the jiggging runs.
- A narrower PSD range of the feed coal could be used which should in turn decrease separation based on coal particle size which is not desirable during coal beneficiation processes.
- A secondary visual control system could be designed and implemented. For example, a camera could be attached next to the fluidized bed and changes to the air-flow rate could be made according to the visual characteristics of the bed (refer to the run videos on the attached CD-ROM). A pressure drop system is also a very good indicator of fluidization but due to a large bed diameter the probe does not always capture the true pressure drop of the entire bed. Therefore as a secondary control system the visual process could be beneficial to the fluidized bed equipment.
- Magnetite could be added to the feed with a larger particle size than the magnetite used in this study ($d_{50} = 24\mu\text{m}$). This particle size should be small enough to cancel out the coal/magnetite particle interactions, but also large enough to reduce the effects of channelling air through the bed. The recommended estimated d_{50} of the magnetite is $150\mu\text{m}$.
- Further experiments could be conducted with higher ash percentage coals to compare the upgrading capabilities of the fluidized bed between higher and lower ash percentage coals.

Bibliography

- AMINOV, A. 2011. Mongolian coking-coal producer. *Mining journal*:3-14. October.
- CHEN, Q. & WEI, L. 2003. Coal dry beneficiation technology in China: The state-of-the-art. *China Particuology*, 1(2):52-56. 18 March.
- CHEN, Q. & WEI, L. 2005. Development of coal dry beneficiation with air-dense medium fluidized bed in China. *China Particuology*, 3:42.
- CHEN, Q. & YANG, Y. 2003. Development of Dry Beneficiation of Coal in China. *Coal Preparation*, 23:3–12. 20 January.
- CHIKEREMA, P. & MOYS, M. 2012. Effects of Particle Size, Shape, and Density on the Performance of an Air Fluidized Bed in Dry Coal Beneficiation. *International Journal of Coal Preparation and Utilization*:80-94. 20 March.
- DWARI, R.K. & RAO, K.H. 2007. Dry beneficiation of coal - A review. *Mineral Processing & Extractive Metall*, 28:177-234.
- EBERHARD, A. 2011. *The future of South African coal: Market, investment, and policy challenges*. Stanford.
- EBERHARD, A. 2012. Overview of South African coal sector. *Coal International* January.
- ENGLAND, T., HAND, P.E., MICHAEL, D.C., FALCON, L.M. & YELL, A.D. 2002. Coal preparation in South Africa. Pietermaritzburg: Natal witness commercial printers.
- ERDENETSOGT, B.O., LEE, L., BAT-ERDENE, D. & JARGAL, L. 2009. Mongolian coal-bearing basins: Geological settings, coal characteristics, distribution, and resources. *International Journal of Coal Geology*:87–104. 4 August.
- ESCUDERO, D. & HEINDEL, T.J. 2011. Bed height and material density effects on fluidized bed hydrodynamics. *Chemical Engineering Science*:3648–3655. 27 April.
- FAN, M., CHEN, Q., ZHAO, Y., GUAN, Z.L.Y & LI, B. 2001. Magnetically stabilized fluidized beds for fine coal separation. *Powder Technology*:208-211. 6 September.

School of Chemical and Minerals Engineering

FEIL, N.F., SAMPAIO, C.H. & WOTRUBA, H. 2011. Influence of jig frequency on the separation of coal from the Bonito seam — Santa Catarina, Brazil. *Fuel Processing Technology*:22–26. 8 December.

GUPTA, S.K., AGARWAL, V.K., SINGH, S.N., SESHARDI, V., MILLS, D., SINGH, J. & PRAKASH, C. 2009. Prediction of minimum fluidization velocity for fine tailings materials. *Powder Technology*:263-271. 6 August.

HE, J., ZHAO, Y., HE, Y., LUO, Z. & DUAN, C. 2013. South Africa using the dense gas-solid fluidized bed beneficiation technique. *The Journal of The Southern African Institute of Mining and Metallurgy*, 113:575-582. July.

HOUWELINGEN, J.A. & DE JONG, T.P.R. 2004. Dry cleaning of coal: Review, fundamentals and opportunities. *Geologica belgica*, 7:335-343.

JEFFREY, L.S. 2005. Characterization of the coal resources of South Africa. *The South African Institute of Mining and Metallurgy*:95-102. 9 September.

KUMAR, P., SAH, R., ARI, V. & DAS, A. 2010. Dry beneficiation of coal fines using air table. *Mineral Processing Technology*:446–451.

KUNII, D. & LEVENSPIEL, O. 1991. Fluidization Engineering. Newton: Butterworth-Heinemann.

LEONARD, J.W. & HARDINGE, B.C. 1991. Coal Preparation. 5th ed. Littleton: Society for mining, metallurgy, and exploration, inc.

LEVIN, D. 2012. *In Mongolia, a New, Penned-In Wealth*.

LUO, Z. & CHEN, Q. 2001. Dry beneficiation technology of coal with an air dense-medium fluidized bed. *International journal of mineral processing*:167-175. 3 April.

LUO, Z., FAN, M., ZHAO, Y., TAO, X., CHEN, Q. & CHEN, Z. 2008. Density-dependent separation of dry fine coal in a vibrated fluidized bed. *Powder Technology*, 187:119-123. 8 February.

School of Chemical and Minerals Engineering

- LUO, Z.F., TANG, L.G., DAI, N.N. & ZHAO, Y.M. 2012. The effect of a secondary gas-distribution layer on the fluidization characteristics of a fluidized bed used for dry coal beneficiation. *International Journal of Mineral Processing*:28-33. 9 December.
- LUO, Z., ZHAO, Y., CHEN, Q., FAN, M. & TAO, X. 2002. Separation characteristics for fine coal of the magnetically fluidized bed. *Fuel Processing Technology*:63-69.
- LUO, Z., ZHAO, Y., TAO, X., FAN, M., CHEN, Q. & WEI, L. 2003. Progress in Dry Coal Cleaning Using Air-Dense Medium Fluidized Beds. *Coal Preparation*, 23:13-20. 15 January.
- LUO, Z., ZHU, J., FAN, M., ZHAO, Y. & TAO, X. 2007. Low Density Dry Coal Beneficiation Using an Air Dense Medium Fluidized Bed. *Journal of China University of Mining & Technology*, 17:306–309. 5 March.
- MAOMING, F., QINGRU, C., YUEMIN, Z., ZHENFU, L., XINXI, Z., XIUXIANG, T. & GUOHUA, Y. 2003. Fine coal dry classification and separation. *The European Journal of Mineral Processing and Environmental Protection*, 3(2):196-201. 10 June.
- MOHANTA, S., CHAKRABORTY, S. & MEIKAP, B.C. 2011. Influence of Coal Feed Size on the Performance of Air Dense Medium Fluidized Bed Separator Used for Coal Beneficiation. *Industrial and Engineering Chemistry Research*:10865–10871. 19 August.
- MOHANTA, S., RAO, C.S., DARAM, A.B., CHAKRABORTY, S. & MEIKAP, B.C. 2013. Air Dense Medium Fluidized Bed for Dry Beneficiation of Coal: Technological Challenges for Future. *Particulate Science and Technology*:16-27.
- MUKHERJEE, A.K., DWIVEDI, V.K. & MISHRA, B.K. 2005. Analysis of a laboratory jigging system for improved performance. *Minerals Engineering*:1037-1044. 9 March.
- OSBORNE, D.G. 1988. Preparation Technology. Graham & Trotman Ltd.
- PHILANDER, G. 2010. www.cosechaypostcosecha.org. Date of access: 16 October 2011.
- ROUX, R. 2012. *Air dense medium fluidisation of fine coal*. Potchefstroom.

School of Chemical and Minerals Engineering

RÜDISÜLI, M., SCHILDHAUER, T.J., BIOLLAZ, S.M.A. & RUUD VAN OMMEN, J. 2011. Scale-up of bubbling fluidized bed reactors — A review. *Powder Technology*:21-38. 1 October.

SAHU, A.K., BISMAL, S.K. & PARIDA, A. 2009. Development of air dense medium fluidized bed technology for dry beneficiation of coal – A review. *International Journal of Coal Preparation and Utilization*:216-241. 10 June.

SAMPAIO, C.H., ALIAGA, W., PACHECO, E.T., PETTER, E. & WOTRUBA, H. 2007. Coal beneficiation of Candiota mine by dry jigging. *Fuel Processing Technology*:198-202. 5 September.

STEYN, M. & MINNITT, R.C.A. 2010. Thermal coal products in South Africa. *The Journal of The Southern African Institute of Mining and Metallurgy*, 110:593-599. October.

TERBLANCHE, A.N. 2011. *Dry beneficiation of fine coal using a fluidized bed*. Potchefstroom.

WEI, L., CHEN, Q. & ZHAO, Y. 2003. Formation of Double-Density Fluidized Bed and Application in Dry Coal Beneficiation. *Coal preparation*, 23:21-32. 20 January.

WILLS, B.A. & NAPIER-MUNN, T.J. 2006. *Wills' mineral processing technology*. Burlington: Elsevier Ltd.

YANG, X., ZHAO, Y., LI, G., LUO, Z., CHEN, Z. & LIANG, C. 2012a. Establishment and Evaluation of a United Dry Coal Beneficiation System. *International Journal of Coal Preparation and Utilization*:95-102. 20 March.

YANG, X., ZHAO, Y., LUO, Z., SONG, S., DUAN, C. & DONG, L. 2012b. Fine coal dry cleaning using a vibrated gas-fluidized bed. *Fuel Processing Technology*:338-343. 22 Augustus.

ZHAO, Y., LI, G., LUO, Z., LIANG, C., TANG, L., CHEN, Z. & XING, H. 2011. Modularized dry coal beneficiation technique based on gas-solid fluidized bed. *National Natural Science Foundation of China*, 18:374-380. 10 Desember.

School of Chemical and Minerals Engineering

ZHAO, Y.M., LIU, X.J., LIU, K.L., LUO, Z.F., WU, W.C., SONG, S.L. & TANG, L.G. 2010b. Fluidization characteristics of a gas-paigeitite-powder bed to be utilized for dry coal beneficiaton. *International Journal of Coal Preparation and Utilization*:149–160. 28 July.

ZHAO, Y.M., LUO, Z.F., CHEN, Z.Q., TANG, L.G., WANG, H.F. & XING, H.B. 2010a. The effect of feed-coal particle size on the separating characteristics of a gas-solid fluidized bed. *The Journal of The Southern African Institute of Mining and Metallurgy*, 110:219-224. May.

ZHAO, Y., TANG, L., LUO, Z., LIANG, C., XING, H., WU, W. & DUAN, C. 2010c. Experimental and numerical simulation studies of the fluidization characteristics of a separating gas–solid fluidized bed. *Fuel Processing Technology*:1819-1825. 1 August.

Appendix A – Experimental results

A.1. Feed coal washability data tables

Table 7-1: Washability data table: Witbank filter feed

Witbank filter Feed					
Sample Identity		Mass g		% Yield	
		Total	Fract	Fract	Cumul
FILTER FEED FFT		ISO 7936:1992 *			
Sample Mass		170			
F1.20	1.2		1.25	0.76	0.76
F1.30	1.3		12.09	7.30	8.05
F1.40	1.4		42.78	25.81	33.86
F1.50	1.5		29.02	17.51	51.36
F1.60	1.6		45.51	27.45	78.82
F1.70	1.7		11.80	7.11	85.93
F1.80	1.8		8.33	5.02	90.96
Si1.80			14.99	9.04	100
Total			165.7846	100	

Table 7-2: Washability data table: Witbank spiral feed

Witbank spiral Feed					
Sample Identity		Mass g		% Yield	
		Total	Fract	Fract	Cumul
SPIRAL FEED SFT		ISO 7936:1992 *			
Sample Mass		248.03			
F1.20	1.2		3.75	1.53	1.53
F1.30	1.3		30.67	12.52	14.05
F1.40	1.4		58.23	23.76	37.81
F1.50	1.5		46.73	19.07	56.88
F1.60	1.6		46.34	18.91	75.79
F1.70	1.7		6.97	2.84	78.64
F1.80	1.8		8.77	3.58	82.22
Si1.80			43.57	17.78	100
Total			245.0299	100	

Table 7-3: Washability data table: Waterberg

Waterberg (bright coal)					
Sample Identity		Mass g		% Yield	
		Total	Fract	Fract	Cumul
WATERBERG FEED WBT		ISO 7936:1992 *			
Sample Mass		240			
F1.20	1.2		1.15	0.52	0.52
F1.30	1.3		6.45	2.92	3.44
F1.40	1.4		61.94	28.06	31.50
F1.50	1.5		36.99	16.75	48.26
F1.60	1.6		37.53	17.00	65.26
F1.70	1.7		11.12	5.04	70.29
F1.80	1.8		27.40	12.41	82.70
Si1.80			38.19	17.30	100
Total			220.7664	100	

A.2 Repeatability graphs

Run 2

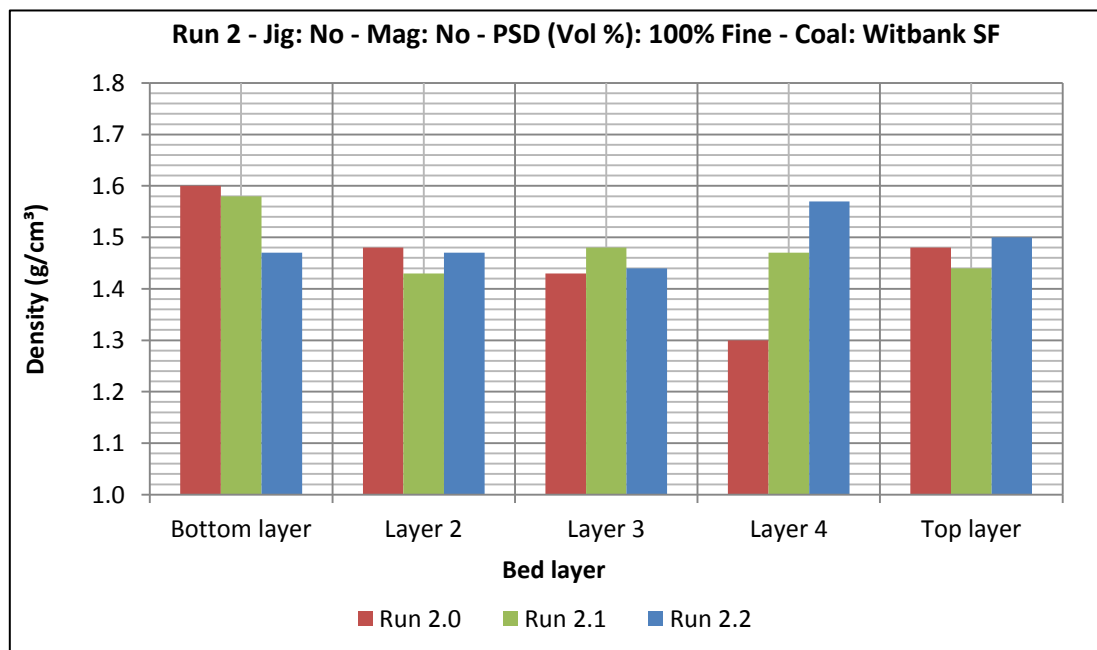


Figure 7-1: Run 2 density repeatability graph

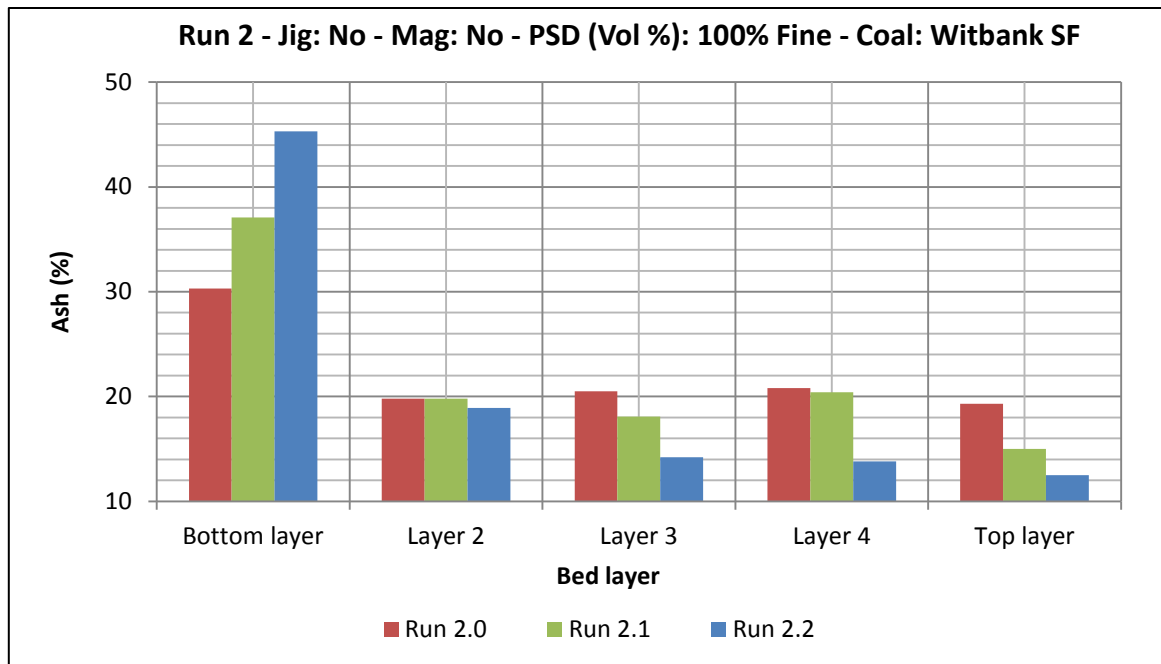


Figure 7-2: Run 2 ash repeatability graph

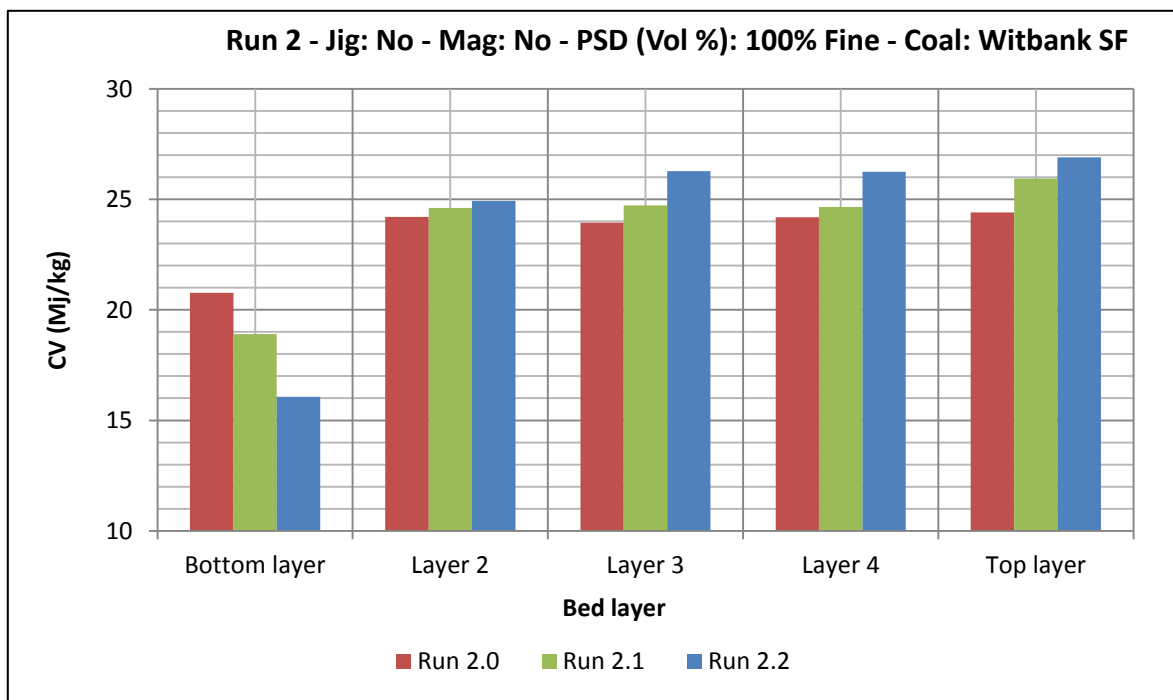


Figure 7-3: Run 2 CV repeatability graph

Run 3

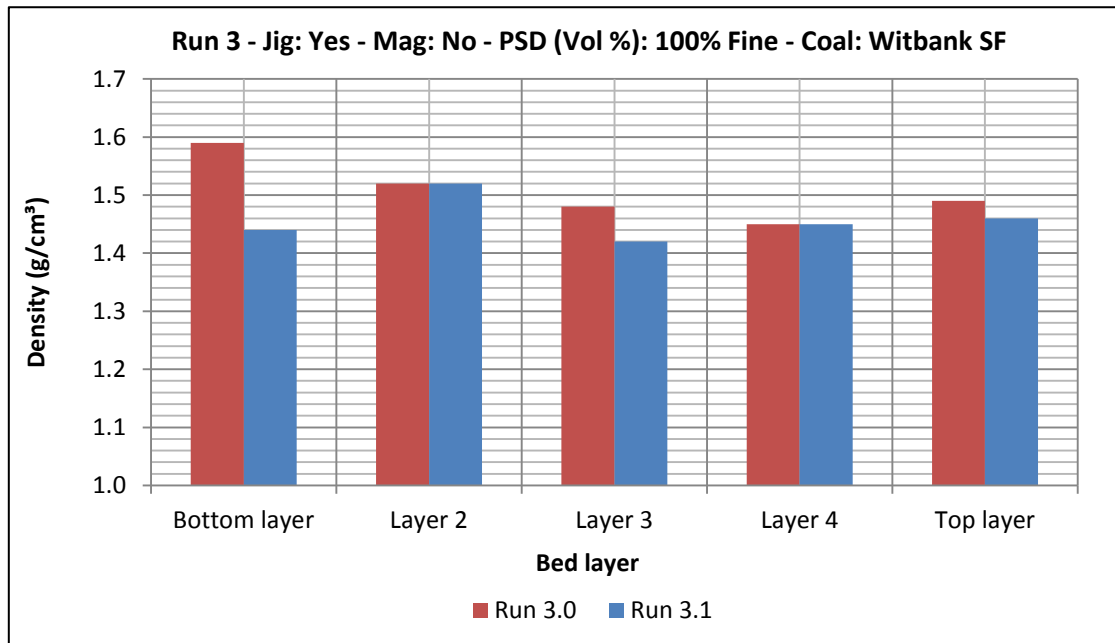


Figure 7-4: Run 3 density repeatability graph

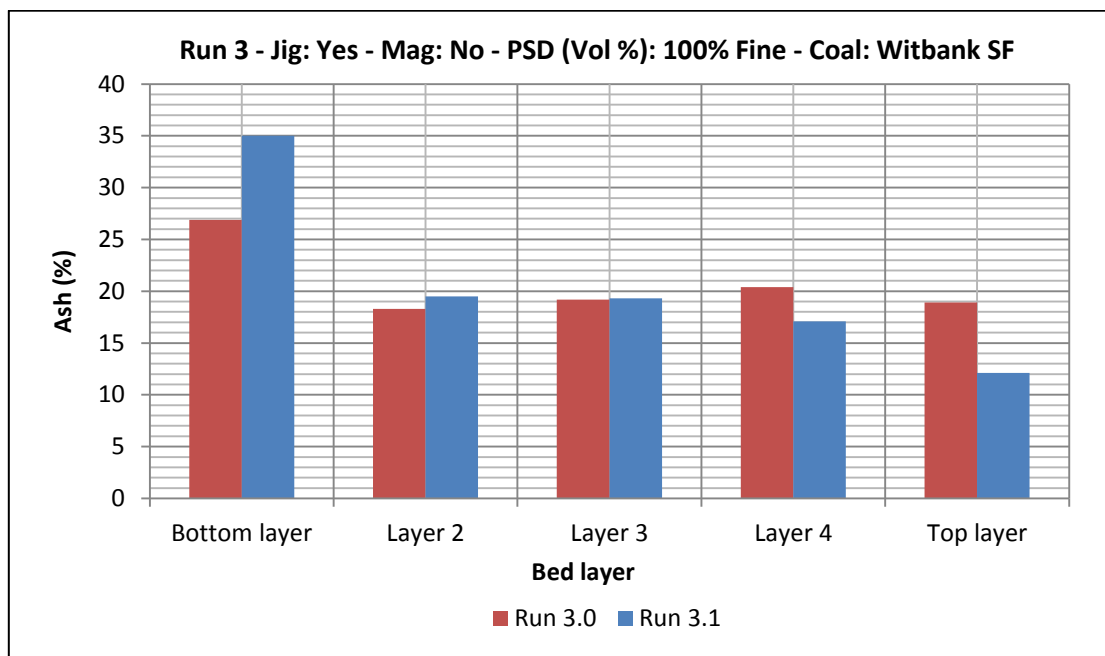


Figure 7-5: Run 3 ash repeatability graph

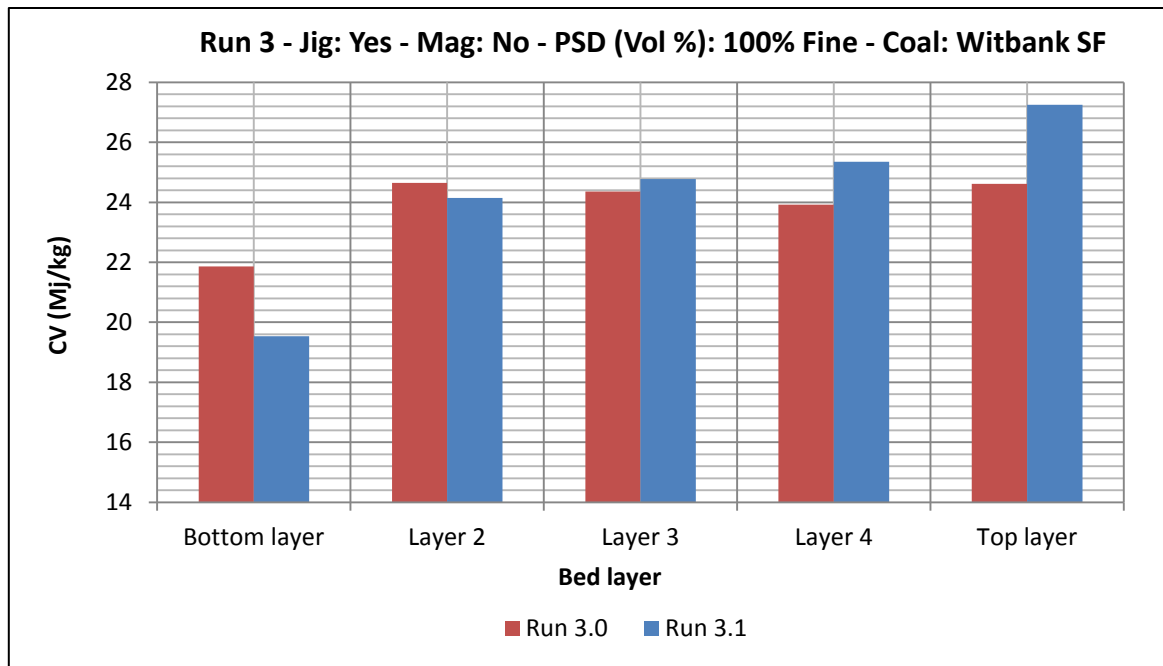


Figure 7-6: Run 3 CV repeatability graph

Run 8

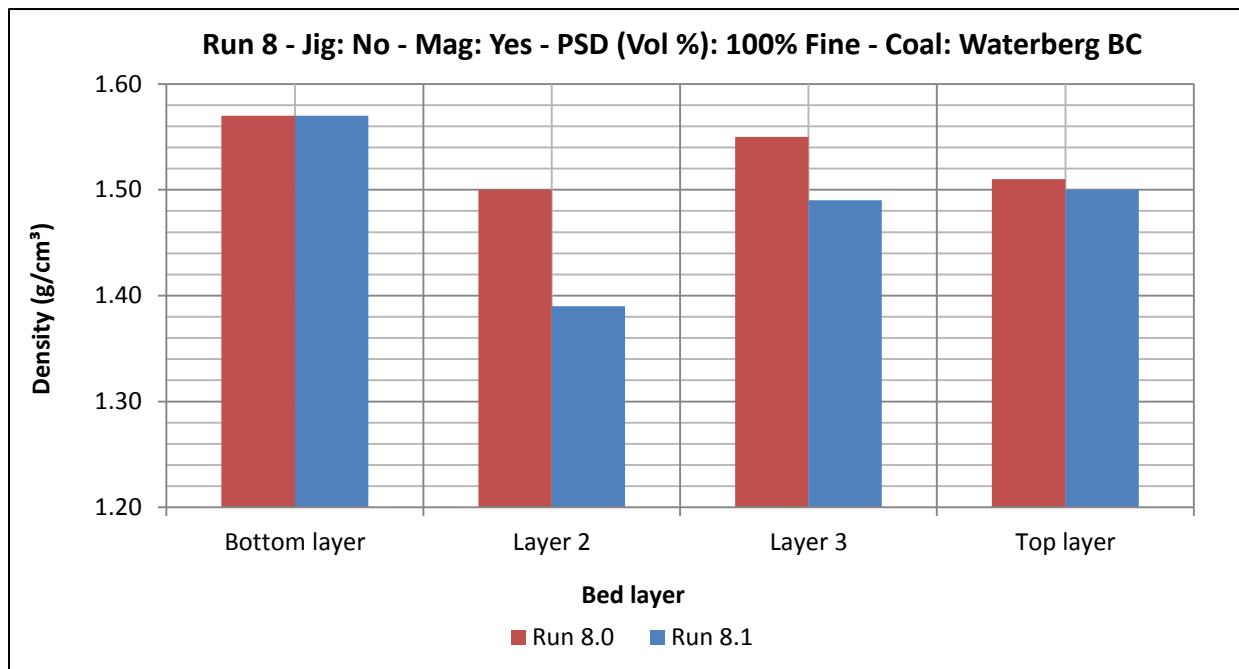


Figure 7-7: Run 8 density repeatability graph

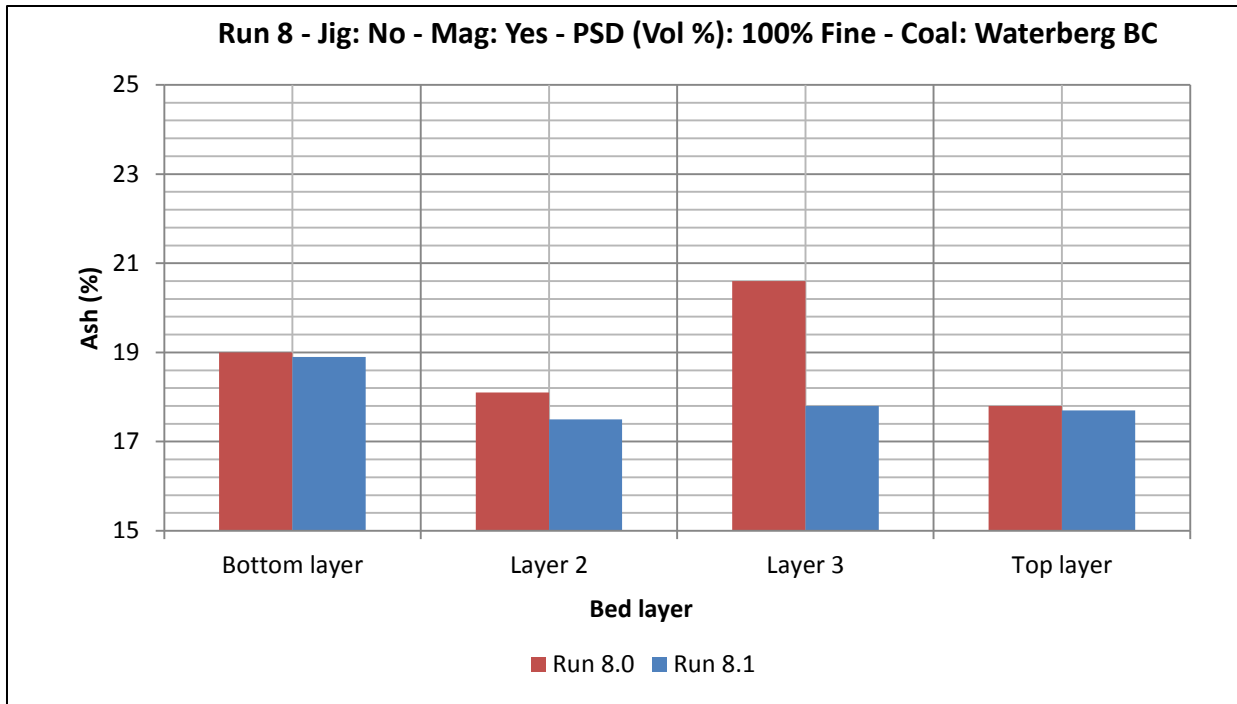


Figure 7-8: Run 8 ash repeatability graph

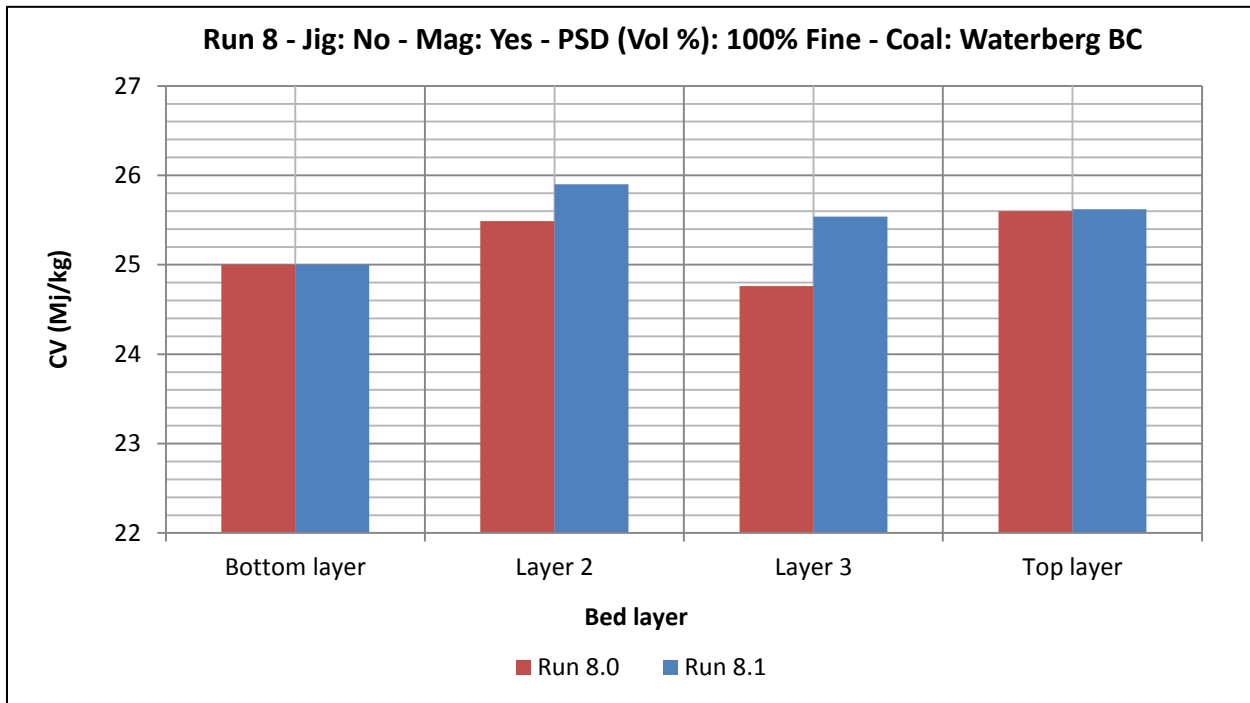


Figure 7-9: Run 8 CV repeatability graph

Run 9

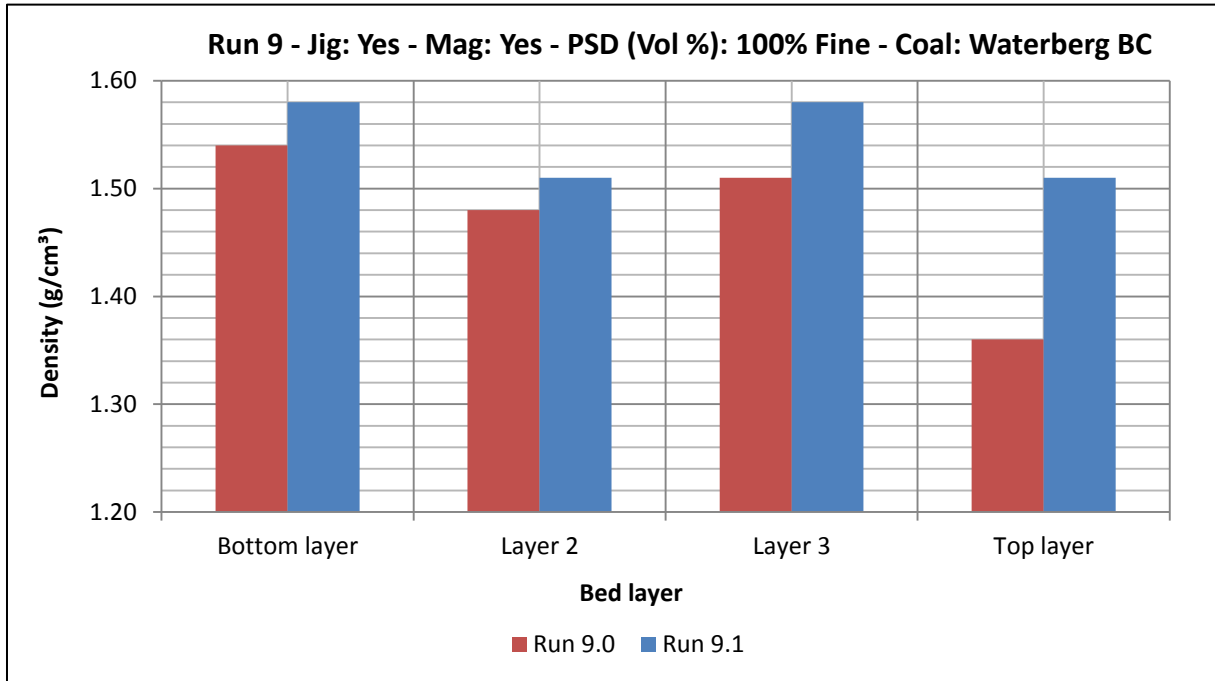


Figure 7-10: Run 9 density repeatability graph

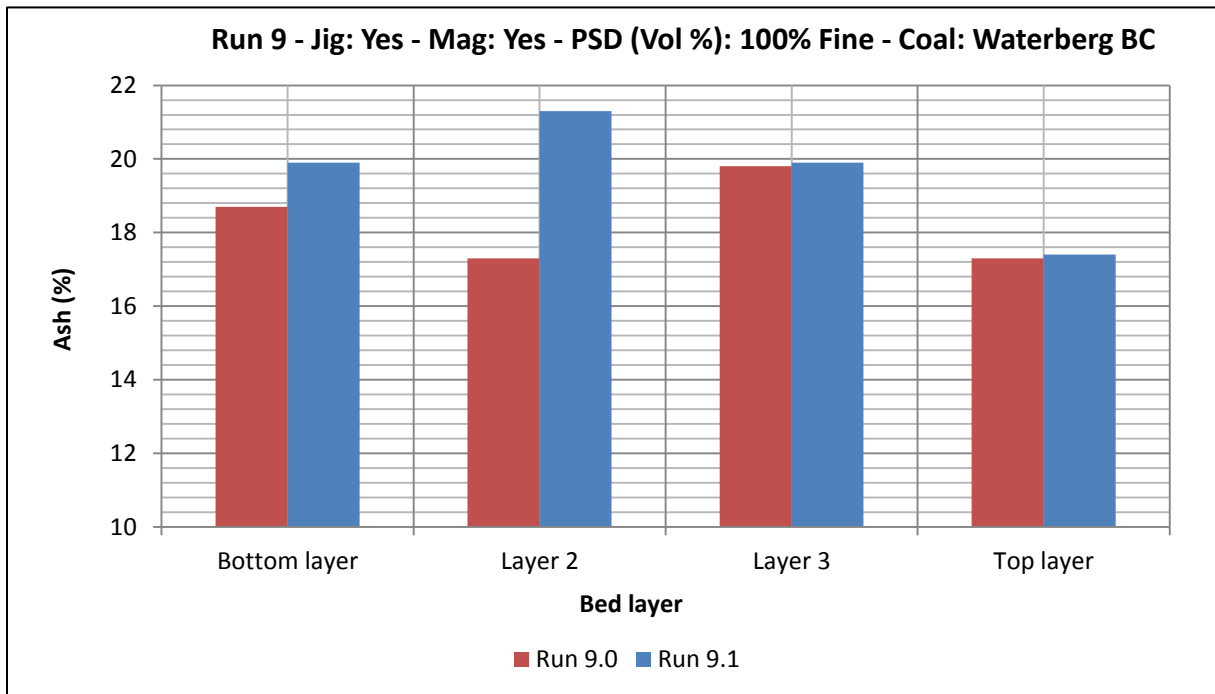


Figure 7-11: Run 9 ash repeatability graph

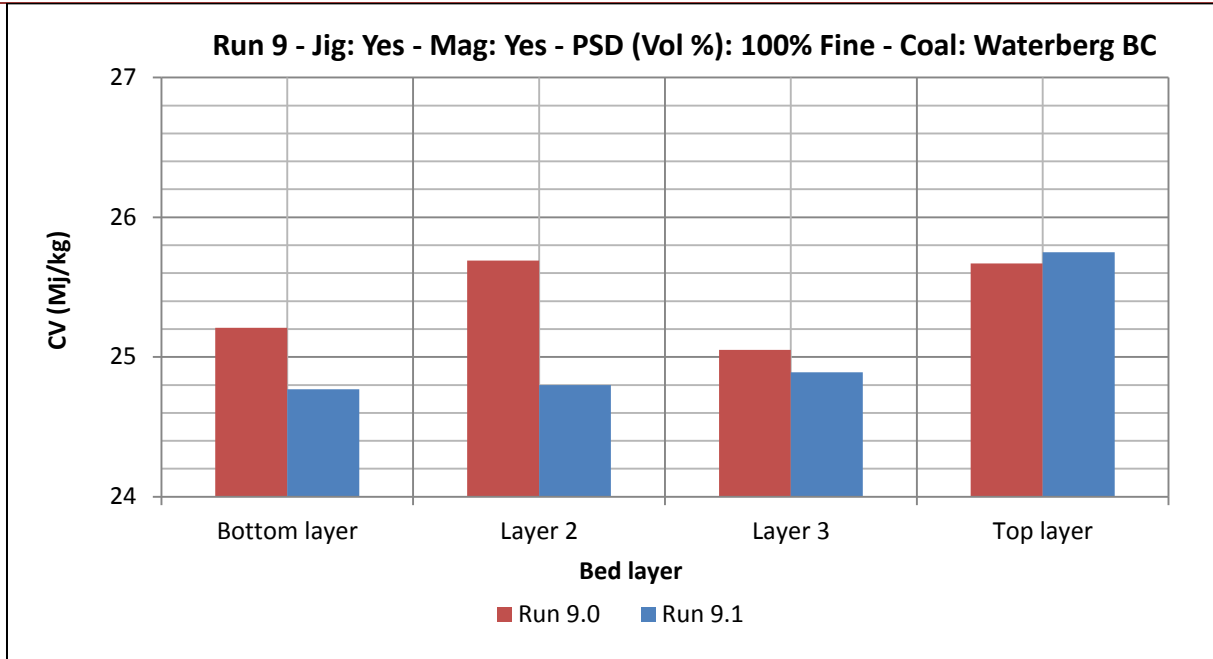


Figure 7-12: Run 9 CV repeatability graph

Appendix B

Due to the large amount of graphs and experimental data, Appendix B is attached to reduce the use of printing paper. Appendix B is included on the DVD attached to this dissertation and includes the following relevant information:

- All relevant result graphs and tables constructed during this study for all runs,
- Statistical analysis graphs and tables.